Functional Characterization of the Human RECQ5 Protein

Dissertation zur Erlangung der naturwissenschaftlichen Doktorwürde
(Dr. sc. nat.)

vorgelegt der
Mathematisch-naturwissenschaftlichen Fakultät der Universität Zürich

von
Sybille Schwendener
aus
Buchs SG

Promotionskomitee
Prof. Dr. Josef Jiricny (Vorsitz)
Prof. Dr. Ulrich Hübscher
Dr. Pavel Janscak (Leitung der Dissertation)

Zürich, 2009

TABLE OF CONTENTS

1 SUMMARY

RecQ DNA helicases are involved in processing of complex DNA structures arising during DNA metabolism to prevent aberrant mitotic recombination. Inherited defects in three of the five human RecQ helicases give rise to cancer predisposition syndromes. RECQ5 has not been associated with human disease. However, deletion of the *Recq5* gene in mice results in cancer susceptibility. How RECQ5 could act as a tumor suppressor is not yet clear. Recent findings suggest that RECQ5 has a role in DNA replication and homologous recombination. RECQ5 associates with the replication machinery and accumulates at sites of stalled replication forks and DNA double-strand breaks. In addition, RECQ5 interacts physically with the RAD51 recombinase and possesses the ability to disrupt RAD51 presynaptic filaments.

In a first study, we analyzed the activity of RECQ5 helicase on DNA structures that resemble stalled replication forks. RECQ5 was found to convert M13-based forked DNA substrates with a long leading-strand gap into four-way junctions as revealed by restriction-enzyme digestion of the reaction products. However, these structures were not sensitive to cleavage by the Holliday-junction resolvase RusA. These controversial findings and the observed low extent of RECQ5-promoted fork-regression reaction argue against a role for RECQ5 in the repair of stalled replication forks by template switching.

In a second study, we explored the mechanism underlying RECQ5-mediated disruption of RAD51 presynaptic filaments. We investigated whether the observed physical interaction between RECQ5 and RAD51 is required for RECQ5-mediated displacement of RAD51 from ssDNA. To do so, we mapped precisely the RAD51-interaction site on RECQ5 and tested RECQ5 mutants that fail to interact with RAD51 for the ability to displace RAD51 from ssDNA in a topoisomerase-linked RAD51-trap assay. We found that direct RAD51 binding enhances the RAD51 filament-disruption activity of RECQ5 but it is not essential for it. In addition, we found that the helicase core fragment of RECQ5 was not able to displace RAD51 from ssDNA, suggesting a mechanistic difference between DNA unwinding and protein-DNA complex-disruption activity of RECQ5.

2 ZUSAMMENFASSUNG

RecQ DNA Helikasen sind in die Verarbeitung von komplexen DNA Strukturen involviert, die während dem DNA Metabolismus entstehen und verhindern unangemessene mitotische Rekombination.

Vererbte Gendefekte in drei der fünf humanen RecQ Helikasen verursachen Krebsprädispositions-Syndrome. RECQ5 ist nicht assoziiert mit einer Erkrankung beim Menschen. Ein inaktiviertes *Recq5* Gen in der Maus verursacht hingegen eine Disposition für Krebserkankungen. Wie RECQ5 als Tumorsuppressor agiern könnte, ist bis jetzt nicht klar. Neuere Daten weisen auf eine Funktion von RECQ5 in der DNA Replikation und homologer Rekombination hin. RECQ5 ist assoziiert mit der Replikationsmaschinerie und akkumuliert an blockierten Replikationsgabeln und DNA Doppel-strangbrüchen. Zusätzlich interagiert RECQ5 direkt mit der RAD51 Rekombinase und besitzt die Fähigkeit präsynaptische RAD51 Filamente zu zerlegen.

Im ersten Teil der Studie untersuchten wir die RECQ5 Helikase Aktivität auf M13-basierten DNA Strukturen, die blockierten Replikationsgabeln glichen. Durch Restriktionsenzym-Verdau der Reaktionsprodukte wurde sichtbar gemacht, dass RECQ5 gabelförmige DNA Substrate mit einer grossen Lücke im Folgestrang in kreuzförmige DNA Strukturen umwandeln konnte. Diese Strukturen wurden aber nicht vom Holliday-Struktur spezifischen Enzym RusA geschnitten. Diese kontroversen Ergebnisse und das geringe Ausmass der Regressionsreaktion katalysiert durch RECQ5 sprechen gegen eine Funktion von RECQ5 in der Reparatur von blockierten Replikationsgabeln durch einen Matrizenwechsel-Mechanismus.

Im zweiten Teil dieser Studie untersuchten wir den Mechanismus durch den RECQ5 präsynaptische RAD51 Filamente zerlegt. Wir untersuchten, ob die beobachtete direkte Interaktion zwischen RAD51 und RECQ5 dazu notwendig ist. Dafür kartierten wir die präzise Interaktionsstelle von RAD51 auf RECQ5. RECQ5 Mutanten, die nicht mit RAD51 interagieren konnten, wurden dann in einem Topoisomerase-basierten RAD51 Assay getestet auf ihre Fähigkeit RAD51 von einzelsträngiger DNA zu entfernen. Wir konnten zeigen, dass direkte RAD51-RECQ5 Interaktion stimulierend auf das Entfernen von RAD51

Filamenten durch RECQ5 wirkt, aber nicht notwendig dafür ist. Zusätzlich beobachteten wir, dass das Helikase-core Fragment von RECQ5 nicht in der Lage war RAD51 von einzelsträngiger DNA zu entfernen, was auf einen mechanistischen Unterschied zwischen dem Entwinden von DNA und dem Entfernen von an DNA gebundene Proteine durch RECQ5 hindeutet.

3 INTRODUCTION

3.1 Maintenance of genome integrity and suppression of tumorigenesis

Numerous alterations in the genome of cancer cells are found. The spectrum ranges from point mutations, small insertions and deletions of nucleotides (nt) to gross chromosomal aberrations that can result from breakage and rejoining of chromosomes and aneuploidy, the condition in which a cell has extra or missing chromosomes. In addition, epigenetic changes may contribute to the development of neoplasia (1). In this process, changes in gene expression are not accompanied by changes in DNA sequence but arise from covalent modifications of histones or other chromatin components and changes in DNA cytosine-methylation patterns.

That cancer is an extremely heterogeneous disease becomes also obvious by the large number of genes identified to be causally implicated in tumorigenesis. In an ongoing effort to catalogue those cancer critical genes (cancer gene) in humans, 291 genes were reported in an original census conducted in 2004 (2), and now, this list contains a collection of over 400 genes (www.sanger.ac.uk/genetics/CGP/Census/). Despite this variability, cancer cell behavior on molecular basis can be explained by a relatively small number of events leading to deregulation in crucial cellular pathways (3-5). It is proposed that mutations in a minimum of four to seven cancer genes are sufficient to transform a cell and alter its properties in proliferation, differentiation, and survival to confer growth advantage. However, it might be rare that cancer develops because of only four to seven mutations that hit or deregulate exactly a set of cancer genes in the huge human genome with approximately 23.000 protein-coding genes (www.ensembl.org/Homo_sapiens/Info/Index). It does not astonish that in cancer typically much higher number of mutations are found. Analysis of breast and colorectal cancers revealed that individual tumors accumulate an average of approximately 90 mutant protein-coding genes, most of it accidental passenger or bystander mutations that are not involved in tumorigenesis (6). Dysfunction of genes involved in genome maintenance is

implicated in increased mutation rate and an important driving force for tumor progression. This phenomenon underlies the accelerated tumor progression observed in patients with hereditary nonpolyposis colorectal cancer (HNPCC). Loss of post-replicative mismatch repair (MMR) leads to an increased rate of somatic mutations, which, in turn, might increase the likelihood of cancer critical growth-control genes being mutated (7,8). HNPCC is a rare cancer predisposition syndrome due to germ line mutations in key MMR genes. In the cancer gene catalogue, 73 genes are reported to predispose carriers to cancer when mutated in the germ line (www.sanger.ac.uk/genetics/CGP/Census/germline_mutation.shtml). In this catalogue, genes associated with DNA maintenance and repair are clearly overrepresented, which indicates the importance of functional genome surveillance system to suppress tumorigenesis (Tab.1). Three members of the RecQ family of DNA helicases (*BLM, WRN, RECQL4*) are also among those genes that cause, if mutated, hereditary cancer syndromes. The focus of my thesis is on a further member of this helicase family, RECQ5, and its role in DNA metabolism.

3.2 DNA damage and DNA repair

Efficient detection and repair of DNA damage is particularly important for dividing cells to transmit the correct complement of genetic material to their progeny. DNA damage is not a rare event. It occurs at high frequency also under normal physiological conditions. For example, it has been estimated that loss of purine bases due to spontaneous hydrolysis of N-glycosyl bonds is in the order of 10^4 events per day for a mammalian cell (9). Other frequent DNA lesions, caused by endogenous sources, are deamination and methylation of bases and oxidative damage of bases and sugars in the DNA backbone (Fig. 1) (10). Furthermore, during DNA replication the cell has to cope with misincorporated bases (11), nicked DNA, single-stranded (ss) gaps and double-stand breaks (DSBs). In addition, environmental agents, such as UV light, ionizing radiation, and numerous genotoxic chemicals including alkylating agents and polycyclic aromatic hydrocarbons, can cause alterations in DNA structure (12).

Cancer Syndrome	gene	Molecular activity/Cellular function	Tumor Types
Ataxia-telangiectasia	ATM	Serine-threonine protein kinase/ Checkpoint signaling upon DNA double strand breaks	leukemia, lymphoma, medulloblastoma, glioma
Bloom Syndrome	BLM	DNA helicase (RecQ family member)/ DNA replication, repair and homologous recombination	leukemia, lymphoma, skin squamous cell, other cancers
Hereditary breast/ovarian cancer	BRCA1, BRCA2	BRCA1: E3 ubiquitin ligase/ DNA repair and homologous recombination	breast, ovarian, pancreatic (BRCA2), leukemia (BRCA2)
Fanconi anaemia J, breast cancer susceptiblity	BRIP1	DNA helicase/ DNA repair and homologous recombination	AML, leukemia, breast
Mosaic variegated aneuploidy	BUB1B	Serine-threonine protein kinase/ Component of the mitotic checkpoint	rhabdomyosarcoma
Familial breast cancer	CHEK2	Serine-threonine protein kinase/ Checkpoints singnaling upon DNA damage	breast
Xeroderma pigmentosum (E) (D), (B), (F), (G), (A), (C)	DDB2 ERCC-2, 3, 4, 5 XPA, XPC	DDB2: Component of UV-damaged DNA-binding protein complex; ERCC-2 ,-3: DNA helicases (components of the core-TFIIH basal transcription factor); ERCC-4, -5: DNA endonucleases/ Nucleotide excision repair	skin basal cell, skin squamous cell, melanoma
Fanconi anaemia A, C, D2, E, F, G	FANC-A, C, D2, E, F, G	DNA repair and homologous recombination (DNA crosslink repair)	AML, leukemia
Multiple Endocrine Neoplasia Type 1	MEN1	May be involved in DNA repair	parathyroid adenoma, pituitary adenoma, pancreatic islet cell, carcinoid
Hereditary non-polyposis colorectal cancer	MLH1, MSH2, MSH6, PMS1, PMS2	MSH2-MSH6: MutS alpha; MLH1-PMS2: MutL alpha, PMS2: endonuclease activity/ DNA mismatch repair	colorectal, endometrial, ovarian, CNS (MLH1), medulloblastoma (PMS2), glioma (PMS2)
Nijmegen breakage syndrome	NBS1	DNA damage repair and DNA damage checkpoint signaling	NHL, glioma, medulloblastoma, rhabdomyosarcoma
Fanconi anaemia N, breast cancer susceptibility	PALB2	Recombinational repair (partner of BRCA2)	Wilms tumor, medulloblastoma, AML ,breast
Rothmund-Thompson Syndrome	RECQL4	DNA-dependent ATPase (RecQ family member)/ DNA replication, repair and homologous recombination	osteosarcoma, skin basal and sqamous cell
Rhabdoid predisposition syndrome	SMARCB1	Chromatin-remodeling (core component of the hSWI/SNF complex)	malignant rhabdoid
Li-Fraumeni syndrome	TP53	DNA damage signaling	breast, sarcoma, adrenocortical carcinoma, glioma, multiple other tumour types
Werner Syndrome	WRN	DNA helicase, DNA exonuclease (RecQ family member)/ DNA replication, repair and homologous recombination	osteosarcoma, meningioma, others

Table 1

Cancer syndromes associated with defect in DNA maintenance and repair. Table 1 lists the genes of the germline mutated cancer gene catalogue (www.sanger.ac.uk/genetics/CGP/Census/germline_mutation.shtml) that are implicated in genome surveillance and stability. The listed cancer syndromes are all recessive disorders. Carriers are predisposed to develop cancer because of one defective allele and loss of the second allele is usually observed in tumor cells. In addition, associated with several of these germ line mutations are pathologies other than cancer. AML, acute myelogenous leukemia; CNS, central nervous system; NHL, non-Hodgkin lymphoma.

Cells have evolved pathways to prevent genome from excessive mutagenesis. Most of these pathways are conserved through evolution. In bacteria, yeast and vertebrates similar sets of molecular players are found that detect DNA lesions and repair or tolerate them. Alternatively, multicellular organisms can activate a programmed cell-death process to eliminate cells with severely damaged DNA (13).

Five major DNA repair mechanisms have evolved: (i) direct repair, (ii) base excision repair (BER), (14) nucleotide excision repair (NER), (iv) mismatch repair (MMR), and (v) DSB repair (12,15). DSBs can be repaired either by non-homologous end joining (NHEJ) or homologous recombination (HR). Since one topic of this thesis deals with the regulatory role of RECQ5 helicase in HR, the HR pathway is described in detail in chapter 3.3. The other repair systems are described here only briefly with emphasis on the overall mechanism of the DNA repair reaction.

Direct repair is catalyzed by highly specific repair proteins, which recognize a particular base modification and reverse it in a single-step reaction. In humans, the enzyme O^6-methylguanine-DNA methyltransferase (MGMT or AGT) corrects O^6-methylated guanine by transferring the methyl group to a cysteine residue in its active site (16,17). In BER, NER and MMR, DNA lesions are excised and the original DNA sequence is restored by DNA synthesis using the intact opposite strand as template. The remaining nick is then sealed by DNA ligases. BER is a multi-step process that is initiated by DNA glycosylases. These enzymes recognize specific types of modified bases and remove them by cleavage of the N-glycosidic bond. Abasic sites are then processed by an apyrimidinic/apurinic (AP) endonuclease. In humans, eight different DNA-glycosylases with partially overlapping substrate specificities have been described (18). NER is an elaborate repair mechanism where more than 30 proteins are involved and function in multi-protein complexes (19). DNA damage is rather indirectly recognized through distortion of the DNA helix structure (20). Such distortions can occur by bulky DNA adducts or by UV induced crosslinking of adjacent pyrimidine bases in the same DNA chain (cyclobutane pyrimidine dimers (CPDs) or 6-4 photoproducts). Defects in components of NER pathway are linked to the cancer syndrome xeroderma pigmentosum (XP). The failure to repair UV

photoproducts predisposes these patients to develop skin cancer associated with sunlight exposure (21). A second branch of the NER system senses lesions *via* stalled RNA polymerase II and is called transcription-coupled NER (22). The MMR system corrects errors during DNA replication that have been missed by the proofreading activity of the polymerases (23). In humans, generally, base-base mismatches and small insertion/deletion loops (IDL) are recognized by the heterodimer MutSα (MSH2-MSH6), whereas larger IDLs are detected by MutSβ (MSH2-MSH3). The DNA bound MutS forms a ternary complex with MutLα (MLh1-PMS2) and in an ATP-driven process the complex slides along DNA and searches for a nick in the DNA that serves as a signal to distinguish the newly synthesized erroneous DNA stand from the correct template strand. Loss of MMR becomes apparent in the instability of short repetitive DNA sequences (microsatellites) that are prone to be incorrectly synthesized by DNA poymerases and require post-replicative repair (24).

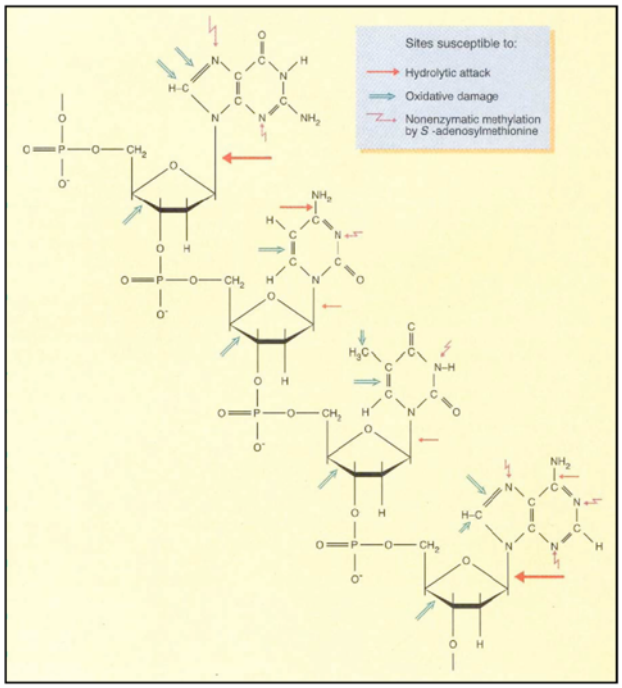

Figure 1

Target sites for intracellular DNA decay. A short segment of one strand of the DNA double helix is shown with the four bases (from top: guanine, cytosine, thymine, adenine). Sites susceptible for hydrolytic attack, oxidative damage, and non-enzymatic methylation by S-adenosylmethionine are indicated. The large arrows highlight major sites of damage. Adapted from (10).

3.3. Homologous recombination

Homologous recombination (HR) serves to eliminate DSBs from chromosomes by using an intact homologous DNA sequence as template for

repair. DSBs can be programmed, such as in meiosis to induce recombination between homologous chromosomes (25) or they can occur as unscheduled events during DNA replication or result from direct damage induced, for example, by ionizing radiation. Unprogrammed DSBs pose a serious threat for the cell. They must be repaired quickly and with sufficient accuracy to restore the integrity and functionality of the genome. As mentioned above, the cell has two distinct pathways to repair DSBs. In NHEJ the DNA ends are bound by the Ku70/80 heterodimer and a process is initiated that joins the DNA ends directly (26). This repair process can lead to sequence alterations at the breakpoint (27). In contrast, HR is an accurate repair mechanism, but requires the presence of a homologous DNA sequence elsewhere in the genome. HR functions therefore preferentially during the S and G2 phase of the cell cycle where the sister chromatid is available (28). How DSBs are directed for repair by the different pathways is not yet clear. In a recent study, it has been suggested that phosphorylation of CtIP as cell enters S phase could shift the balance of DSB repair from NHEJ to HR (29). CtIP promotes the resection of DNA ends and by this generates ssDNA tails, which could serve as substrate for HR (30).

3.3.1 Mechanism of homologous recombination

The classical DSB repair (DSBR) model was worked out in yeast studies on meiotic recombination and helps to explain several key features of mitotic HR to repair a spontaneous DSB (31). To initiate HR the end of a DSB is resected to generate a 3'-ssDNA tail that serves as substrate for the HR machinery (Fig. 2 A). The MRE11/RAD50/NBS1 (MRN) complex is a central player in the cellular response to DSBs. It binds to DSBs, promotes DNA end processing, and is involved in activation of the damage checkpoint kinase ATM (32). As mentioned above CtIP, is another protein required for DSB resection and interacts directly with the MRN complex (30).

Next, a catalytic nucleoprotein filament assembles on the ssDNA tail. The subunits of this filament belong to the RecA/Rad51 family of recombinases that promote strand invasion into a homologous DNA duplex and thus create a three-stranded DNA intermediate called displacement loop (D-loop) (Fig. 2 A). Presynaptic filament assembly as well as D-loop formation

is dependent on several recombination mediators and accessory factors (33). Firstly, for Rad51 to nucleate on ssDNA, the inhibitory effect of bound replication protein A (RPA) must be overcome. At least in yeast, Rad52 has a key role in the delivery of Rad51 to RPA-bound HR substrates (34,35), and *S. cerevisiae* rad52 mutants exhibit severe defects in DSB repair (36). Although vertebrates possess a Rad52 ortholog, other proteins seem to mediate Rad51 filament assembly on ssDNA. In humans, five RAD51 paralogs (RAD51B, RAD51C, RAD51D, XRCC2, XRCC3) have been described that might participate in assembly and/or maintenance of RAD51 presynaptic filaments (37). In addition, two main mediators are BRCA1 and BRCA2. Both are required for normal levels of HR and cell lines defective in BRCA2 fail to accumulate RAD51 foci after DNA damage (38-41). Secondly, ATP-dependent dsDNA translocases like RAD54 and RAD54B assist RAD51 in search for DNA homology and stimulate D-loop reaction (42).

In a next step of HR, the invaded DNA strand is extended from the 3'-end by DNA synthesis (Fig. 2 A). A candidate for this DNA transaction is the translesion synthesis (TLS) polymerase η (Pol η). Human Pol η was identified to promote efficiently extension of an artificial D-loop substrate by a biochemical approach (43).

In the classical DSBR model, the displaced strand of the D-loop anneals to the ssDNA tail of the second DSB end (Fig. 2 B). Rad52 is suggested to promote this step. Rad52 exhibits ssDNA annealing activity even in presence of saturating amounts of RPA (44). Furthermore, yeast Rad52 in the presence of RPA was shown to capture ssDNA and facilitate the annealing with the displaced strand after Rad51-mediated strand exchange *in vitro* (45,46). The resulting DNA structure after second end capture, gap filling and ligation contains two Holliday junctions (HJs). This intermediate needs to be resolved to allow the repaired DNA molecules to separate (Fig. 2 B).

The resolution step of HR is much better understood in bacteria. The bacterial RuvABC enzyme complex acts on HJs and cleaves them symmetrically into linear duplex products (47). How the corresponding process takes place in eukaryotic cells is not well characterized. Mus81-Eme1 was identified as a candidate protein complex with resolvase activity. However, at least *in vitro*, it shows higher activity on 3'-flaps, fork structures or

nicked HJs than on intact HJs (48-50). Recently, West's laboratory reported a novel resolvase GEN1 (yeast otholog Yen1) that cleaves HJs, like RuvC, symmetrically to produce nicked duplexes that can be readily ligated (51). Depending on which pairs of DNA strands are nicked, HJ-cleavage products can give rise to crossover or non-crossover DNA molecules (Fig. 2 C). Crossovers that lead to exchange of chromosome arms are observed in meiosis and are essential for proper chromosome segregation (25).

Mitotic HR differs from meiotic HR. In mitotic cells, crossovers between homologous DNA molecules, that are usually sister chromatids, seems to be actively suppressed. The BLM helicase has an important role to suppress sister chromatid exchanges (SCEs). Acting together with topoisomerase IIIα (TOPOIIIα), BLM is thought to migrate HJs between paired duplexes inward and the resulting hemicatenane structure is then resolved by TOPOIIIα to yield only non-crossover products (Fig. 2 D). This double HJ dissolution mechanism was demonstrated *in vitro* (52) and helps to explain the elevated level of SCEs observed in cells from Bloom's syndrome patients (53).

Synthesis-dependent strand annealing (SDSA) is another proposed HR repair mechanism that is not associated with crossovers (54,55). By D-loop migration the invading strand is displaced after repair synthesis and re-anneals with the second resected DSB end, which is not captured into the recombination intermediate (Fig. 2 E). Gap-repair DNA synthesis followed by ligation is then used to complete the repair process (Fig. 2 E). The yeast helicase Srs2 was recently suggested to promote SDSA, since it shows preference to unwind synthetic DNA structures that mimic a D-loop and is stimulated by Rad51 bound to double-stranded (ds) DNA (56).

DNA helicases are in general thought to control HR at different stages (57). They can negative regulate early steps of HR by direct disruption of Rad51 presynaptic filaments formed on ssDNA (see Chapter 3.5.3). Furthermore, the complex DNA structures that arise during HR such as D-loops and HJs are preferred substrates for DNA helicases. Evidence that helicases have important roles in disruption/resolution of HR intermediates comes from studies in yeast. *S.cerevisiae* double mutants srs2 sgs1 that lack both Srs2 and the BLM ortholog Sgs1, show low viability. Interestingly, the low

viability of sgs1 srs2 mutants is suppressed by mutation in rad51 (58). These findings suggest that in the absence of Srs2 and Sgs1, Rad51-promoted DNA intermediates are not removed or maturated properly and become toxic for the cell.

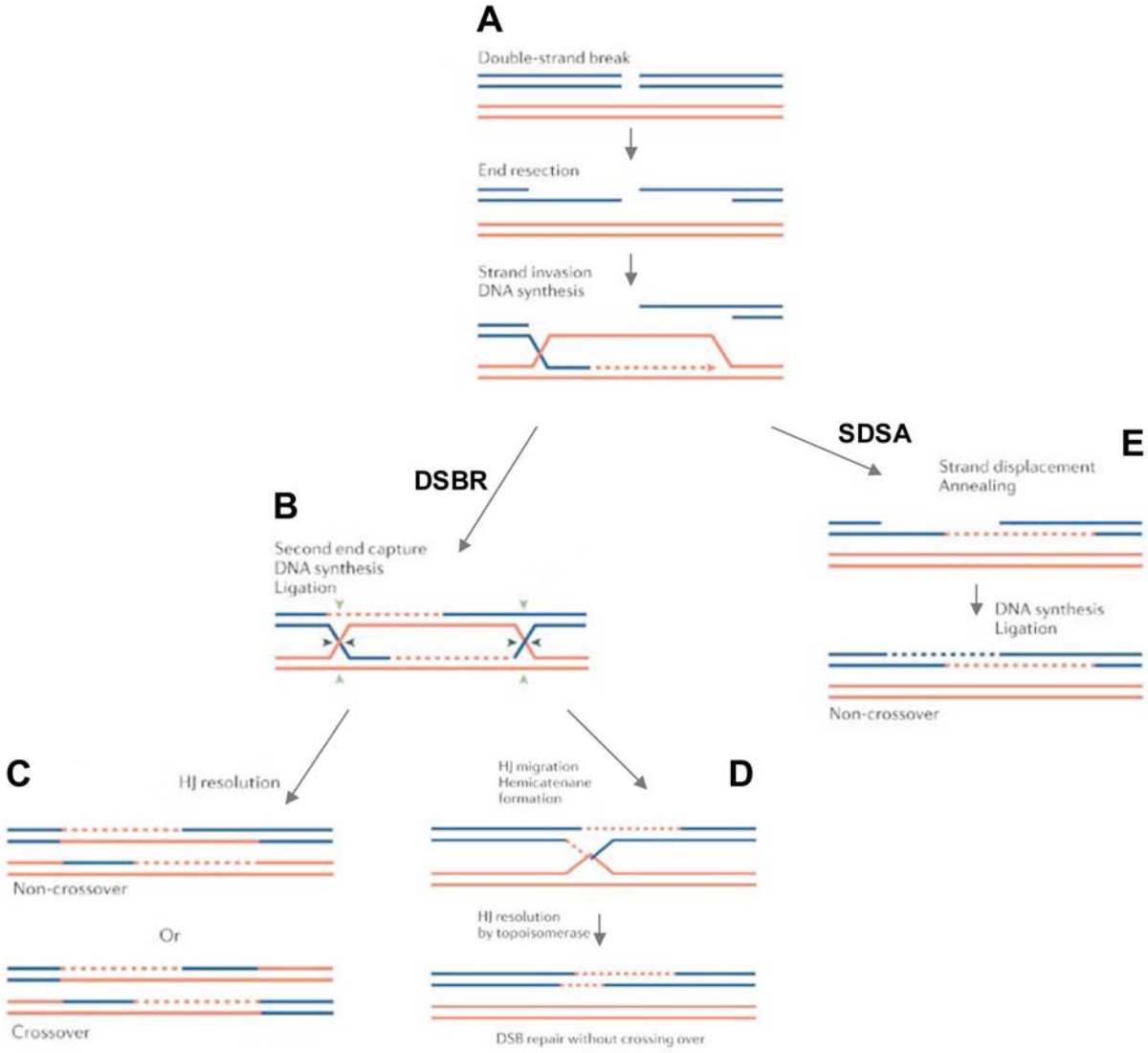

Figure 2
Repair of DNA double-strand breaks. Double-strand breaks (DSBs) can be repaired by several homologous recombination (HR)-mediated pathways, including double-strand break repair (DSBR) and synthesis-dependent strand annealing (SDSA). **(A)** Repair is initiated by resection of a DSB to provide 3'-ssDNA overhangs. Strand invasion by a 3'-ssDNA overhang into a homologous sequence is followed by DNA synthesis at the invading end. **(B)** In the DSBR pathway the second DSB end is captured and after gap-repair DNA synthesis and ligation a DNA intermediate with two Holliday junctions (HJs) is formed. **(C)** This structure can by resolved at the HJs in a non-corossover (black arrow heads) or crossover mode (green arrow heads). **(D)** Alternatively, double HJs can be dissolved by migration of the HJs inwards and decatenation of the DNA molecules to give non-crossover products. **(E)** Another pathway to generate non-crossover products is SDSA. The reaction includes displacement of the invaded strand after DNA synthesis, re-annealing to the other resected DSB end, gap-filling DNA synthesis and ligation. Adapted from (57).

3.3.2 The RAD51 recombinase

The catalytic core of the HR machinery consists of proteins belonging to the RecA/Rad51 family of recombinases that assemble into nucleoprotein filaments on ssDNA and promote homologous DNA pairing and strand exchange. In eukaryotes, two orthologs of the *E.coli* recombinase RecA exist, RAD51 and DMC1. RAD51 is needed for mitotic and meiotic HR, whereas DMC1 function is restricted to meiotic HR as it is only expressed in meiosis. *S.cerevisiae* rad51 mutants are viable. However, RAD51 is essential in higher eukaryotes. Deletion of *Rad51* from the genome in mice is lethal (59,60) and vertebrate cells rapidly accumulate chromosome aberrations and stop dividing when RAD51 expression is suppressed (61).

The human RAD51 recombinase is a relatively small protein of about 37 kDa and the core domain, homologous to RecA, contains the Walker A and B motifs responsible for ATP binding and hydrolysis (Fig. 3 A). As other recombinases, RAD51 exists as homo-oligomer in solution and forms heptameric ring structure (62) (Fig. 3 B). RAD51 binds both ss and dsDNA showing preference for dsDNA with a ssDNA tail (63,64). The catalytically active form of RAD51 is a highly ordered right-handed helical nucleoprotein filament on ssDNA (65) (Fig. 3 B). In this complex, the DNA is held in an extended conformation, being stretched by as much as 50% of the length of a canonical B-form DNA helix (66,67).

The reaction catalyzed by the competent RAD51 filament, which is search for homologous sequence in duplex DNA and strand exchange, is not completely understood. It is thought that rapid exchange of A:T base pairs is essential for homology recognition and formation of initial paranemic joints (68). Interestingly, RAD51 filament was reported to localize homologous sequence even on the surface of nucleosomal DNA and promote formation of paranemic joints that can be converted into stable plectonemic joints by RAD54 (69).

One important prerequisite for catalytically competent RAD51 filament is bound ATP. Under *in vitro* conditions, inhibition of the ATPase activity of RAD51 leads to stabilized presynaptic filaments and an enhanced ability of RAD51 filaments to catalyze the strand-exchange reaction. As a consequence, the use of a nonhydrolyzable nucleotide analogue (such as

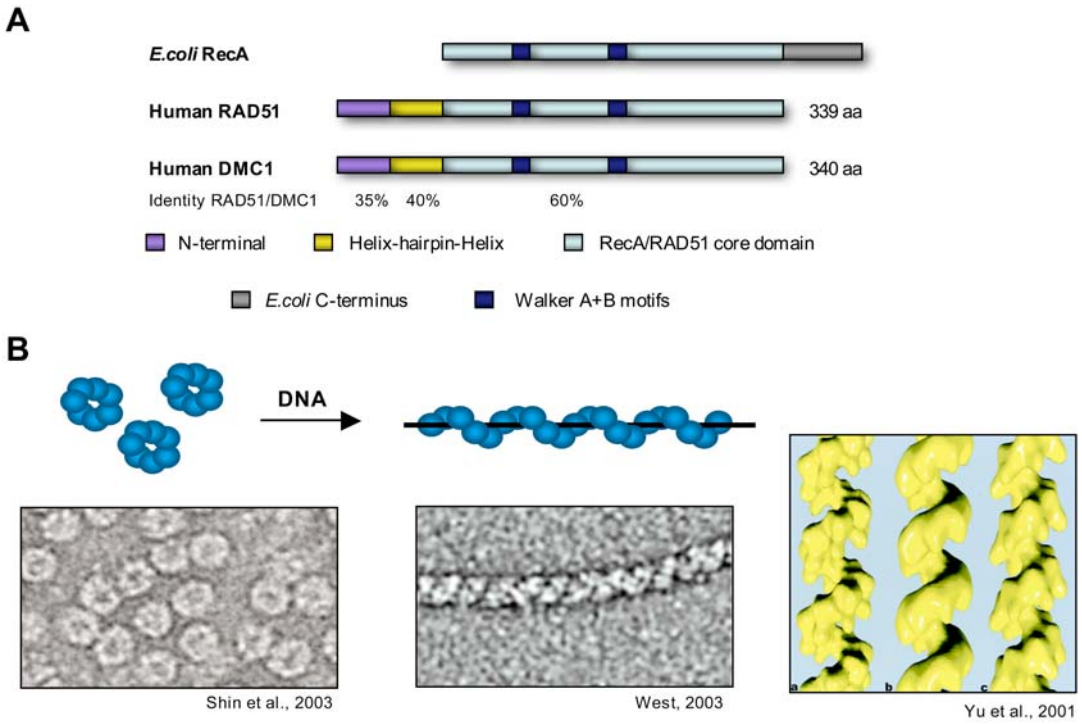

Figure 3
Structures of RecA/Rad51 family recombinases. (A) Schematic representation of *E. coli* RecA, human RAD51 and human DMC1, showing their characteristic motifs (adapted from (70). **(B)** RAD51 forms heptameric ring structures in solution, as indicated schematically and in the electron microscope (EM) image of archaeal RAD51 (adapted from (62)). The catalytically active RAD51 is associated with ssDNA in the form of a highly ordered right-handed helical nucleoprotein filament, indicated schematically. The nucleoprotein filament has a pitch of 95-100Å, comprising 6 RAD51 proteins and 18 nucleotides of the DNA ligand per helical repeat (67). The EM image shows a nucleoprotein filament assembled from human RAD51 (adapted from (71)). Filaments formed on ssDNA by human RAD51 (a), *S. cerevisiae* Rad51 (b), and *E. coli* RecA (c) are illustrated by three-dimensional surfaces reconstructions (adapted from (67)).

AMP-PNP) (63,69,72), calcium ions in the reaction (72,73) or RAD51 mutants that bind but cannot hydrolyze ATP (63), highly stimulates RAD51 function. Moreover, over expression of such ATPase-defective RAD51 mutants, yeast Rad51K191R or human RAD51K133R, is needed to compensate for the loss of endogenous RAD51 *in vivo* (74,75). These findings raise at least two questions. Firstly, what is the role of ATP hydrolysis for the RAD51-promoted reaction, and secondly, how can a stable filament form *in vivo*. It is demonstrated that ATP hydrolysis is linked to dynamic disassembly of the filament (72). The fast turnover of the RAD51 filament is thought to generate an intracellular pool of free RAD51 proteins available for HR and DNA repair reactions (63). A crucial role in the stabilization of RAD51 filaments *in vivo*

might have the several known HR mediators and accessory factors (33). Especially, BRCA2 is reported as universal RAD51 regulator. BRCA2 interacts directly with RAD51 *via* BRC repeats and a C-terminal region. BRCA2 is reported to target RAD51 to ssDNA, influences its oligomerization state and the stability of the formed RAD51 filament on DNA (70,76).

3.4 DNA Replication

DNA replication is the process by which the cell copies its genome. To maintain genetic information each DNA strand must be accurately and completely duplicated exactly once before each cell division. In the first part of the chapter (3.4.1) the global process during undisturbed DNA replication is explained. In the second part of the chapter (3.4.2) it is described how the replication machinery copes with damaged DNA or other situations that block the replication process.

3.4.1 Global DNA replication process

Duplication of the genome starts at replication origins. At these sites, the DNA double helix is melted and two replication forks are initiated. The replication forks then move along the DNA, replicating each strand as they progress. At the fork, several factors are organized in a complex called a replisome that allows coordinated copying of the antiparallel template strands by DNA polymerases (Pols). These enzymes synthesize DNA in 5'→3' direction. Therefore, the two polymerase molecules copying the template strands move in opposite directions, one producing a continuous leading strand, while the other generates a lagging strand in a discontinuous fashion by synthesis of short so-called Okazaki fragments (Fig. 4). In *E. coli*, both nascent strands are synthesized by Pol III. Efficient replication of the eukaryotic genome requires three major DNA polymerases: Pol α, Pol δ, and Pol ε (77). Pol α-primase complex initiates DNA synthesis by generating a short RNA primer that is elongated by its DNA polymerase activity to form a short stretch of DNA, allowing Pol δ and Pol ε to perform the bulk of chain elongation. Pol δ and Pol ε are both highly selective for correct nucleotide insertion and have intrinsic proofreading exonuclease activities. Hence, the error rate of these

polymerases is in the 10^{-6} to 10^{-8} range (11). Recent studies in yeast specify Pol ε as the leading-strand and Pol δ as the lagging-strand polymerase during undisturbed DNA replication (78,79) (Fig. 4). This division of labor model at the eukaryotic replication fork is based on analysis of error patterns caused by mutator variants of Pol ε or Pol δ in a target sequence inserted next to a well-defined replication origin (78,79). Evidence implicating Pol δ in lagging-strand replication is in addition provided by its role in Okazaki fragment maturation (80). Every 100-200nt on the lagging strand, Pol δ runs into the RNA primer of the previous Okazaki fragment and is able to perform strand-displacement DNA synthesis, thus generating a 5'-flap structure that can be cleaved by flap endonuclease 1 (Fen1) or Dna2 and ligated by DNA ligase I (80,81). Furthermore, Pol δ seems to correct errors made by Pol α that has a lower fidelity because of lack of intrinsic proofreading activity (82).

A key factor that coordinates proteins at the replication fork is the proliferating cell nuclear antigen (PCNA). PCNA is proposed to encircle dsDNA as a trimer (83), forming a siding clamp that enhances the processivity of polymerases and recruits proteins to DNA (84). Other important factors participating in DNA replication are the ssDNA binding protein RPA, DNA helicases and topoisomerases. DNA strand separation by helicases at the replication fork generates ssDNA that is bound and protected by RPA. DNA unwinding leads to accumulation of positive supercoiling ahead of the fork that opposes further fork progression and requires the action of topoisomerases (85).

Apart from the higher complexity observed in eukaryotes, the mechanism of DNA replication seems fairly conserved from bacteria to higher eukaryotes. However, an important difference concerns the shape of the genome. Most bacteria have a single circular chromosome. *E. coli*, for example, replicates its 4.7 10^6bp genome from a single sequence-defined origin. Not only the initiation of bacterial DNA replication, but also its termination is a controlled process. Termination (Ter) sequences and bound Tus proteins allow progression of the replication fork only in one direction and constrain the replication forks to converge at a terminus region located opposite to the origin (86). The situation in eukaryotes is much more complex.

Replication of several linear chromosomes in the cell needs to be synchronized. On each chromosome, a large number of origins are used, typically spaced 30-100kb apart (87). Origins are established at origin recognition complex (ORC) bound DNA sites, which are often not defined by sequence in metazoa (88). During late mitosis and G1, pre-replication complexes (pre-RCs) are assembled by loading the minichromosome maintenance (MCM) 2-7 proteins (87). MCM2-7 proteins are essential for initiating and elongating replication forks during S phase. Hence, these proteins are suggested to function as a replicative helicase. Eukaryotic cells seem to control the replication from their multiple origins in a flexible way. More pre-RCs are assembled than are activated during S-phase, thus firing of individual origins is inefficient and it is proposed that pre-RCs at silent origins are destroyed by passage of replication forks from active origins (88).

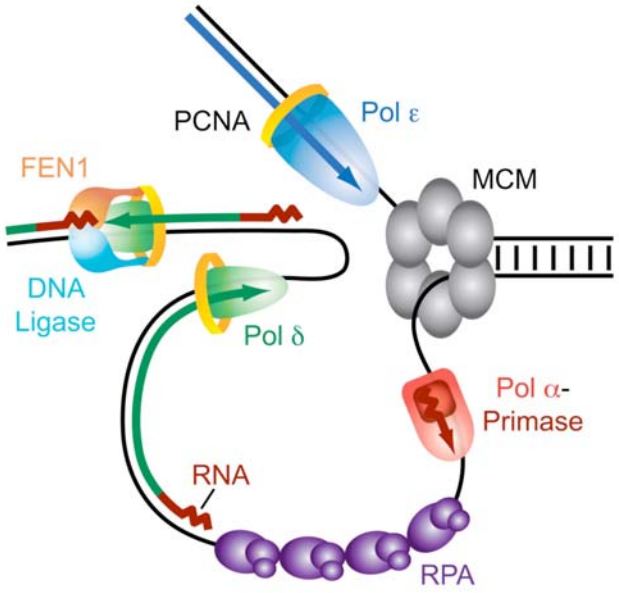

Figure 4

The eukaryotic replication fork model. During undisturbed DNA replication, synthesis of the leading and lagging strand is performed by Pol ε and Pol δ, respectively. A minimal replisome is shown consisting of the MCM helicase, RPA, PCNA, Pol α-primase complex that synthesizes RNA/DNA primers, Pol ε and Pol δ responsible for the bulk of DNA replication, and the Okazaki fragment maturation proteins FEN1/DNA Ligase. By loop formation of the lagging-strand template, Pol δ is thought to move coupled with Pol ε in direction of the progressing fork. Arrows represent the 3'-end of DNA strands. Adapted from (79).

3.4.2 Processing of stalled replication forks

DNA replication is exposed to a variety of situations that may challenge the progression of replication forks, thus endanger genome integrity. In *E. coli,* it is assumed that about 18% of cells require replisome reloading outside the origin during a single round of chromosome duplication in the absence of

exogenous DNA damaging agents (89). In both, prokaryotes and eukaryotes, replication-fork blockage, eventually collapse of the fork because of replisome disassembly is though to arise often from different sources. A damaged DNA base can stall the replicative polymerase on one arm of the fork; a roadblock in the template duplex ahead of the fork, such as tightly bound proteins or a inter-strand DNA crosslink, can stall the whole replisome; a nick in the template strand can result in a one-ended DSB. Therefore, recovery from the different types of replication-fork damage requires multiple fork-reactivation pathways.

3.4.2.1 Pathways in bacteria

In *E. coli,* replication arrest by defects in replicative enzymes or as a result of DNA damage has been the subject of extensive studies in the past years. To replicate the circular chromosome from a single origin, the bacterial replication machinery relies on a close interplay with recombination and DNA repair proteins (90,91). Two studies on *E.coli* replication mutants led to the proposal of a replication-reactivation model in which a HJ forms at blocked replication forks. In the first study, replication-associated DSBs were demonstrated in helicase-defective mutants (dnaB and rep) in the absence of functional HR due to a lack of RecBCD (92). The *E. coli* RecBCD, a helicase-exonuclease complex, is a key factor in HR that degrades DNA from a DSB end and generates the 3'-ssDNA overhang substrate for RecA upon encountering a regulatory sequence called Chi (93). In the second study, the fragmentation of chromosomal DNA in cells lacking Rep helicase and the RecBCD complex could be suppressed by inactivation of the RuvABC proteins (94). Therefore, it is thought that replication arrest leads to a reaction called replication-fork regression. This reaction involves the unwinding of the two arms of the fork, annealing of the nascent strands and repairing of the parental strands to form a four-way DNA structure, similar to a HJ (Fig. 5 B). In RecBCD-proficient cells the regressed arm can be processed from the end without breakage (Fig. 5 F). In the absence of RecBCD, the RuvABC complex alternatively processes the four-way DNA and generates a one-ended DSB that depends on functional HR to be repaired (Fig. 5 D). The genetic data support this model. The viability of rep recBC mutants could be restored by inactivation of

the ruvAB operon (94). Hence, no irreparable DSBs are formed at arrested forks and replication is channeled in an alternative restart pathway. This concept of chromosome fragmentation after HJ formation at the arrested replication fork was confirmed with other replication mutants (dnaE, dnaN, and holD) and a priA mutant, defective in the main replication-restart pathway (95-97).

Originally, it was thought that conversion of an arrested fork into a HJ facilitates replisome reloading in a HR-dependent way and promotes restart of collapsed replication forks (90,94). Biochemical studies showed later that the replicative helicase DnaB can be loaded directly on a fork structure and DNA synthesis can be re-initiated even on the leading strand outside the origin (98,99). Two different direct enzymatic restart systems are reported. The first system depends on PriA that can restart a collapsed replication fork when the 3'-end of the nascent leading strand is near the fork junction and in addition can promote restart from a D-loop substrate (98-100). The second system, which is PriC-dependent, initiates replication on a fork with a leading-strand gap (98,99).

Fork structures with a long leading-strand gap were observed *in vivo*. A lesion in the leading-strand template can uncouple nascent strand polymerization at the fork; while the leading-strand polymerase is blocked, unwinding of the replication fork and lagging-strand synthesis can continue for some distance (101). Replication through base lesions requires specialized DNA polymerases called translesion synthesis (TLS) polymerases (Fig. 5 A) (100). TLS polymerases are able to insert bases opposite DNA lesions that block the major replicative polymerases at the expense of low-fidelity (11). Alternatively, in the direct PriC-dependent restart pathway, the gaps with a lesion left behind are proposed to be repaired in error-free manner by HR using undamaged sister chromatid (Fig. 5 C). Mutants in priA, in which only the PriC restart system is functional, require the RecFOR gap-filling recombination proteins for viability (102). Furthermore, Courcelle's laboratory reported that UV lesions that block replication are processed and repaired through a transient X-shaped DNA structure in *E.coli* (103). They propose that fork regression sets back the replication-blocking lesion to the parental duplex allowing repair enzymes to gain access. In a recent study, they provided

evidence for the involvement of the RecJ-RecQ nuclease-helicase complex in rapid recovery of DNA synthesis after UV damage (104). RecJ-RecQ preferentially degrades the nascent lagging strand at blocked forks (105). Therefore, processing of a stalled fork with a leading-strand gap by RecJ-RecQ is thought to allow re-annealing of the parental strands and removal of the lesion by the excision repair machinery from the parental duplex (104). In the absence of RecJ, or to a lesser extent RecQ, both recovery of replication and cell survival become dependent on the TLS Pol V (104).

In most conditions of replication inactivation, the mechanism by which a blocked replication fork is converted into a HJ remains unknown. Replication-fork regression can in principle be spontaneous or enzyme-driven. Positive superhelical stress built up in front of the replication fork can be relived by fork regression. It has been demonstrated that introduction of positive supercoiling into partially replicated plasmids causes fork regression *in vitro* (106,107). Alternatively, helicases or recombinases could actively drive the regression process at blocked forks. The bacterial helicase RecG binds and unwinds forked DNA structures and can promote HJ branch migration (108). Furthermore, it can convert fork structures into HJ (109,110) and shows an efficient fork-regression activity on a M13-based fork structure with a long leading-strand gap (111). The crystal structure of RecG bound to a synthetic forked DNA suggests that monomeric RecG can promote fork regression by simultaneously unwinding of the two nascent arms and annealing of the parental strands (112). RecG is though to translocate along the parental duplex in opposite direction to replication. A motif called a wedge domain is involved in stripping off the nascent strands at the fork junction and frees them for annealing, while the complementary parental strands are directed to narrow channels on each side of the wedge domain that can only accommodate ssDNA. *In vivo* data further suggested a role for the UvrD helicase in fork regression (113,114), and also implicated the branch migration complex RuvAB in converting a stalled fork into a HJ (115). By an alternative mechanism, fork regression can also be promoted by the RecA recombinase. On fork structures with a ssDNA gap, RecA can form a nucleoprotein filament and catalyze strand exchange with the homologous

sister arm. *In vitro*, RecA was found to regress a M13-based fork structure with a 2.1kb leading-strand gap (116).

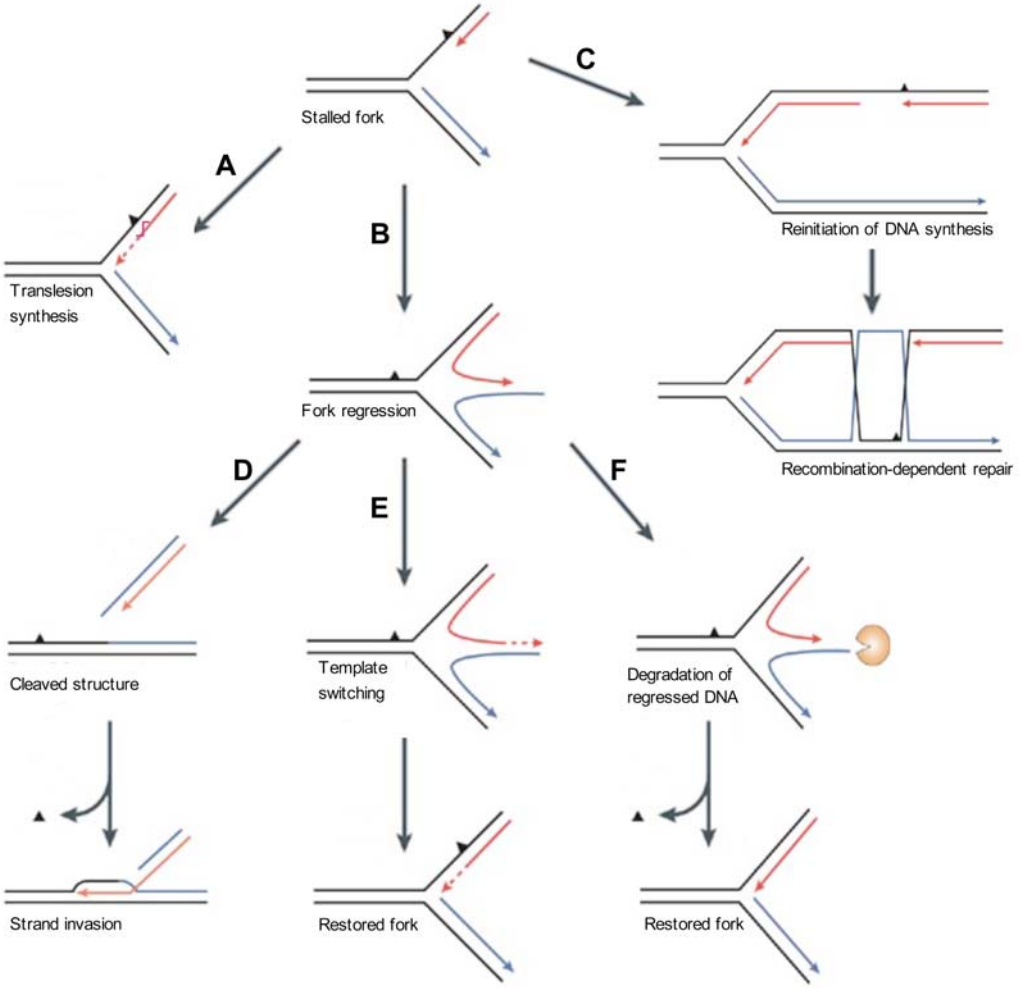

Figure 5
Potential pathways resulting in reactivation of replication forks stalled by a leading-strand specific lesion. When the replisome encounters a lesion (black triangle) in the leading-strand template leading- and lagging-strand synthesis can become uncoupled resulting in a stalled fork with a leading-strand gap. **(A)** Specialized DNA polymerases called translesion synthesis polymerases are able to replicate past lesions in an error-prone pathway. **(B)** Fork regression is thought to convert a stalled replication fork into a four-way DNA structure similar to a Holliday junction (HJ) that serves as intermediate for several reactivation mechanisms (D-F). **(C)** Alternatively, DNA synthesis may directly reinitiate and the gap with the lesion could be repaired later in a recombination-mediated error-free pathway using complementary DNA from the sister duplex. **(D)** After HJ cleavage the broken DNA end can undergo a strand invasion into the intact homologous duplex and DNA synthesis can be restarted from a D-loop. **(E)** By template switching, the complementary nascent strand is used for DNA synthesis, following reversal of the regressed fork. Thereby the lesion is bypassed in a error-free manner without removal. **(F)** Furthermore, fork regression sets back the blocking lesion to the parental duplex where it can be removed by excision repair. The fork structure could be restored by an exonuclease (indicated in orange) that degrades DNA of the regressed arm. The arrow heads represent the 3'-end of DNA strands and the dotted lines DNA extension past the lesion. This figure is adapted from (117).

3.4.2.2 Pathways in eukaryotes

Processing of damaged replication forks might be of similar importance in eukaryotic cells, so there could be analogous systems for reactivation of arrested forks to those in prokaryotes. However, eukaryotes could also use the presence of multiple origins on each chromosome. Hence, a fork from an adjacent origin might converge on a damaged fork to complete replication from the opposite site. Two major pathways are thought to operate on blocked replication forks in eukaryotes: an error-prone pathway that relies on TLS polymerases that can progress though certain types of lesions that block replicative polymerases and an error-free repair pathway largely dependent on HR.

Replication of SV40 derived plasmids with a CPD in the leading-strand template in human cell extracts showed a temporary arrest at the lesion, leading to uncoupling of the leading- and lagging-strand synthesis and finally lesion bypass without repair in about 50% of the daughter plasmids (118,119). Replication–competent extracts from XP-variant cell line were found severely impaired in CPD bypass (118,119). XP-variant cells are defective in the TLS Pol η that is able to replicate past CPDs (120). The switch to a TLS polymerase is proposed to involve post-translational modifications including monoubiquitination of the sliding clamp PCNA at stalled replication forks (121).

Also in eukaryotes, recombination is believed to assist replication. RAD51 function is indispensable in the maintenance of chromosomal DNA during normal cell cycling (61). Substrate for HR repair machinery is likely generated by collapse of replication fork at endogenous single strand breaks (SSBs). Challenging replicating cells with SSBs following camptothecin treatment or using cells deficient in SSB repair (XRCC1-deficient) triggers RAD51-dependent HR events (122), suggesting a role for HR in reactivation of broken replication forks. Programmed replication-fork barriers (RFBs) in certain regions of the chromosomes that slow down fork progression have often been invoked to explain the nature of specific hot spots for recombination (123). In a study in yeast, the consequence of fork arrest by introducing a RFB at an ectopic site was analyzed (124). The used RFB consists of a non-histone protein/DNA complex. Proteins implicated in HR

were found to be recruited to the ectopically blocked replication site and promote recombination events that allow cells to survive, but are sometimes associated with gross chromosomal rearrangements (124).

How transiently blocked replication forks are processed is not yet completely understood. A reactivation pathway through a transient HJ was originally also suggested for eukaryotes. Moreover, fork regression was postulated to allow bypass of a lesion by using the complementary nascent strand as template for error-free DNA synthesis (125) (Fig. 5 E). This mechanism called template switching, although conceptually attractive, is controversial. Direct visualization of replication intermediates by electron microscopy (EM) in yeast showed regressed replication forks only in checkpoint-defective mutants (rad53) after hydroxyurea (HU) treatment (126). HU is an inhibitor of ribonucleotide reductase that slows down replication by limiting dNTP pools. Rad53 is an effector kinase that is activated after DNA damage (127). The authors proposed therefore that Rad53 activity maintains the stability of stalled replication forks and prevents accumulation of pathological DNA rearrangements including regressed forks (126).

Nevertheless, enzymatic activities that could promote fork regression are reported for eukaryotes as well. Recently, a FA protein, FANCM, which functions as DNA translocase, has been shown to promote extensive fork regression of a plasmid-based fork structure with a short lagging-strand gap (128). In another study, the BLM DNA helicase has been shown to catalyze the regression of a plasmid-based model fork with a short leading-strand gap *in vitro* (129). Moreover, another human RecQ helicase, WRN, is capable to regress synthetic fork structures (130). In addition, human RECQ5 protein has been shown to promote efficiently strand-exchange reactions between homologous arms of oligonucleotide-based fork structures (131). Whether RECQ5 is able to carry out a regression reaction of a large M13-based model fork is analyzed in the first part of this thesis.

In yeast, there is evidence for a transient template-switching mechanism for error-free damage bypass following PCNA polyubiquitination (132,133). Rad5, a protein with DNA-dependent ATPase activity and a RING finger motif characteristic of ubiquitin ligase proteins (134), presumably mediates PCNA polyubiquitination. In biochemical experiments, Rad5 was

shown to be able to regress plasmid-based fork structures (135). Hence, Rad5 could directly act at stalled replication forks and promote template switching by fork regression. Two human orthologs of the yeast Rad5, SHPRH and HLTF, both involved in PCNA polyubiquitination have been described, suggesting the existence of this DNA damage bypass mechanism in human cells (136,137).

Finally, EM analysis of replication intermediates in yeast mutants challenged with irreparable UV lesions suggests repriming of DNA synthesis downstream of the lesions on both leading and lagging strands (138). After UV treatment of excision-repair defective mutants (rad14) uncoupling of leading- and lagging-strand synthesis was observed. Long ss gaps up to 3kb length at forks are seen. Furthermore, internal ssDNA gaps accumulate along replicated duplexes on both arms of the fork. Interestingly, defects in TLS (rev1 and rev3) and HR (rad52) did not affect fork progression over damaged template, but increased internal gap accumulation, suggesting repriming of DNA synthesis, post-replicative recombination-mediated repair and TLS that might take place behind the replication fork (138).

In conclusion, multiple reactivation pathways seem to operate also in eukaryotes. How stalled forks are directed to distinct repair/bypass pathways is unclear. However, failure to process stalled forks, which might lead to breakage, is an important source of genomic instability.

3.5 Helicases

3.5.1 Overview

Helicases are nucleic acid-dependent ATPases that are capable of unwinding DNA or RNA duplexes (139-141). As a consequence, they are involved in almost all biological processes where complementary nucleic acid strands have to be separated. More recently, it has become clear that several putative helicases do not unwind duplex DNA or RNA. Helicases therefore represent only a subgroup of motor proteins that all translocate directionally along ss or ds nucleic acids but do not necessarily have unwinding activity (142). Other transactions performed by these enzymes are displacement of proteins bound to DNA (chapter 3.5.3) or RNA and chromatin remodeling (143).

Helicases/translocases have been classified into six superfamilies (SFs) based on short conserved amino acid motifs (142). These helicase motifs include key residues of the functional translocase domain. SF1 and SF2 are related, are the largest SFs and contain at least seven conserved helicase motifs (1, 1a, 2-6) (144) (Fig. 6). Additional motifs have later been included for SF1 and SF2 helicases: TxGx (145), Q-motif (146), motif 4a (147), and TRG (148). SF1 and SF2 members function mainly as monomers or dimers (142). Well-characterized representatives of SF1 are the bacterial helicases Rep, PcrA, UvrD and the *S. cerevisiae* Srs2. Intensively studied members belonging to SF2 are, for example, the bacterial RecG and the RecQ family helicases. SF3-6 consist of helicases that form hexameric ring structures and share three to five superfamily-specific motifs (142). SF3 includes putative helicases found in the genome of small DNA and RNA viruses. SF4 consists of proteins that are related in sequence to the *E. coli* replicative helicase DnaB and SF5 is exemplified by the bacterial transciption termination factor Rho. Finally, SF6 consists of a subgroup of proteins belonging to the AAA^+ (ATPases Associated with various cellular Activites) family and includes the MCM proteins and RuvB.

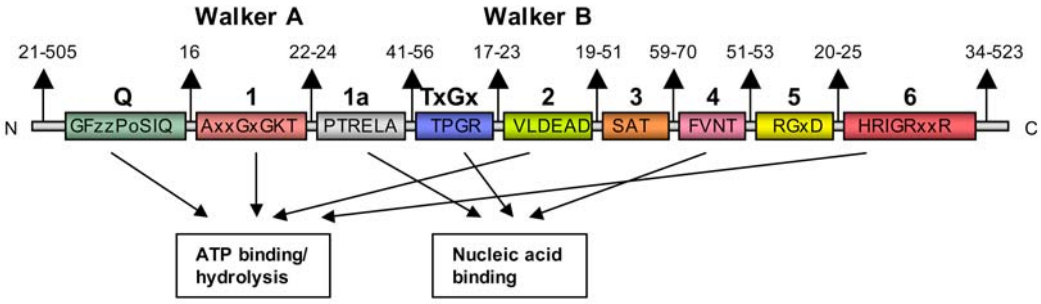

Figure 6
Schematic diagram representing organization and involvement in the catalytic functions of conserved motifs of DEAD-box helicases (Superfamily 2). Open boxes represent the conserved helicase motifs. The consensus amino-acid (aa) sequence of each motif is shown by the single-letter code inside the boxes (z = D, E, H, K, R; o = S, T; x = any aa). Motifs are labeled above the boxes according to new nomenclature (142). Numbers above the arrows are typical ranges of aa residues found between the motifs. Adapted form (141).

3.5.2 Mechanism of DNA unwinding

DNA helicases convert the chemical energy from ATP hydrolysis into mechanical energy to translocate along ssDNA with either 3'→5' or 5'→3' polarity and unwind duplex DNA in the process. A monomeric enzyme is thought to contain at least two DNA-binding sites: the leading (L) site binds to ssDNA or ss/dsDNA and the trailing (T) site binds only ssDNA. Coupled to ATP binding and hydrolysis, the enzyme changes its conformation from a compact form to an extended form. In the process, the L and T sites sequentially alter DNA-binding affinity from weak to tight which results in a directional inchworm-like movement (149) (Fig. 7). The DNA strand separation can then proceed *via* an active or a passive mechanism. In the passive mechanism, the helicase does not make contacts with the duplex. Instead, it operates by trapping ssDNA at a thermally fraying ss-dsDNA junction. In the active mechanism, the helicase interacts directly with dsDNA and destabilizes the duplex. For PcrA, such a dsDNA contact is described. Residues located outside of the helicase core mediate this contact. This causes double helix distortion and is therefore proposed to facilitate strand separation (150).

From crystal structures of diverse enzymes, it turns out that the minimal structural unit of a translocase, also called core domain, folds into neighboring RecA-like domains either within the same polypeptide chain or between subunits (140,142). In the cleft between two RecA-like domains the ATP binding and hydrolysis takes place. The conserved helicase motifs are located on the surface of the cleft. For SF1 and SF2 enzymes, motifs 1 and 2 are equivalent to the Walker A and B motifs found in ATPases, respectively (151) (Fig. 6). Motif 1 has a consensus sequence GK(T/S). The lysine residue in motif 1 interacts with the phosphates of ATP/ADP and the hydroxyl of the threonine or serine residue ligates the Mg^{2+} ion. Motif 2 takes the general form of DExx across SF1 and SF2. Subgroups of SF2 are classified according to the DExx motif into DEAD-, DExD- or DExH-box families (141). The carboxyl of the aspartate residue in Motif 2 coordinates the Mg^{2+} ion of MgATP/MgADP, whereas the glutamic acid residue is suggested to act as a catalytic base in ATP hydrolysis. Another universal feature of the RecA-like ATPase core is an "arginine (R) finger" that plays a key role in energy

coupling (142). Both, SF1 and SF2 members have an R in the middle of motif 6. In the structure of PcrA complexed with an ATP analog, the guanidinium group of the corresponding R forms a salt bridge with the γ phosphate of ATP (151). Other contacts with ATP are mediated by motif Q containing an invariant glutamine within an amino acid stretch upstream of motif I. Motifs 1a, TxGx and 4 are suggested to be involved in ssDNA binding (140).

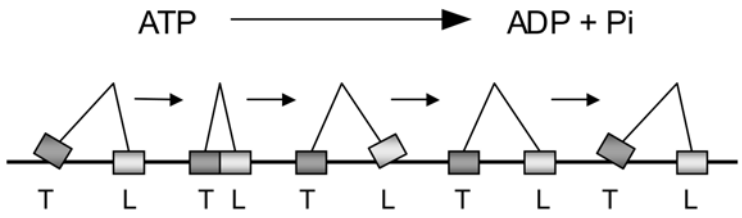

Figure 7
Cartoon of inchworm-like movement of helicases/translocases along DNA. A monomeric enzyme is represented with two DNA-binding sites, a leading (L) site and a trailing (T) site. The enzyme changes its conformation coupled to ATP binding and hydrolysis from compact to extended. In the process altering weak and tight DNA binding of the L and T site results in unidirectional translocation along DNA.

Crystal structures of helicases in complex with DNA substrate and ATP hydrolysis intermediates provide insight into the molecular mechanism of DNA unwinding. Such structures are, for example, available for PcrA and UvrD (152,153). Both enzymes are organized into four domains. Domains 1A and 2A form the RecA-like ATPase core. Crystal structures of UvrD showed that one UvrD molecule is associated with the ss-ds junction of the DNA substrate, which is held in a L-shaped conformation (153) (Fig. 8). The 3'-ssDNA tail binds across the surface of the two RecA-like domains 1A and 2A. Domains 1B and 2B contact the duplex DNA without disturbing the regular B form helix. Upon ATP binding (AMPPNP) the cleft between 1A and 2A is closed (Fig. 8). In addition, domains 2A and 1A/1B/2B with bound DNA duplex are rotated towards each other by 20°. This conformational change of the protein is suggested to be the first part of the ATPase-driven power stroke that leads to separation of the first base pair at the ss-ds DNA junction. Note that the now unpaired base (-1) of the ssDNA tail bound by UvrD is bulged out (Fig. 8 B). The second part of the power stroke, which is coupled to the release of ADP

and Pi after ATP hydrolysis, mediates domain opening and allows translocation of the ssDNA across domains 1A and 2A. This study led to the proposal of a combined wrench-and-inchworm mechanism for DNA unwinding by UvrD at the step size of 1bp per ATP hydrolyzed (153).

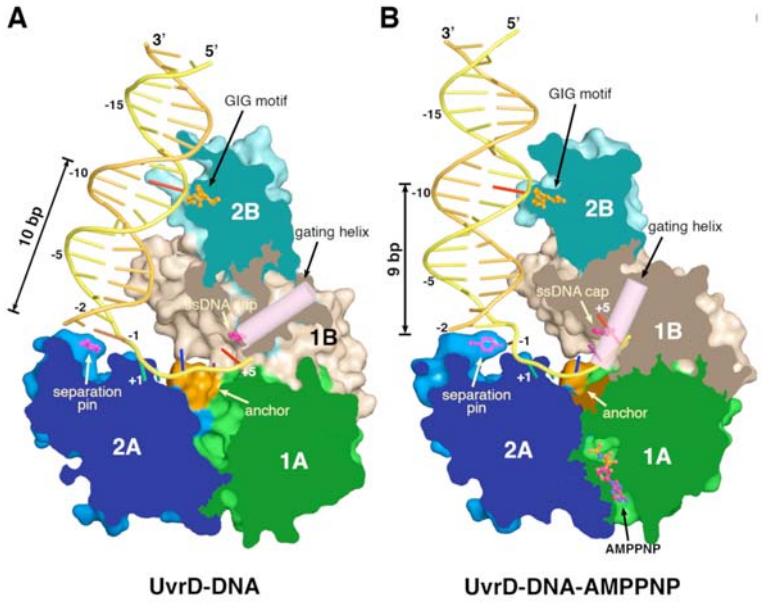

Figure 8
Crystal structures of UvrD complexed with partially ss-ds synthetic DNA. UvrD contains domains 1A (green), 1B (beige), 2A (blue), 2B (cyan). 1A and 2A form the RecA-like ATPase core. UvrD is shown in molecular surface with the front of molecule removed to expose the bound DNA (yellow) **(A)** Binary complex of UvrD and DNA. **(B)** Ternary complex of UvrD-DNA and the ATP analog AMPPNP. Functionally important regions are highlighted. Anchor (orange) is referred to residues in helicase motif 3 that function as an "anchor" for ssDNA during transition from binary to ternary complex. GIG-motif (orange), gating helix (pink), and separation pin (pink), are sequence motifs conserved among UvrD homologs including yeast Srs2. Adapted from (153).

3.5.3 Function in protein-DNA complex disruption

Translocases that move along DNA or RNA are likely to encounter proteins that are bound to nucleic acid. Moreover, some enzymes containing helicase motifs function directly in removing proteins from nucleic acid during various biological processes. For example, progression of replication through chromosomal sites bound by non-histone protein complexes is facilitated by accessory helicases to the replication machinery. These helicases belong to the Pif1-like subfamily and are highly conserved among eukaryotes (154). The best-characterized representative is the *S. cerevisiae* Rrm3. Rrm3 is a 5'→3'

DNA helicase of the SF1 (155). *RRM3* is not an essential gene, but in its absence, replication forks pause at over 1000 discrete sites, including rDNA genes, tRNA genes, centromers, inactive replication origins, telomers and subtelomeric regions (155-157). At rDNA pausing sites, it has been shown that in the absence of functional Rrm3 both fork breakage and recombination are increased suggesting that blocked replication forks collapse (156,158). The second Pif1-like helicase of *S. cerevisiae*, Pif1, has been shown to function at telomeres. Pif1 is a negative regulator of telomerase, the reverse transcriptase that maintains telomeric DNA (159) and was shown to displace active telomerase from DNA ends (160).

Another biological process where protein-DNA complex disruption has a relevant role is HR. Some helicases act as anti-recombinases by disrupting recombinase-nucleoprotein filaments and are thought to prevent thereby inappropriate HR events. Helicases with anti-recombinase function are found from bacteria to man. The *E. coli* UvrD helicase dismantles RecA nucleoprotein filaments and inhibits RecA-mediated strand-exchange reaction *in vitro* (161). In addition, genetic evidence suggests that UvrD acts at blocked replication forks and removes either RecA directely from ssDNA or RecA-promoted structures (114). The *E. coli* replication mutants (dnaE, dnaN) require UvrD for viability. The lethality of those double mutants (dnaE or dnaN and uvrD) can be suppressed by inactivation of recombination proteins (recA, recJ, recFOR, or recQ) (114).

The *S. cerevisiae* Srs2 protein is a 3'→5' DNA helicase (162) structurally and functionally related to UvrD (153,161). Accordingly, srs2 mutants show a hyper-recombination phenotype (163) that can be suppressed by mutations that prevent formation of the Rad51 nucleoprotein filament (58,164). By biochemical studies, Srs2 was demonstrated to act as translocase that disassembles Rad51 nucleoprotein filaments (165,166).

Regulation of HR at an early step by antagonizing RAD51 filament formation is expected to take place in higher eukaryotes as well. However, sequence homologs of *SRS2* are not clearly apparent in the genome of higher eukaryotes. It is therefore expected that alternative helicases carry out presynaptic filament disruption in a way like Srs2. In humans, the F-box DNA helicase 1 (hFBH1) was identified to possess sequence similarities to the

helicase domains of Srs2 and UvrD (167). Furthermore, hFBH1 is able to rescue some recombination defects in yeast srs2 mutants (167). In a screen for functional equivalent of the yeast Srs2 in *C. elegans*, the helicase RTEL-1 was found (168). Purified human RTEL1 was shown to disrupt D-loops, but not RAD51 filaments (168). In contrast, two RecQ family helicases, BLM and RECQ5, were recently demonstrated to be able to displace RAD51 from ssDNA, in the same manner like Srs2 (169,170). The second part of my thesis addresses the mechanism underlying the RECQ5-mediated displacement of RAD51 from ssDNA.

3.5.4 RecQ family of DNA helicases

RecQ DNA helicases belong to SF2. The first RecQ family member was discovered in *E. coli* in a screen for mutations that confer resistance to thymine starvation (171). Most unicellular organisms express only one RecQ family member, whereas higher eukaryotes typically express multiple RecQ proteins. Humans possess five family members, namely RECQ1, BLM, WRN, RECQ4 and RECQ5 (Fig. 9). A feature that makes RecQ proteins of particular interest is their implication in human diseases. Germ line mutations in three of the five human RecQ family genes (*BLM, WRN, RECQ4*) give rise to genetic disorders associated with cancer predisposition, premature aging and/or developmental abnormalities (172,173). RecQ helicases play a crucial role in maintenance of genome stability through their involvement in DNA recombination, replication, and repair (174-177).

RecQ family proteins share a region of primary sequence similarity of approximately 400 aa in which the seven classical helicase motifs (144) and a Q-motif (called O-motif) are located (178). The crystal structure of the catalytic core fragment of *E. coli* RecQ (RecQΔC) shows that the helicase domain consists of two typical RecA-like modules (179) (Fig. 9 domains colored magenta and blue). Unique to RecQ helicases is the so-called RecQ C-terminal (RecQ-Ct) domain that follows the helicase domain in the majority of RecQ family members (180). The RecQ-Ct domain consists of two subdomains: a zinc-binding motif (Fig. 9 yellow) and a helix-turn-helix motif, called winged-helix (WH) domain (Fig. 9 green) (179). The zinc-binding motif has been shown to be important for protein stability and the helicase activity

of the enzyme (181-183). The WH domain is predicted to be important for dsDNA binding (179). However, WH domain is dispensable for unwinding activity, as exemplified by RECQ5β (here RECQ5), which lacks this domain and is active as DNA helicase (184). Some RecQ family members contain another structural domain capable of DNA binding, the helicase and RNaseD C-terminal (HRDC) domain (Fig. 9 beige) (180,185,186). Variations in DNA-binding residues of the HRDC domain are thought to confer DNA substrate specificity among RecQ proteins (185,187). Eukaryotic RecQ family members possess additional domains flanking the RecQ homology regions that show little or no sequence homology (Fig. 9 grey). These domains have been shown to mediate interactions with other proteins or possess additional enzymatic activities (e.g. N-terminus of WRN protein contains an exonuclease domain) (174).

Biochemical studies have shown that RecQ family proteins are ATP-dependent helicases that separate duplex DNA with a 3'→5' polarity (175). The processivity of DNA unwinding by RecQ helicases is relatively low in the absence of accessory factors such as ssDNA binding proteins. In contrast, the same enzymes are capable of migrating HJs over several kb of DNA. Additionally, it has been shown that many RecQ helicases exhibit an intrinsic DNA strand-annealing activity (184,188-192). A common property of RecQ proteins is their ability to bind and unwind DNA structures other than standard B-form DNA duplex. Preferred substrates are branched DNA structures, including forked structures, four-way DNA junctions, D-loops and G-quadruplex DNA (175). This implicates that RecQ helicases function in cellular processes where such DNA structures arise that is DNA replication and recombination.

3.5.4.1 *E. coli* RecQ

Compared to other RecQ family members, the *E. coli* RecQ helicase shows a much wider substrate specificity *in vitro*. Apart from unwinding duplex DNA with a 3'-ssDNA tail, different fork structures, HJs, G-quadruplex DNA and D-loops, *E. coli* RecQ is also able to separate duplex DNA with a 5'-ssDNA tail and blunt-ended duplex DNA (193-196).

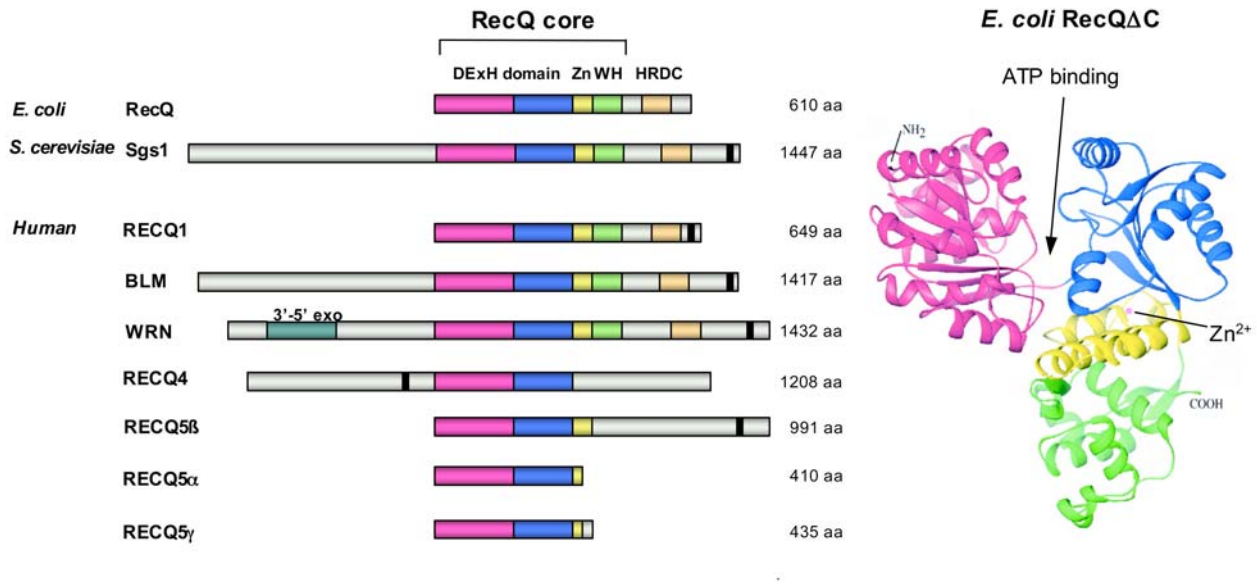

Figure 9
Selected members of the RecQ familiy of DNA helicases. Regions corresponding to the helicase domain (DExH domain), zinc-binding motif (Zn), and winged-helix domain (WH) are indicated and collored accordingly to the domains in the cartoon of crystal structure of *E. coli* RecQΔC (178), shown on the right. In addition, the helicase and RNaseD C-terminal domain (HRDC) as well as the location of the putative nuclear localization signals (black line) (193) are indicated.

RecQ is suggested to have multiple biological functions in the bacterial cell. Controversially, some of them may lead to opposing effects. For example, RecQ functions in the initiation of HR, but can also suppress illegitimate recombination. RecQ is a member of the RecF recombination pathway, which includes RecA, RecF, RecG, RecJ, RecO, RecR and RuvABC, and mediates recombination on DNA substrates that lack a DSB, including gaps and nicks. RecQ is proposed to act at the initiation phase of this HR pathway by generating ssDNA for assembly of the RecA filament. RecQ helicase is capable to initiate RecA-catalyzed homologous pairing and strand-exchange reactions from duplex DNA substrates *in vitro* (195). *In vivo*, it appears likely that RecQ in conjunction with RecJ degrades the nascent lagging strand at stalled replication forks (105) allowing either fast repair (104) or induction of DNA damage signaling, called SOS response (196). The ssDNA generated by RecQ/RecJ at the fork serves as substrate for RecA filament formation that is, besides catalyzing strand exchange, required for SOS response *via* proteolysis of the transcription repressor LexA and

consequent induction of several stress genes (196). In a recent study, RecQ was demonstrated to promote the formation of HR intermediates *in vivo* (198). Cells defective for HJ resolution (ruv) and anti-recombinase (uvrD) accumulated toxic recombination intermediates and displayed failed chromosome segregation. Viability of these ruvB uvrD double mutants could be restored by inactivation of recQ, recF or recA (198). On the other hand, RecQ was reported to act as an anti-recombinase. RecQ is capable to disrupt recombination intermediates, including D-loops *in vitro* (195) and suppresses illegitimate recombination between DNA sequences with limited homology (199).

E. coli RecQ cooperates with the topoisomerase III (Top3). This functional coupling seems conserved among several RecQ family proteins and the RecQ-Top3 pairs appear to conduct an important role in maintaining genome stability. *E. coli* RecQ stimulates strand-passage activity of Top3 *in vitro* (200). If *E. coli* RecQ-Top3 functions in a similar way as human BLM-TOPOIIIα, which mediate double Holliday junction (DHJ) dissolution, is not yet clear. A recent study also suggested that the RecQ-Top3 complex could be involved in resolution of converging replication forks (201).

3.5.4.2 *S. cerevisiae* Sgs1

Slow growth suppressor 1 (Sgs1) is the sole RecQ helicase in budding yeast. Biochemical analysis has been carried out with a N- and C-terminally truncated protein designated Sgs1$^{400\text{-}1268}$. The enzymatic properties of this recombinant protein are similar to those of the other RecQ helicases. Sgs1$^{400\text{-}1268}$ can unwind, in an ATP-dependent manner, duplex DNA with a 3'-ssDNA tail, three- and four-way DNA structures and G-quadruplex DNA. In addition, it is able to disrupt RNA/DNA duplexes (202-205).

Sgs1 expression is cell cycle regulated. It is very low in the M and G1 phase, peaks in S phase and decreases again in G2 (206). Sgs1Δ strains are sensitive to UV light, methylmethane sulfonate (MMS) and HU and display intra- and inter-chromosome hyper-recombination, as well as an elevated frequency of SCEs (174).

Sgs1 appears to play multiple roles in DNA metabolism. Its function is coupled to all three topoisomerases (Top1, Top2, Top3) expressed in *S. cerevisiae.* A genetic interaction between Sgs1 and Top1 was reported (207). Sgs1 was further identified in a search for Top2 interaction partners (208) and mutation in the *SGS1* gene was found to suppress the top3 slow-growth phenotype (209). Sgs1 forms a complex with Top3 (210) and Rmi1/Nce4 protein (211,212) that has been proposed to process HJs in the same manner as the human BLM-TOPOIIIα complex to suppress crossover during DSB repair (213). Consistent with the proposed DHJ dissolution activity of Sgs1-Top3, sgs1 mutants accumulate Rad51-dependent recombination intermediates during a perturbed S phase (214). Further evidence that Sgs1 has a role in removing HR intermediates is demonstrated by the synthetic lethality of sgs1 srs2 double mutants that is suppressed by mutation in Rad51 (58). As mentioned above, Srs2 is suggested to act as anti-recombinase through disrupting other HR intermediates, namely Rad51 presynaptinc filaments (chapter 3.5.3) or eventually channeling HR into the SDSA pathway (56).

Furthermore, Sgs1 is implicated to act at stalled replication forks. Sgs1 is required for the stabilization of the replisome in HU treated cells. In its absence, Pol α and Pol ε fail to remain associated with the fork and, as a consequence, the reestablishment of replication is impaired (215,216). Further evidence that Sgs1 could modulate the replisome function comes from analysis of DNA replication in sgs1 mutant cells. Surprisingly, in the absence of Sgs1, fork progression was faster as measured by DNA combing (217). However, in absence of Sgs1, completion of DNA replication was strongly retarded at the rDNA array, presumably because recombination takes place at naturally pausing sites when replisome is not stabilized (217).

Sgs1 plays a role in S phase checkpoint that monitors DNA integrity. In HU treated cells, activation of the effector kinase Rad53 depends on Sgs1 in addition to a parallel signaling pathway *via* Rad17/Rad24 (206). Hence, rad24 sgs1 double mutants have a severely compromised intra S phase checkpoint and fail to suppress late-origin firing in the presence of DNA damage (206). In addition a synthetic lethality is observed in the double mutants mus81 sgs1

and mms4 sgs1 (218), suggesting a bypass pathway *via* the nuclease complex Mus81-Mms4 in the absence of Sgs1-Top3. (219).

3.5.4.3 Human RECQ1

Of the five human RecQ helicases RECQ1 (also RECQL or helicase Q1) is the smallest. Purified RECQ1 is a 3'→5' helicase of rather low processivity. On its own it is capable to unwind only short M13 partial duplex DNA of less than 30bp (220). However, addition of human RPA stimulates its unwinding activity specifically allowing duplex-substrate separation of more than 500bp in length (221). Further biochemical analysis demonstrated that RECQ1 could unwind a wide variety of DNA structures, including fork structures, HJs, and D-loops (191). As the other human RecQ proteins, RECQ1 can catalyze annealing of short complementary DNA strands in a reaction that is modulated by ATP binding (191). The balance between the two opposing functions, DNA unwinding and annealing, is proposed to be linked to the oligomeric state of RECQ1 (222). In the absence of ATP, RECQ1 is assembled into ring-like oligomeric structures of five or six subunits and capable to promote strand annealing. Addition of ATP or ATPγS results in the disruption of higher oligomeric structures and allows strand-separation reaction by dimeric or monomeric RECQ1 (222).

The cellular function of RECQ1 is not yet clear. RECQ1 is the most abundant RecQ helicase in human cells (223), but mutations in RECQ1 are not linked to a human disease condition. Recent data indicate a potential role of RECQ1 in genome maintenance. *Recq1*-knockout mice do not show particular abnormalities, but cells from these mice showed an elevated frequency of chromosomal instability (193). Furthermore, RECQ1 was shown to interact with mismatch repair factors MSH2-MSH6 and exonuclease 1 (224) and identified as the major HJ processing enzyme in HEK293 cell nuclear extract (225).

3.5.4.4 Human BLM

The Bloom syndrome helicase (BLM) is one of the most intense studied human RecQ family member. Loss of BLM function causes a rare autosomal

recessive disorder called Bloom's syndrome (BS). The BS phenotype is multifaceted and is generally associated with death before the age of 30 (172). Affected individuals show growth retardation, impaired fertility, immune deficiency and a dramatic predisposition to development of most cancer types (173,174). Genomic instability is proposed to drive tumorigenesis in BS (173). Cells from BS patients show DNA gaps, breaks and structurally rearranged chromosomes at an elevated frequency. However, the hallmark feature of BS cells, which is used in diagnosis in humans, is the approximately 10-fold increase in the frequency of SCEs (174). In addition, BS cells are reported to be sensitive to DNA damaging agents such as UV light and HU, but not to γ-irradiation (174). A viable mouse model for BS has been established (226). BLM-deficient mice are cancer prone; cell lines from these mice display an elevated rate of mitotic recombination and a high frequency of somatic loss of heterozygosity (147), which helps to explain how BLM could suppress tumorigenesis (226).

Purified human BLM was demonstrated to form hexameric and tetrameric ring structures in solution (227), which is mediated by the N-terminal part of the protein that is not important for the helicase activity of the enzyme (228). A BLM core fragment (aa 642-1290) that lacks this domain exists as a monomer and exhibits similar DNA unwinding activity as full-size BLM (229). *In vitro*, BLM helicase alone is capable to unwind DNA duplexes up to 70bp in length, but can be stimulated to unwind up to 300bp by association with RPA (230). Like other RecQ helicases, BLM is active on aberrant DNA molecules (231), catalyzing efficiently disruption of D-loops (14,232), G-quadruplex DNA (205,233), HJ-branch migration (234) and is able to promote the regression of a model replication fork (129). Besides unwinding activity, BLM also displays a ssDNA annealing activity *in vitro* (188,190).

BLM is expressed in all tissues where cell proliferation takes place. The BLM protein level is very low in G1 and peaks in S/G2 phase of the cell cycle (174). BLM is generally found in PML nuclear bodies, large nuclear structures that are defined by the presence of the promyelocytic leukemia (PML) protein. The function of those PML nuclear bodies is not yet clear and they are proposed to represent a protein storage depot (235). Exposure of cells to

DNA damaging agents or replication inhibitors causes relocalization of BLM to sites of ongoing DNA repair (236,237). Under such conditions, BLM co-localizes with several other proteins that are required for DNA repair, including RPA, RAD51, BRCA1, and the MRN complex. BLM is found in multi-protein complexes in the cell and makes numerous contacts with other DNA repair or DNA damage signaling proteins (172,174). A selection of those proteins is shown in Figure 10.

BLM is recruited to sites of stalled replication forks in cells treated with HU (238). Analysis of chromosome fibers revealed that BLM-defective cells are compromised in replication-fork restart after HU and aphidicolin treatment as well as in suppression of new origin firing (239). Recent findings suggested mechanisms for how BLM could suppress excessive mitotic HR and thereby counteract genome instability. BLM was shown to be very efficient in displacing the invading strand of mobile D-loop structures *in vitro* (232). However, when RAD51 was bound to D-loop substrates, BLM was only capable of disrupting those structures after inactivation of the RAD51 filament by removal of Ca^{2+} ions (170). In addition, it was demonstrated that BLM is able to displace human RAD51, but not yeast Rad51, from ssDNA, thus BLM may inhibit the initial strand invasion step of HR (170). Furthermore, BLM in complex with TOPOIIIα and BLAP75/RMI1 is proposed to act late in HR pathway by processing of DHJs (240,241). In biochemical experiments, BLM-TOPOIIIα was demonstrated to resolve DHJs exclusively into non-crossover products (52). The catalysis of this reaction is highly specific for BLM (187,240) and may explain how loss of BLM function leads to increased

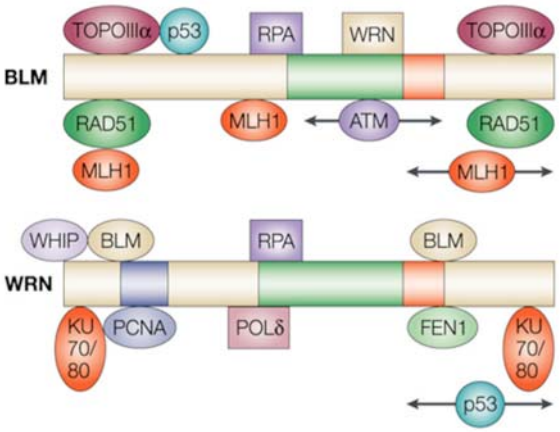

Figure 10

Selected protein partners of BLM and WRN. The helicase, RecQ-Ct and exonulease domains are shown as green, orange and blue boxes, respectively. All proteins indicated interact with BLM and/or WRN. Horizontal arrows indicate approximately limits of binding domains for proteins whose interaction sites have been mapped less accurately. Adapted from (172).

frequency of SCEs in BS patients. Recently, it has been shown that BLM-TOPOIIIα and BLAP75/RMI1 are localized to ultrafine anaphase bridges, suggesting a role for BLM in decatenation of chromatid disjunctions during anaphase (242).

3.5.4.5 Human WRN

The Werner syndrome helicase (WRN) is another RecQ member implicated in human disease. Germ line mutation in *WRN* gene gives rise to Werner's syndrome (WS), an autosomal recessive disorder associated with multiple progeroid pathologies and a greatly increased cancer incidence (173). Individuals with WS are phenotypically normal until puberty, at which time they fail to show the usual growth spurt. Consequently, affected individuals are of short stature and start to develop a battery of symptoms that are normally seen only in the elderly people, including skin changes, hair loss, osteoporosis, cataracts and arteriosclerosis (174). Death usually occurs before the age of 50 due to vascular diseases or cancer, with a high rate of mesenchymal malignancies being observed (172).

WRN is unique among all RecQ proteins in having an N-terminal exonuclease domain whose structure has been recently determined (243). Biochemical analysis showed that WRN possesses both 3'→5' exonuclease activity (244,245) and ATP-dependent 3'→5' helicase activity (246,247). WRN nuclease functions on a variety of DNA substrates, including DNA bubbles, stem-loops, forks and HJs, as well as on RNA-DNA duplexes (248). WRN helicase shows low processivity. On its own, it can unwind DNA duplexes up to about 70bp in length, but in the presence of RPA it can catalyze unwinding of longer duplex DNA substrates up to 849bp (249). Preferred substrates for WRN helicase are DNA bubble structures, forked DNA and G-quadruplex DNA (231). WRN is capable of promoting branch migration of HJs (250), displays fork-regression activity (130) and ssDNA annealing activity (188).

Expression of WRN is cell cycle regulated, being the highest in G2/M phase (174). Cells from WS patients show an increased frequency of chromosomal rearrangements, including translocations, inversions, and manly extensive deletions, but no elevated frequency of SCEs (174). Furthermore,

WS cells show a reduced ability to proliferate, which may be one of the underlying reasons for premature aging observed in WS patients (173).

A role for WRN in DNA replication has been proposed. WRN was reported to interact with proteins required for DNA replication, such as RPA, PCNA, FEN1 and Pol δ (Fig. 10) (172,174). *In vitro*, WRN was shown to assist DNA Pol δ to catalyze DNA synthesis through G-quadruplex structures (251). Cells lacking WRN helicase were reported to be defective in lagging-strand synthesis of the G-rich template strand of telomeres (252). It appears that WRN plays an important role in the maintenance of telomere structure. WS cells with compromised DNA damage response rapidly accumulate chromosome fusions that can be rescued by either expression of WRN or telomerase (253). Evidence for the function of WRN in telomere metabolism comes also from the mouse model for WS. The WS phenotype in *Wrn*$^{-/-}$ mice only manifests when the mice also lack telomerase (254).

There are further potential roles for WRN. For example, WRN may be involved in NHEJ through its direct contact with Ku70/80 (174). It can also participate in BER *via* interaction with Pol β (255). It also interacts physically and functionally with the MMR factors MutSα, MutSβ, and MutLα, suggesting a role in rejection of recombination between divergent sequences (256). A role in HR is possible since abnormal recombination intermediates accumulate in WS cells that can be resolved by expression of the bacterial HJ resolvase RusA (257,258).

3.5.4.6 Human RECQ4

There are three autosomal recessive disorders associated with mutations in the *RECQ4 (also RECQL4)* gene: Rothmund-Thomson syndrome (RTS), RAPADILINO syndrome and Baller-Gerold syndrome (BGS) (173,259). The three syndromes are rare and phenotypically complex showing some overlapping symptoms such as short stature and skeletal abnormalities. Poikiloderma is characteristic for RTS and BGS whereas joint dislocation is mainly seen in RAPADILINO syndrome. RTS patients display premature aging symptoms and a predisposition to malignant tumors, particularly osteosarcomas.

RECQ4 protein lacks the RecQ-Ct domain. Accordingly, RECQ4 does not show conventional DNA helicase activity although it is proficient in promoting ATP hydrolysis in the presence of ssDNA (189). It also possesses a strong ssDNA annealing activity residing in the N-terminal part of the protein (189,192). Interestingly, a recent study demonstrated that in the presence of excess complementary ssDNA, RECQ4 can mediate DNA duplex unwinding in a manner dependent on ATP. The authors suggested that under classical helicase conditions, the strong intrinsic DNA annealing activity of RECQ4 might mask its unwinding activity (192). Paradoxically, RECQ4 Walker A and Walker B mutants were still able catalyzing DNA duplex unwinding. An additional helicase activity that resides in the N-terminal RECQ4 domain may explain this finding (192).

Cells derived from RTS patients show genomic instability, including aneuploidy (e.g. trisomy 8) and chromosomal rearrangements (173). How RECQ4 prevents genomic instability as well as the molecular pathways in which it might be involved remain poorly understood. A potential role in the initiation of DNA replication has been suggested by recent studies using *Xenopus laevis* egg extracts. It has been shown that immunodepletion of xRTS protein results in a reduction and delay in sperm chromatin replication, an effect that can be rescued by complementing the extracts with recombinant human RECQ4 (260). In addition, the following interaction partners of RECQ4 were reported: RAD51 (261); UBR1/2 ubiquitin ligases (262); and poly(ADP-ribose)polymerase 1 (263).

3.5.4.7 Human RECQ5

The human RECQ5 protein exists in at least three different isoforms, RECQ5α, RECQ5β (here RECQ5), and RECQ5γ, resulting from alternative splicing of the RECQ5 transcript (Fig. 9) (264,265). The two short isoforms, RECQ5α and RECQ5γ lack the zinc-binding motif, and in a recent biochemical analysis RECQ5α failed to exhibit DNA-dependent ATPase and helicase activity (183). In agreement with these results, the zinc-binding motif has been shown to be important for DNA binding, ATPase and helicase activities of the *E. coli* RecQ (181) and human BLM (182). The largest isoform

RECQ5 contains the zinc-binding motif and exhibits ATP-dependent 3'→5' helicase activity (184). Like other RecQ helicases, RECQ5 is a helicase with a low processivity that is stimulated in its unwinding capacity by RPA and possesses an intrinsic ssDNA annealing activity (184). RECQ5 functions probably as a monomer and acts on forked substrates and HJs (131,184).

RECQ5 gene is expressed throughout the cell cycle in normal human fibroblast cell lines (223). In contrast to the other human RecQ members, RECQ5 protein is also expressed in resting G0 cells (223). Only the large isoform, RECQ5, harboring a potential nuclear localization signal in its C-terminal domain, is found in the nucleus (131,265). RECQ5α and RECQ5γ were found in the cytoplasm if expressed as fusions with GFP (265). At present, no human disease has been linked to mutation in the *RECQ5* gene. *Recq5*-knockout mice have been generated (266). These mice do not show particular abnormalities, but they are prone to cancer development (169,266). Cells from these mice exhibit an increased frequency of RAD51 foci and gross chromosomal rearrangements after camptothecin treatment, but an increase in the frequency of LOH was not obvious (169). Moreover, *Recq5*$^{-/-}$ mouse embryonic stem (ES) cells showed a mild slow growth phenotype and a significantly higher frequency of SCEs compared to wild-type cells, a phenotype similar to *Blm*$^{-/-}$ cells (266). Interestingly, the rate of SCEs in the *Recq5 Blm* double-knockout cells was even higher than that in either single mutant, suggesting that RECQ5 and BLM operate in different pathways to suppress mitotic recombination (266). In chicken DT40 cells, *Recq5* deletion did neither manifest in slow growth phenotype nor in an increase in the frequency of SCEs (267). But again, the rate of SCEs in *Recq5*$^{-/-}$ *Blm*$^{-/-}$ double mutant DT40 cells was much higher than that in *Blm*$^{-/-}$ cells (267).

RECQ5 interacts with RAD51 *in vivo* and *in vitro* and can disrupt RAD51 presynaptic filaments in a reaction dependent on ATP hydrolysis and the presence of RPA, suggesting a mechanism for how RECQ5 regulates HR (169). There is also evidence that RECQ5 assists during DNA replication. RECQ5 associates with the replication machinery and accumulates at sites of stalled replication forks and DSBs (131,268). RECQ5 is linked to sites of DNA damage *via* its interaction with the MRN complex (268). Other protein

interactions with potential biological relevance were reported for RECQ5: for example, interaction with TOPOIIIα and β (265), and with the RNA Pol II complex (269,270). In Figure 11, selected interaction partners of RECQ5 identified in our laboratory and the cellular processes in which they are involved are shown.

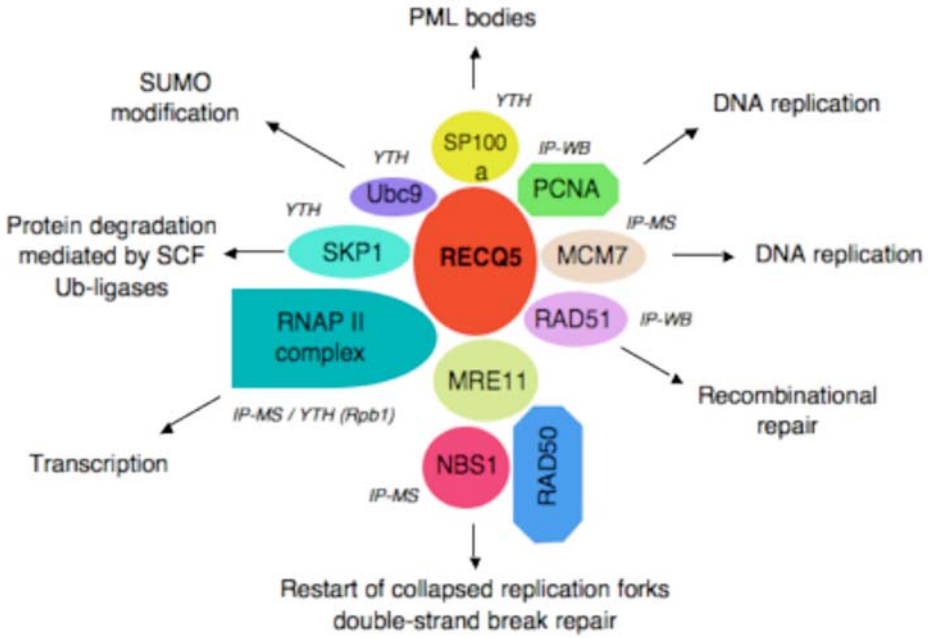

Figure 11
Selected interaction partners of RECQ5. Methods used to identify protein-protein interactions are given as following abbreviations: IP-MS/WB, Analysis of RECQ5 immunoprecipitate from 293T cell extracts by mass spectrometry/Western blot; YTH, yeast two hybrid assay.

4 AIM OF MY STUDIES

RecQ DNA helicases are involved in processing of complex DNA structures arising during DNA metabolism and prevent excessive mitotic recombination that can destabilize the genome. Like other RecQ family members, the human RECQ5 protein is proposed to act during DNA replication and repair. However, its exact role in these processes has not yet been clearly defined. The main objectives of my PhD project are:

(i) to characterize the activity of RECQ5 on DNA structures that resemble stalled replication forks and

(ii) to elucidate the mechanism underlying RECQ5-mediated disruption of RAD51 nucleoprotein filaments that initiate homologous DNA recombination.

In the first study, we further characterized the strand-exchange activity of RECQ5 observed with oligonucleotide-based forked DNA structures. We tested if RECQ5 can promote regression of a M13-based model DNA that mimics a stalled replication fork with a leading-strand gap. In the second study, we asked whether physical interaction between RECQ5 and RAD51 is required for RECQ5-mediated displacement of RAD51 from ssDNA. To address this issue, we mapped precisely the RAD51-interaction domain on RECQ5 and tested RECQ5 mutants that fail to interact with RAD51 in a topoisomerase-linked RAD51-trap assay for the ability to disrupt RAD51 filaments.

5 RESULTS

5.1 Characterization of fork-regression activity of RECQ5

The human RECQ5 protein has been shown to possess three distinct biochemical activities: a 3'→5' DNA unwinding activity, a ssDNA annealing activity and a Holliday junction (HJ) branch migration activity (184). It is not yet clear whether all three activities are relevant or even coordinated for RECQ5 function. A DNA transaction that could be promoted by the three mentioned catalytic activities is replication-fork regression. In this process the arms of the replication fork are unwound, the parental strands are repaired and the nascent strands are annealed to form a HJ-like structure that can be stabilized by branch migration. Recently, RECQ5 has been shown to promote strand exchange between homologous arms of a synthetic forked DNA structure (131). The DNA substrate used in this study was assembled from oligonucleotides and had arms with length of 30nt. Furthermore, in the same study it was demonstrated that RECQ5 preferentially unwinds the lagging-strand arm of a synthetic forked DNA structure with non-complementary arms. In contrast, BLM and WRN unwind preferentially the parental duplex. In addition, RECQ5 was suggested to be present at replication forks through physical interaction with proteins of the DNA replication machinery, like PCNA (131) and MCM proteins (unpublished data). These findings let us to test the hypothesis that RECQ5 promotes replication-fork regression, hence could act in the recovery of damaged replication forks. For testing the fork-regression activity of RECQ5, we used a large M13-based forked DNA structure that allows trapping intermediates of the fork-regression reaction containing HJ.

5.1.1 DNA structures for fork-regression assay

For testing fork-regression activity of RECQ5, we used a modified version of a biochemical assay previously established for testing fork-regression activity of the bacterial proteins RecA and RecG (111,116). The DNA structures used in this assay mimic a stalled replication fork with a ssDNA gap (of 2.1kb or 0.2kb) on the leading-strand arm. These branched DNA structures consisted of a gapped duplex (gd) DNA circle and a homologous DNA arm ligated to the

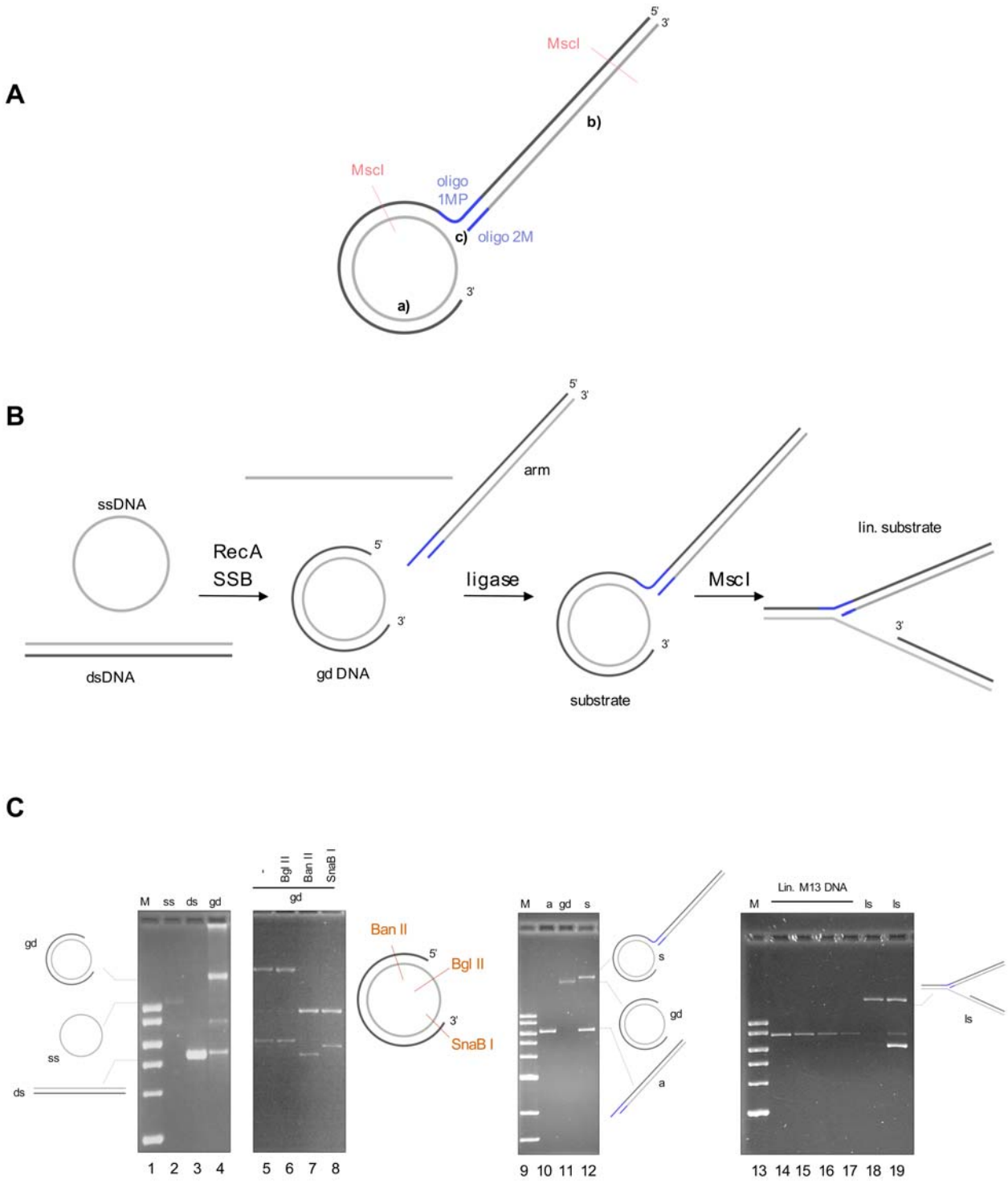

Figure 12
Preparation of DNA substrate for fork-regression assay. (A) The structure of the DNA substrate used for testing fork-regression activity of RECQ5. The structure mimics a stalled replication fork with a leading-strand gap: the arm fragment represents the lagging-strand arm; the parental duplex and the leading-strand arm are linked. The indicated MscI sites are the cleavage sites used to generate a linear fork structure. The components used to construct this structure are: (a) gd DNA (7.3kb circle with a 2.1kb or 0.2kb ssDNA gap); (b) homologous dsDNA arm (7.3kb), and (c) a linker DNA (annealed oligo1MP (49-mer) and oligo 2M (30-mer)). **(B)** Schematic illustration of the preparation of DNA substrate. **(C)** DNA species from

individual steps of substrate preparation resolved by agarose gel electrophoresis. Lanes 1-4: gd DNA was prepared by a RecA-mediated strand-exchange reaction between circular M13mp8.32 ssDNA and a defined homologous linear dsDNA fragment (shown here for M13mp8.32 5.2kb-[BsrGI-EcoRI] fragment). Lanes 5-8: The structure of the gd DNA was verified by restriction analysis. The recognition sites of the used enzymes are indicated in the scheme on the right. Lanes 9-12: The branched DNA substrate was assembled from the purified gd DNA and the homologous arm fragment (M13mp8.32 7.3kb-[SapI-SmaI]) using the linker DNA described above. Lane 13-19: MscI-linearized substrate before and after gel purification (lanes 19 and 18, respectively) and known amount of linearized M13mp8.32 dsDNA used to estimate branched substrate concentration (lanes 14-17). M, 1kb DNA ladder (New England Biolabs); gd, gapped duplex DNA; ss, circular single-stranded DNA; ds, linear dsDNA fragment; a, homologous arm fragment already ligated with the linker DNA; s, circular branched DNA substrate; ls, MscI-linearized substrate; Lin. M13 DNA, linearized M13mp8.32 dsDNA.

free 5'-end of gd DNA through a synthetic linker (Fig. 12 A) (116). The gd DNA was generated by a RecA-mediated strand-exchange reaction between circular M13mp8.32 ssDNA and a defined dsDNA fragment generated by restriction-enzyme digestion of the ds form of M13mp8.32 DNA (Fig. 12 B and C lanes 2-4). The structure of the gd DNA was verified by restriction analysis (Fig. 12 C lanes 5-8). The homologous linear arm fragment was also prepared from M13mp8.32 DNA by restriction-enzyme digestion. It was ligated to purified gd DNA in two successive reactions. Firstly, we ligated a synthetic linker that consisted of two annealed oligonucleotides to the linear arm fragment. Secondly, the purified linker-arm fragment could be annealed and ligated with the gd DNA *via* a 16-nt overhang of the linker DNA that was complementary to the 5'-proximal end of the gd DNA (Fig. 12 B and C lanes 10-12). The linker DNA contained six heterologous bases with respect to the M13mp8.32 sequence at the positions 1,2,3,6,9 and 12 from the fork junction to prevent spontaneous branch migration. The DNA structure for fork-regression assay was usually linearized by MscI and purified by agarose gel electrophoresis followed by electroelution (Fig. 12 B and C lanes 18 and 19).

5.1.2 Analysis of fork-regression activity of RECQ5

The fork-regression reaction with the above-described branched DNA structure is shown in Figure 13 A. On such structures, fork regression includes unwinding of the lagging-strand arm, migration of the branch point towards the 3'-end of the ssDNA gap, annealing of the liberated strands to form a HJ-like structure and finally migration of this four-way DNA junction

unidirectionally to complete strand exchange. For the circular branched structure, the ssDNA region is transferred to the end of the dsDNA arm (Fig. 13 A). For the linearized structure, the fork-regression end-products are two linear DNA fragments (Fig. 13 A).

To test fork-regression activity of RECQ5, we first used linearized DNA structures containing a 2.1kb or a 0.2kb leading-strand gap. In addition to wild-type RECQ5, an ATPase-defective RECQ5K58R mutant and the bacterial helicase RecG were used in these assays as negative and positive controls, respectively. The fork-regression products were analyzed by agarose gel electrophoresis and Southern blotting using ^{32}P-labeled probes complementary to the DNA region indicated in red (Fig. 13 B). RecG has been described to promote efficiently regression of such a forked DNA structure *in vitro* (111). In our assay, RecG converted both DNA substrates into the expected linear 7.3kb products (Fig. 13 B lanes 6 and 13). With RECQ5, we could observe complete disappearance of the substrate in the presence of ATP (Fig. 13 B lanes 2 and 9), but not in the presence of the poorly hydrolysable ATP analog ATPγS (lanes 3 and 10) or in a reaction without nucleotide co-factor (lanes 4 and 11). These findings indicated that RECQ5 processed the DNA substrates in a helicase-dependent manner, which was further confirmed using the ATPase-defective RECQ5K58R mutant that showed no activity in the assay (Fig. 13 B lanes 5 and 12). In contrast to the RecG-promoted reactions, a clear increase in the linear 7.3kb product was not observed with RECQ5 (Fig. 13 B compare lanes 2 to 6 and 9 to 13) indicating that RECQ5 may not promote the regression reaction unidirectionally for more than 6kb, which is required to generate the linear end products.

5.1.3 Restriction analysis of the fork-regression products

Next, we employed restriction enzymes to be able to monitor the formation of early regression intermediates. We used three different restriction enzymes, namely HindIII, PvuI and BglII, having recognition sites in the lagging-strand arm of the forked DNA substrate (Fig. 14 A). These sites are transferred into the parental arm by fork regression. Therefore, digestion of fork-regression intermediates with these enzymes will give rise to defined linear duplex fragments if the fork junction has moved beyond the site of cleavage.

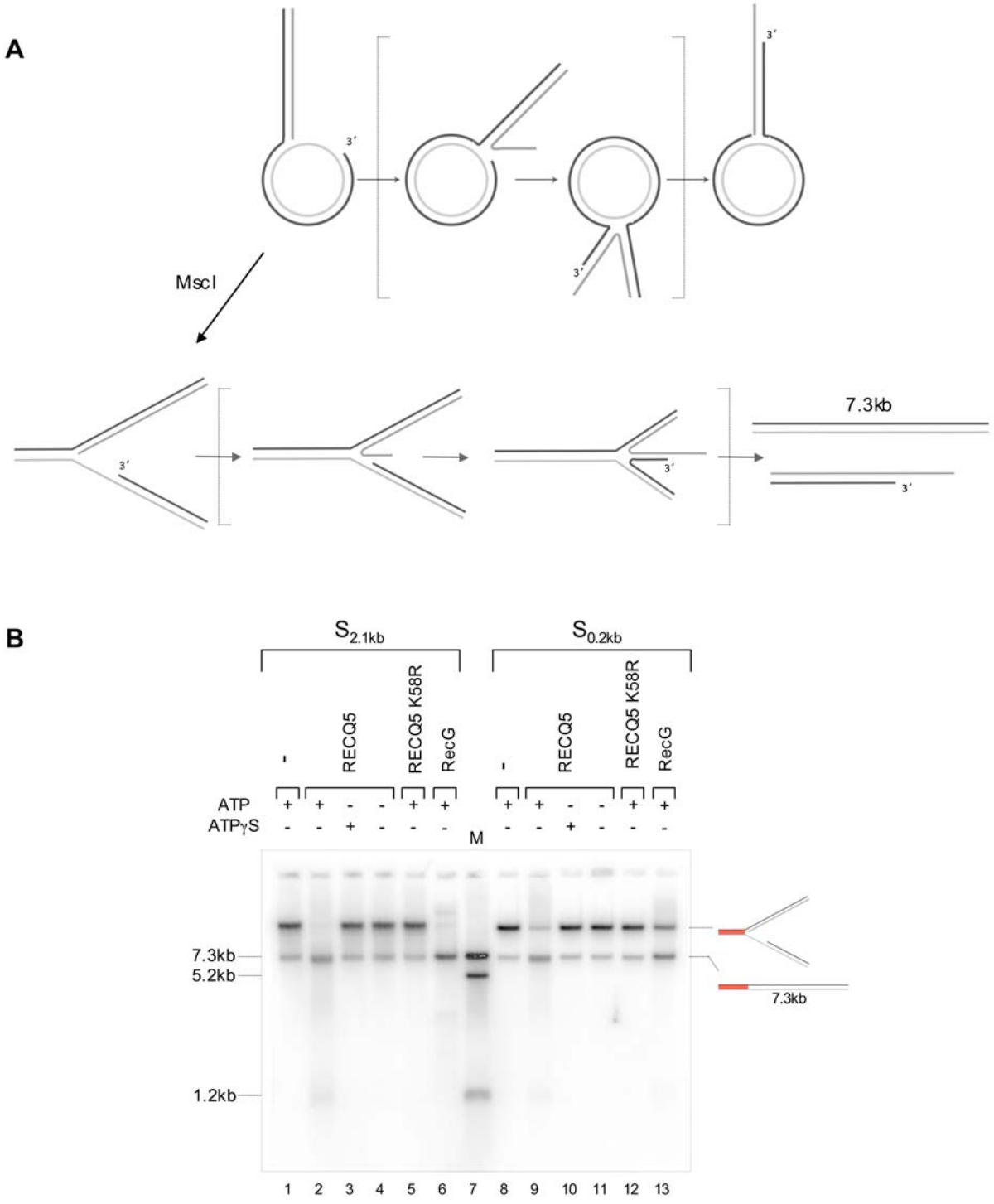

Figure 13
Fork-regression activity of RECQ5. (A) Schematic of fork-regression reaction with circular or MscI-linearized fork structure containing a leading-strand gap. See text for explanations. **(B)** Processing of forked DNA structures with a 2.1kb or a 0.2kb leading-strand gap by RECQ5 depends on ATP hydrolysis. About 10 pM linearized DNA substrate was incubated with 100 nM RECQ5, 100 nM RECQ5 K58R or 40 nM RecG as indicated in the presence or absence of 2 mM nucleotide co-factor ATP or ATPγS for 30 min at 37°C in 1 x NEB4 buffer supplemented with 50 μg/ml BSA. The reaction products were deproteinized, separated by 0.7% agarose gel electrophoresis and transferred to a Zeta-Probe membrane by Southern

blotting. DNA was visualized by autoradiography using ^{32}P-labeled probes specific for a 1.2kb region of the DNA molecule indicated in red. M, M13mp8.32 linear duplex DNA of 7.3kb, 5.2kb and 1.2kb lengths; $S_{2.1kb}$ and $S_{0.2kb}$, substrate with 2.1kb and 0.2kb leading-stand gap, respectively.

Appearance of HindIII, PvuI and BglII linear duplex fragments indicates that the fork junction has regressed more than 40bp, 170bp or 700bp, respectively. When RECQ5 was incubated with the forked substrate containing a 2.1kb leading-strand gap, followed by restriction-enzyme digestion, we could detect all three linear fragments both in the absence and the presence of RPA (Fig. 14 lanes 5,6,9,10,13,14). This indicates that RECQ5 could promote fork regression through a region of at least 0.7kb. As judged from the intensity of the linear fragments, RPA appeared to slightly stimulate the regression reaction (Fig. 14, compare lanes 6,10 and 14 to lanes 5, 9 and 13).

Next, we investigated if RECQ5 could promote the regression of the forked substrate to form a four-way DNA junction. To detect the presence of the regressed arm, reaction products were digested with the restriction endonuclease AclI (Fig. 14 C). The AclI-dependent release of a characteristic regressed arm fragment and a 1.7kb duplex fragment could be detected for both RECQ5 and RecG in reactions with the forked substrate containing a 0.2kb strand gap (Fig. 14 Di lanes 4,5). Formation of the AclI restriction fragments was dependent on RECQ5 protein concentration (Fig. 14 Dii). Again, RPA appeared to slightly stimulate the reaction judged by the intensity of the 1.7kb fragment that represents the re-annealed parental strands (Fig. 14 Dii, compare 1.7kb bands in lanes 4-8 to lanes 10-14). However, RPA seemed to interfere with annealing of the liberated nascent strands since the intensity of the regressed arm fragment was weaker in reactions where RPA was included (Fig. 14 Dii, compare regressed arm fragment to 1.7kb band in lanes 4-8 to lanes 10-14).

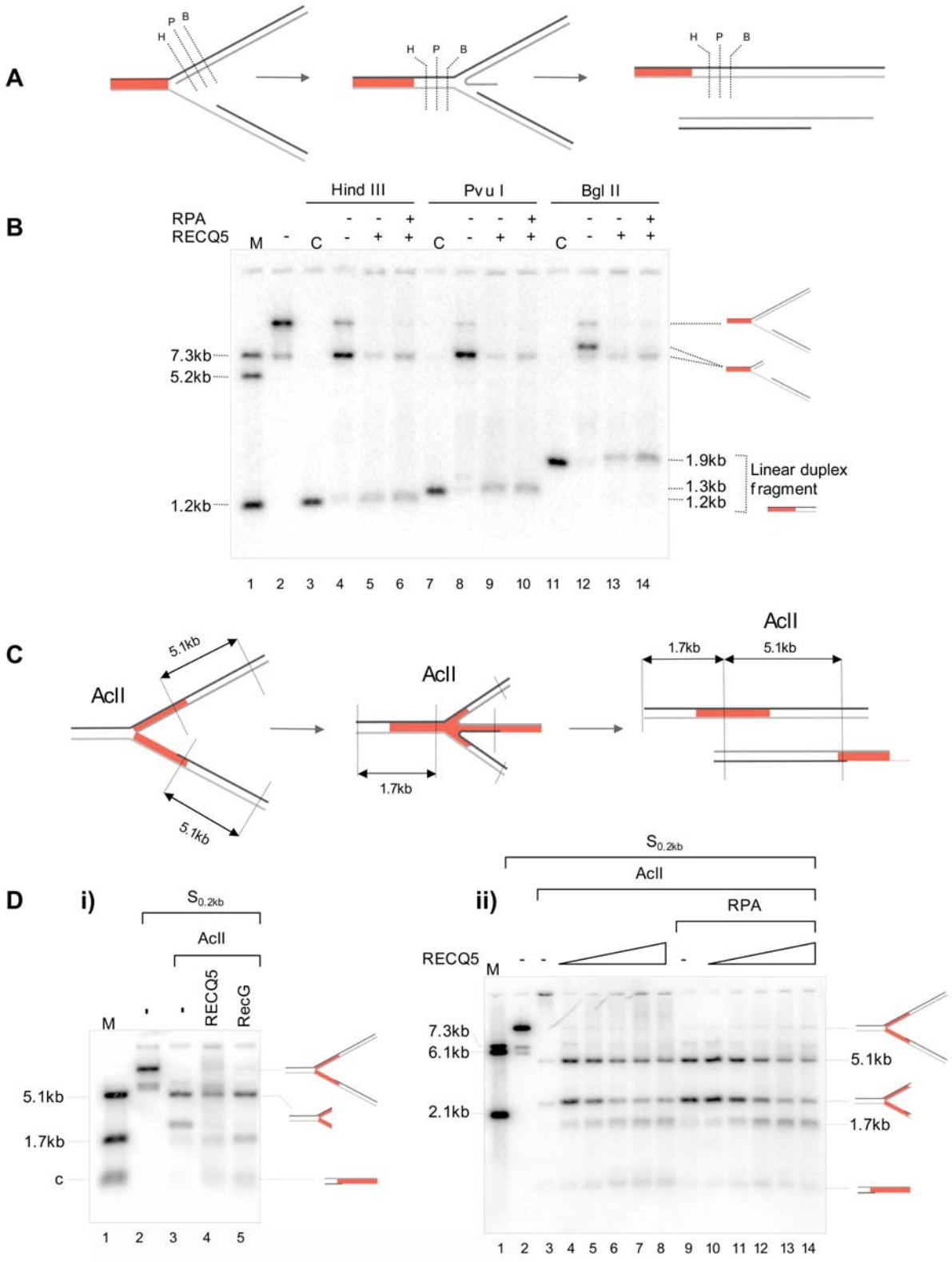

Figure 14

Restriction analysis of fork-regression products of RECQ5. (A) Schematic of the fork-regression reaction with the forked structure containing a 2.1kb leading-strand gap. HindIII, PvuI and BglII recognition sites are indicated on the substrate, early regression intermediate and end product. H, HindIII; P, PvuI; B, BglII. **(B)** RECQ5 promotes fork regression through a long leading-strand gap. The Southern blot shows DNA products after fork-regression assay

and restriction-endonuclease cleavage. About 10 pM of the linearized substrate containing a 2.1kb leading-strand gap was incubated with 40 nM RECQ5 and 40 nM RPA as indicated at 37°C in 1 x NEB4 buffer supplemented with 2 mM ATP and 50 μg/ml BSA for 1h, followed by a further 2h incubation with the restriction enzymes: HindIII (10 U), PvuI (3.5 U), BglII (7 U). Reaction products were analyzed as described in Figure legend 13 B. The 1.2kb DNA region recognized by the ^{32}P-labeled probes is indicated in red. M, M13mp8.32 linear duplex DNA of 7.3kb, 5.2kb and 1.2kb lengths; C, control linear duplex fragments of 1.9kb, 1.3kb or 1.2kb lengths. **(C)** Schematic of fork-regression reaction with indicated AclI sites on substrate, four-way DNA intermediate and end products. **(D)** RECQ5 promotes regression of forked DNA structure to generate a four-way junction. Fork-regression assays were carried out with a linearized substrate containing a 0.2kb leading-strand gap. **i)** About 10 pM substrate DNA was incubated with 100 nM RECQ5 or 40 nM RecG as indicated for 30 min at 37°C, followed by an additional 30 min incubation with 1.5 U of AclI. **ii)** About 10 pM substrate DNA was incubated with RECQ5 (10, 20, 40, 80, 160 nM) with or without 20 nM RPA as indicated for 1 h at 37°C, followed by an additional 1 h incubation with 3 U of AclI. The reaction products were analyzed as described above and DNA detected by ^{32}P-labeled probes specific for a 2.1kb region of the structure indicated in red. M, M13mp8.32 linear duplex DNA of 7.3kb, 6.1kb, 5.1kb, 2.1kb and 1.7kb lengths and a control DNA c for regressed arm fragment composed of a duplex part and a long 5'-ssDNA overhang generated by cleavage of gapped duplex DNA with EcoRI and AclI; $S_{0.2kb}$ linearized substrate containing a 0.2kb leading-stand gap. Note a loading error in lane 3 of Dii).

5.1.4 Monitoring fork regression by RusA cleavage

In order to confirm that RECQ5 converts the forked substrate into a four-way DNA structure, we included the bacterial HJ-specific resolvase RusA in our assay. RusA binds to HJs and introduces two symmetrically orientated nicks at the junction (271,272). We first established RusA cleavage under RECQ5 reaction conditions. The RusA protein was produced in bacteria, purified to homogeneity and tested for its activity on a plasmid-sized DNA containing a mobile HJ. This DNA was generated *in vivo* using the *E. coli* strain RM40 transformed with the plasmid pSD115 containing two *cer* sites in direct orientation (273). Induction of XerC recombinase in this system leads to intra-molecular recombination of the *cer* sites and results in a HJ-containing plasmid with two supercoiled domains resembling a figure 8. The plasmid DNA isolated from induced RM40 cells consisted of a mixture of pSD115 DNA in recombined, non-recombined and resolved conformations (Fig. 15 A). By EcoRI cleavage, HJ-containing pSD115 DNA was converted into an α-structure and this DNA molecule was purified (Fig. 15 A lane 2) and used to test RusA resolution activity. RusA resolved pSD115 α-structure into a 2.35kb nicked circle and a 2.6kb linear fragment or a 4.95kb linear fragment depending on which pair of strands was cleaved (Fig. 15 B and C lane 2). Addition of ATP, ATPγS or ssDNA oligonucleotide in large excess did not

affect significantly RusA resolution reaction (Fig. 15 C lanes 3-6). Furthermore, we could show that RusA can cleave HJs in the presence of RECQ5. RusA cleavage products were also formed after a 15 min pre-incubation of α-structure with RECQ5 (Fig. 15 C lanes 8 and 9).

Finally, we used RusA in our fork-regression assay to monitor the formation of four-way regression-intermediates of the circular substrate containing a 0.2kb leading-strand gap. RusA resolution of the regressed intermediates by cleavage in orientation a gives rise to a nicked circle and a 7.3kb nicked linear fragment, whereas cleavage at orientation b produces a 14.6kb nicked linear fragment (Fig. 15 D). All expected RusA-cleavage products were observed with RecG-promoted fork regression (Fig. 15 E lane 9). However, we did not observe these products with RECQ5 (Fig. 15 E lanes 3-8). This result challenges the earlier finding that regressed arm fragments observed by restriction analysis are formed by RECQ5-promoted fork regression.

Figure 15
Monitoring fork regression by RusA cleavage. (A) Preparation of Holliday junction (HJ)-containing DNA. Plasmid DNA isolated from induced RM40/pSD115 cells was cleaved with EcoRI and subjected to electrophoresis in 0.9% agarose gel (lane 1). The isolated DNA is a mixture of the following species (scheme on the right): 4.95kb plasmid, HJ-containing 4.95kb plasmid formed in a XerC-promoted intra-molecular recombination reaction, and final Xer-recombination product: 2.6kb and 2.35kb plasmids. pSD115 α-structure (lane 2) was generated by EcoRI cleavage of one supercoiled domain of the HJ-containing plasmid and purified by agarose gel electrophoresis followed by electroelution. Lin, linear duplex DNA; α, pSD115 α-structure; χ, pSD115 χ-structure formed by breakage of the uncleaved domain of the α-structure. **(B)** Schematic illustration of RusA cleavage of the pSD115 α-structure. **(C)** RusA can cleave a HJ in the presence of RECQ5. RusA cleavage assay was carried out with about 20 pM pSD115 α-structure in 1 x NEB4 buffer supplemented with 50 μg/ml BSA at 37°C for 30 min. DNA was incubated with 10 nM RusA in the presence or absence of 2 mM ATP, 9 mM ATPγS and 100 ng ssDNA (oligo f-10-C) as indicated. Lanes 7-9: DNA was pre-incubated for 15 min with 50 nM RECQ5. Reaction products were deproteinized, separted by 0.9% agarose gel electrophoresis, blotted to membrane and detected by autoradiography with ^{32}P-labeled probes. For probe preparation the pSD115 0.95kb-[EcoRI-SalI] fragment was used. α, α-structure; nc, nicked circle. **(D)** Schematic diagram of RusA cleavage products arising during regression of a circular fork structure. **(E)** RECQ5 does not generate RusA cleavable fork-regression intermediates. About 10 pM circular substrate DNA containing a 0.2kb leading-strand gap was incubated with increasing concentration of RECQ5 (5, 10, 20, 40, 80, and 160 nM) or 40 nM RecG for 1 h at 37°C, followed by incubation with 5 nM RusA for 30 min in the presence of 100 ng ssDNA (oligo f-10-C) that served as a helicase trap. Reaction products were analyzed as described in Figure legend 13 B. For probe preparation the M13mp8.32 2.1kb-[EcoRI-BsrGI] fragment was used.

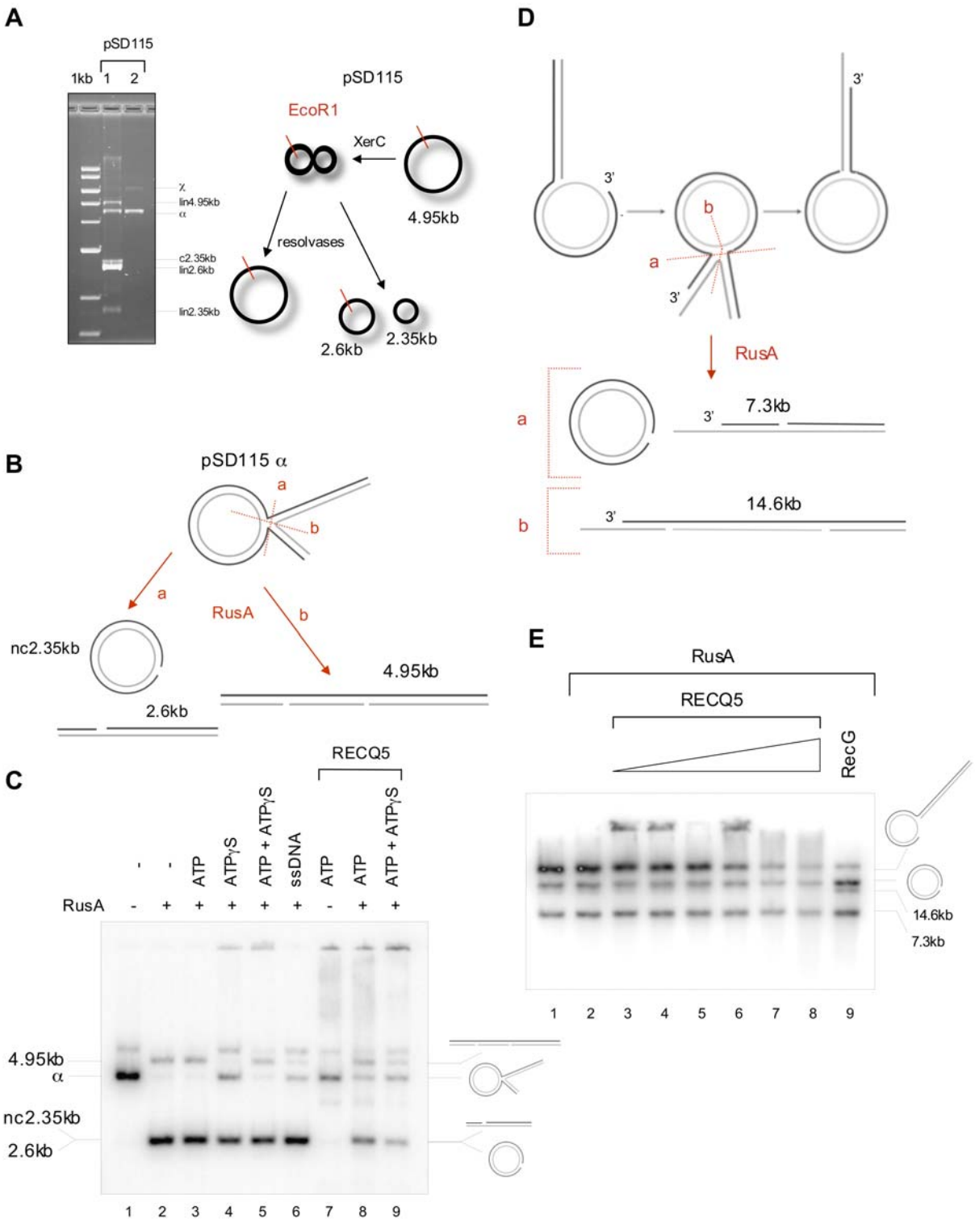
A
pSD115
1kb 1 2
χ
lin4.95kb
α
c2.35kb
lin2.6kb
lin2.35kb
pSD115
EcoR1
XerC
4.95kb
resolvases
2.6kb
2.35kb
B
pSD115 α
a
b
a
RusA
b
nc2.35kb
4.95kb
2.6kb
C
RECQ5
- - ATP ATPγS ATP + ATPγS ssDNA ATP ATP ATP + ATPγS
RusA - + + + + + - + +
4.95kb
α
nc2.35kb
2.6kb
1 2 3 4 5 6 7 8 9
D
3'
3'
b
a
3'
RusA
a
3'
7.3kb
b
3'
14.6kb
E
RusA
RECQ5
RecG
14.6kb
7.3kb
1 2 3 4 5 6 7 8 9

Figure 15

5.2 Analysis of the mechanism of RAD51 nucleoprotein-filament disruption by RECQ5

Homologous recombination (HR) is an important mechanism for repair of DNA double-strand breaks (DSBs) and restoration of productive DNA synthesis following disruption of replication forks (33). This process must be tightly regulated since inappropriate and untimely HR events can destabilize the genome (71). RecQ helicases have a function in preventing excessive mitotic recombination. Also, RECQ5 is suggested to be involved in suppressing HR. Mouse cells deficient in the RECQ5 homolog exhibit an elevated level of spontaneous sister chromatid exchanges (SCEs) (266). In a recent study, it has been shown that the frequency and lifespan of RAD51 foci are increased in *Recq5*$^{-/-}$ mouse embryonic fibroblasts (MEFs) relative to normal cells and the repair by HR of a defined DSB in a reporter gene is 3.5-fold higher in *Recq5*-deficient embryonic stem (ES) cells than in wild-type ES cells (169). In the same study, a physical interaction between the human RECQ5 protein and the RAD51 recombinase was demonstrated *in vitro* and *in vivo*. Furthermore, RECQ5 was found to inhibit RAD51-mediated D-loop formation through displacement of RAD51 from ssDNA in a biochemical assay with recombinant human proteins (169). Therefore, the authors suggested that RECQ5 could prevent inappropriate HR events *via* RAD51 presynaptic filament disruption.

To date, several helicases have been reported to remove proteins from ssDNA. It is not clear whether this activity is specific for a target DNA-binding protein or if it is rather a side action that results from unidirectional translocation of a DNA helicase on ssDNA. In this study, we analyzed the mechanism of RECQ5-mediated RAD51 filament disruption, the suggested RECQ5 function to negatively regulate early step of HR. Especially, we investigated whether the physical interaction between RECQ5 and RAD51 is required for this activity of RECQ5. To address this issue, we first mapped accurately the RAD51-interaction site on RECQ5. Secondly, using a topoisomerase-linked RAD51-trap assay, we tested RECQ5 mutants that fail to interact with RAD51 for the ability to disrupt stable RAD51 filaments formed on ssDNA by an ATPase-defective mutant of RAD51. In addition, to analyze

the contribution of direct RAD51 binding to RAD51 filament-dissociation activity of RECQ5, we tested a BLM-RECQ5 chimera composed of the translocase part of BLM and the RAD51-interaction domain of RECQ5 and compared this fusion protein with a helicase-competent fragment of BLM and wild-type RECQ5 in the RAD51 filament-dissociation assay.

5.2.1 Mapping of RAD51-interaction site on RECQ5

In order to define the RAD51-interaction site on RECQ5, we performed affinity pull-down assays. Several N- and C-terminal truncation variants of RECQ5 were constructed and expressed in bacteria as fusions with a chitin-binding domain (CBD) and bound to chitin beads (Fig. 16 A upper part). The beads were subsequently incubated with extract from 293T cells as source of RAD51 and RAD51 binding to beads was analyzed by Western blotting. The obtained data indicated that the RAD51-interaction domain of RECQ5 is located between amino acids (aa) 411-725 (Fig. 16 B). To map the location of this domain more precisely, we generated a series of internal deletions within the region of RECQ5 spanning aa 515-725 and tested the resulting mutants for the ability to bind to RAD51 in CBD pull-down assay (Fig. 16 A lower part). The obtained data indicated that the region spanning aa 515-653 is dispensable for RAD51 binding (Fig. 16 C lanes 4-7). In contrast, deletion of aa 652-674 as well as deletion of aa 652-725 of RECQ5 completely abolished its interaction with RAD51 (Fig. 16 C lanes 8 and 9). In addition, we found that a RECQ5 fragment containing aa 529-725 could bind RAD51 with affinity similar to that of full-length RECQ5 (Fig. 16 C compare lanes 3 and 10). Collectively, the above data suggest that RECQ5 contains a single RAD51-interaction domain that is located between aa 654-725.

In an attempt to identify amino-acid residues of RECQ5 that are critical for RAD51 binding, we generated single alanine substitutions at charged and aromatic residues within the region spanning aa 654-674 that was established to be required for RAD51 binding. The following residues of RECQ5 were mutated: R654, F659, F666 and E671. The mutant proteins were again

expressed in bacteria as fusions with CBD and tested for binding to RAD51

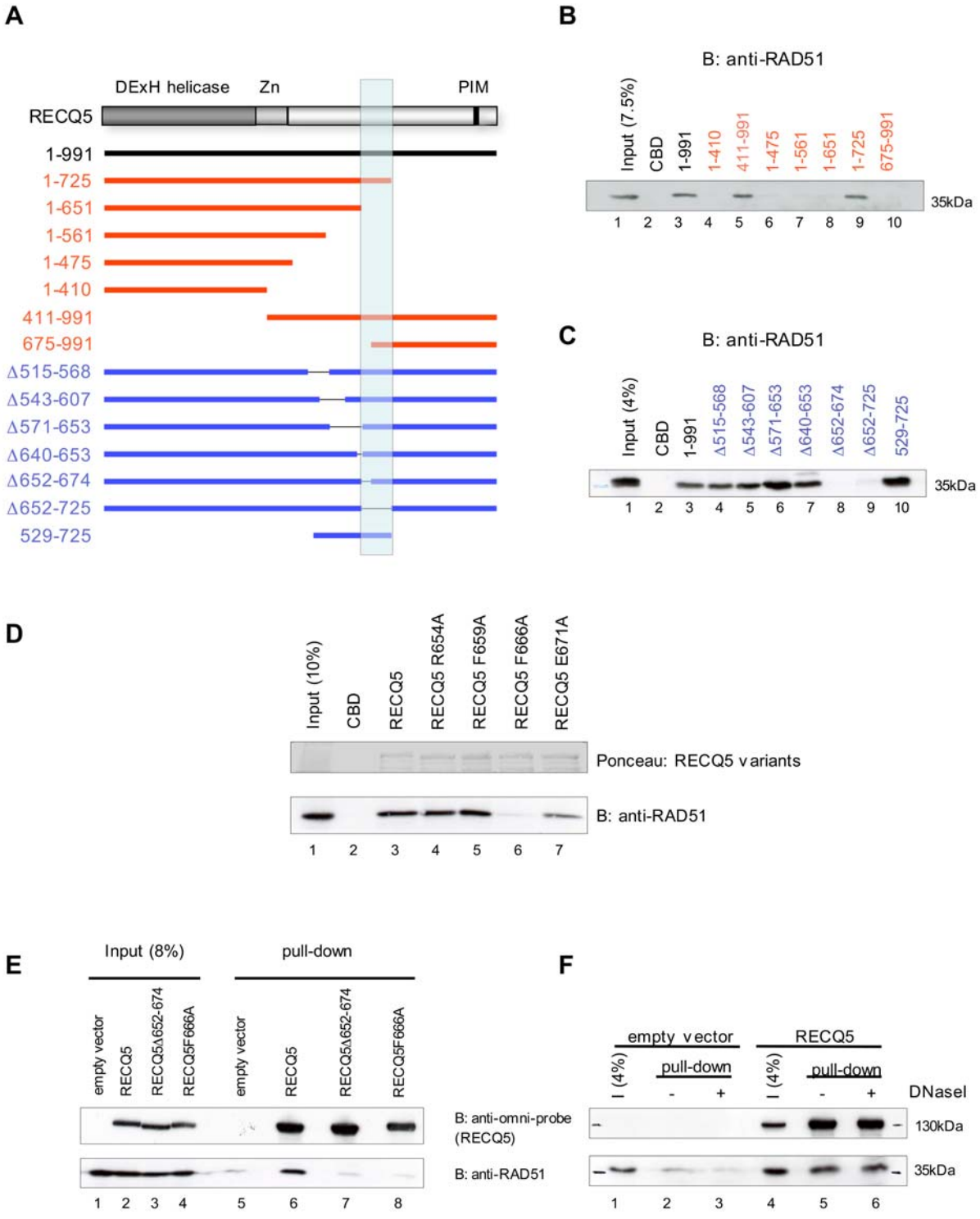

Figure 16
Mapping of RAD51-interaction site on RECQ5. (A) Scheme of RECQ5 variants used in the CBD pull-down assay. The domains of RECQ5 indicated are: DExH helicase domain; Zn, zinc-binding motif; and PIM, PCNA-binding motif. The red and blue thick lines represent the used RECQ5 fragments and the numbers indicate the amino-acid (aa) boundaries. The aa stretch 654-725 is highlighted with a blue box. Δ, deletion. **(B)** and **(C)**: RAD51-interaction site on RECQ5 is localized between aa 654-725. The indicated RECQ5-CBD fusion variants over-expressed in *E. coli* were bound to chitin beads, incubated with 293T cell extracts (B: 600 μg,

C: 800 μg) and bound RAD51 was analyzed by SDS-PAGE and Western blotting using anti-RAD51 antibody (BD Pharmingen). **(D)** Phenylalanine 666 is critical for RAD51 binding. CBD pull-down assay was performed with the indicated RECQ5 point mutants expressed in *E. coli* and 293T cell extract (1 mg) as a source for RAD51. The presence of RAD51 was detected by Western blot analysis using the anti-RAD51 antibody from BD Pharmingen (lower panel). The use of similar protein amounts of the different RECQ5 variants was verified by Ponceau staining (upper panel). **(E)** F666 of RECQ5 is required for RECQ5-RAD51 complex formation *in vivo*. A Nickel pull-down assay was performed with extracts (800 μg) from 293T cells transfected with the expression vector for RECQ5, RECQ5Δ652-674, RECQ5F666A, or the corresponding empty vector. The ectopically expressed RECQ5 variants harboring a C-terminal $(His)_6$-tag were immobilized on nickel beads and bound endogenous RAD51 was analyzed by SDS-PAGE and Western blotting using the anti-RAD51 antibody from BD Pharmingen (lower panel). Upper panel: membrane probed with anti-omni-probe antibody to visualize the $(His)_6$-tagged RECQ5 variants. **(F)** RECQ5-RAD51 interaction is not mediated *via* DNA. Nickel pull-down assay was performed with extract (800 μg) from 293T cells transfected with the vector for wild-type RECQ5 or the corresponding empty vector. Expression and pull-down of $(His)_6$-tagged RECQ5 was analyzed by SDS-PAGE and Western blotting using an anti-omni-probe antibody (upper panel). Co-precipitation of RAD51 was analyzed by an anti-RAD51 antibody (BD Pharmingen) (lower panel). Extracts pre-treated with DNaseI (20 U) are indicated. I, Input.

from 293T cell extract. The data showed that the R654A and F659A substitutions in RECQ5 had no effect on its binding affinity to RAD51, while the F666A substitution completely abolished RAD51 binding and the E671A substitution reduced it significantly (Fig. 16 D). These data establish that phenylalanine 666 of RECQ5 is essential for binding of RECQ5 to RAD51 (Fig. 16 D).

Next, we investigated whether mutational disruption of the RAD51-interaction domain of RECQ5 defined by the above *in vitro* binding experiments affects RECQ5-RAD51 complex formation *in vivo*. For this purpose, 293T cells were transiently transfected with expression vectors for RECQ5, RECQ5Δ652-674, or RECQ5F666A fused N-terminally to a $(His)_6$-tag. The ectopically expressed RECQ5 variants were bound to nickel beads *via* their N-terminal $(His)_6$-tag and analyzed for co-precipitation of endogenous RAD51 by Western blotting. We found that only wild-type RECQ5 could bind RAD51; the two RECQ5 mutants failed to interact with RAD51 (Fig. 16 E). Furthermore, we showed that RECQ5-RAD51 interaction is not mediated *via* ss or dsDNA. Treatment of 293T cell extracts with DNaseI or addition of ethidium bromide did not affect the binding of RAD51 to wild-type RECQ5 (Fig. 16 F and data not shown).

5.2.2 Establishment of RAD51 filament-dissociation assay

To test the RAD51 filament-dissociation activity of RECQ5 mutants that do not bind RAD51, we employed a topoisomerase-linked RAD51-trap assay. A similar assay was previously established to characterize the presynaptic filament-disruption function of Srs2 (165) and recently applied to show RAD51 filament-disruption function of RECQ5 (169). In this assay, RAD51 displaced from ssDNA is trapped by a plasmid DNA and monitored through topological changes in the plasmid DNA caused by RAD51 binding (Fig. 17 A). RAD51 forms also a helical nucleoprotein filament on dsDNA and forces dsDNA to adopt an extended conformation (65,66). Therefore, RAD51 binding to topologically relaxed covalently closed circular dsDNA results in the formation of positive supercoils that can be monitored by treatment with eukaryotic topoisomerase I (165). In our experiments, pre-assembled RAD51 filaments, on circular ssDNA were mixed with RECQ5 and RPA (Fig. 17 A). After a brief incubation, an unrelated relaxed plasmid DNA was added to the reaction to trap the RAD51 molecules displaced from ssDNA. Positive supercoils in plasmid DNA induced by RAD51 binding were fixed upon incubation with wheat germ topoisomerase I and resulted in negatively supercoiling after proteinase K treatment (Fig. 17 A). The different DNA species present in the reaction: ssDNA, dsDNA in relaxed and supercoiled conformation, were separated by electrophoresis in agarose gel and visualized by ethidium bromide staining (Fig. 17 B Lanes 1-4).

Initially, we used wild-type RAD51 in this assay. No spontaneous transfer of RAD51 from ssDNA to dsDNA was observed (Fig. 17 B lane 4). With RECQ5, we could see concentration-dependent formation of supercoiled dsDNA products (lanes 5 and 6). However, the same products were observed with the ATPase-defective mutant of RECQ5 (RECQ5K58R) (lanes 7 and 8), suggesting that RAD51 filament is not stable and can be disrupted by any ssDNA-binding protein. This was further confirmed by the finding that *E. coli* ssDNA binding protein (SSB) as well as the human RPA could disrupt RAD51 presynaptic filaments (data not shown). On the other hand, when the RAD51 filament on ssDNA was assembled in the presence of the poorly hydrolysable ATP analog ATPγS, it was stable and could not be disrupted by wild-type RECQ5 that still binds tightly to DNA under these conditions (data not shown).

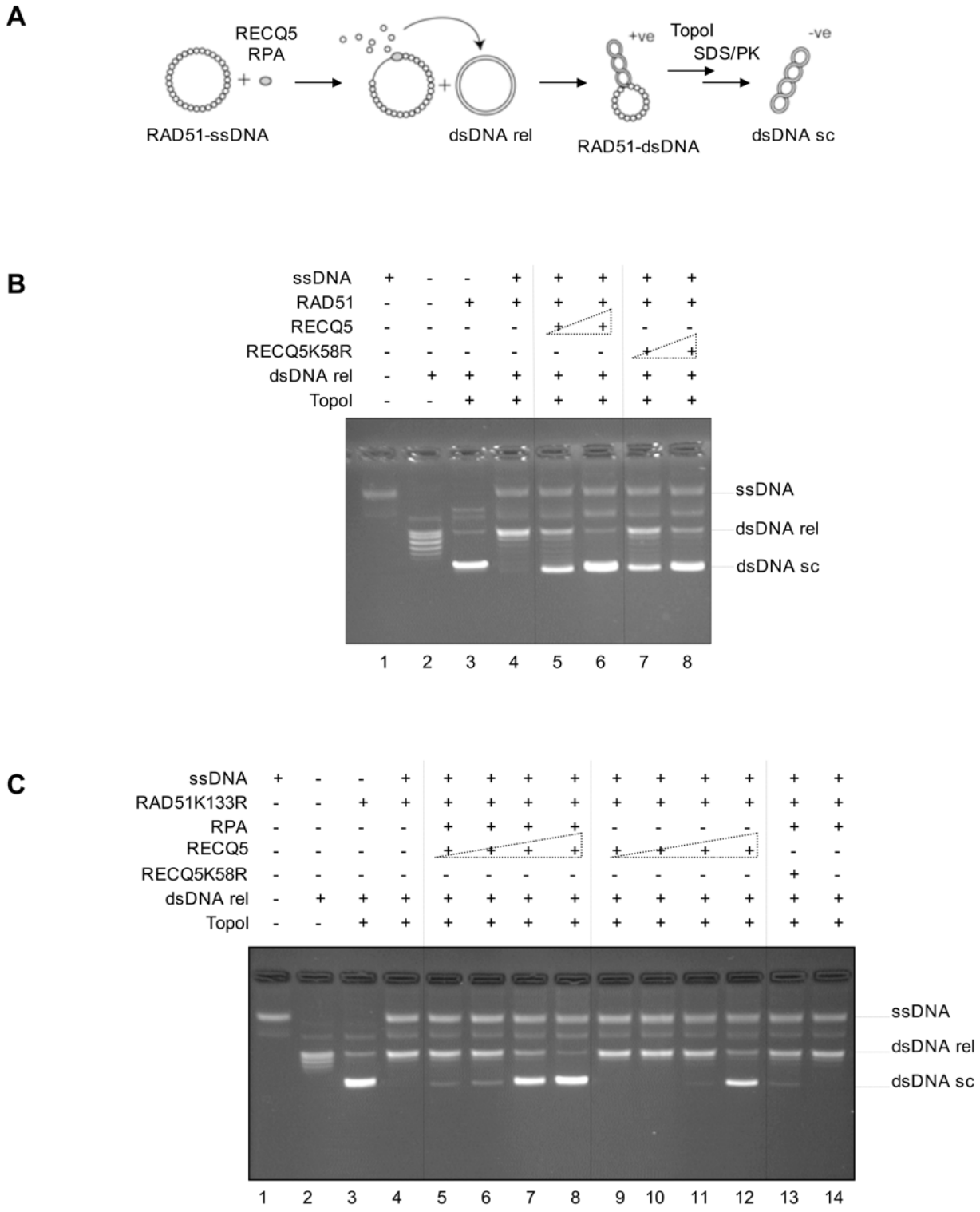

Figure 17
RAD51 filament-dissociation assay. (A) The reaction scheme adapted from (169). See text for explanations. PK, proteinase K; rel, relaxed; sc, supercoiled; TopoI, topoisomerase I. **(B)** Wild-type RAD51 does not form a stable filament on ssDNA in the presence of ATP. The RAD51 presynaptic filament was assembled by a 6-min incubation of 1.5 μM RAD51 with 9 μM circular ssDNA (total nt) in buffer R supplemented with BSA and 2 mM ATP/ATP-regenerating system at 37°C. Where indicated, successively RECQ5 or RECQ5K58R (75 and 150 nM) and 7 μM topologically relaxed dsDNA (total bp) together with 4-5 U wheat germ

topoisomerase I (TopoI) were added, followed by a 6- and 8-min incubation step, respectively. The reaction products were deproteinized with proteinase K, analyzed by agarose gel electrophoresis and visualized by ethidium bromide staining. **(C)** RAD51K133R forms stable presynaptic filaments in the presence of ATP. RAD51K133R filament-dissociation assay was carried out as described above: the filament was pre-formed on 9 μM ssDNA (total nt) with 375 nM RAD51K133R, as indicated successively RECQ5 (20, 40, 80, 160 nM) or RECQ5K58R (160 nM) together with 150 nM RPA and 7 μM relaxed dsDNA (total bp) together with 3 U wheat germ topoisomerase I were added. The reaction products were analyzed as described above.

To have reaction conditions with stable RAD51 filament in the presence of ATP co-factor for helicases, we used the ATPase-defective mutant of RAD51, RAD51K133R. This mutant has been shown to form stable presynaptic filaments in an ATP-bound state and catalyzes strand exchange between homologous DNA more efficiently than wild-type RAD51 (63).

To displace RAD51K133R from ssDNA, the helicase activity of RECQ5 was required. Wild-type RECQ5 promoted the formation of supercoiled dsDNA product in a concentration-dependent manner in the presence of RPA (Fig. 17 C lanes 5-8). In the case of the RECQ5K58R mutant, even at high protein concentration and in the presence of RPA, hardly any supercoiled dsDNA product was found (lane 13). RPA enhanced the RECQ5-mediated release of RAD51K133R from ssDNA (compare lanes 5-8 to 9-12), but could not remove Rad51K133R on its own (lane 14).

5.2.3 Analysis of RAD51K133R filament-dissociation activity of RECQ5 mutants with disrupted RAD51-interaction site

In order to test if the specific physical interaction between RECQ5 and RAD51 is required for disruption of stable RAD51K133R filaments by RECQ5, RECQ5Δ652-674 and RECQ5F666A mutants were compared with wild-type RECQ5 in the RAD51 filament-dissociation assay described above. The helicase domain and zinc-binding motif of the mutants are identical to wild-type RECQ5 suggesting equal translocase activity on ssDNA (Fig. 18 A). The activity of the two RECQ5 mutants was therefore estimated from their DNA-dependent ATPase activity. The formation of inorganic phosphate released by

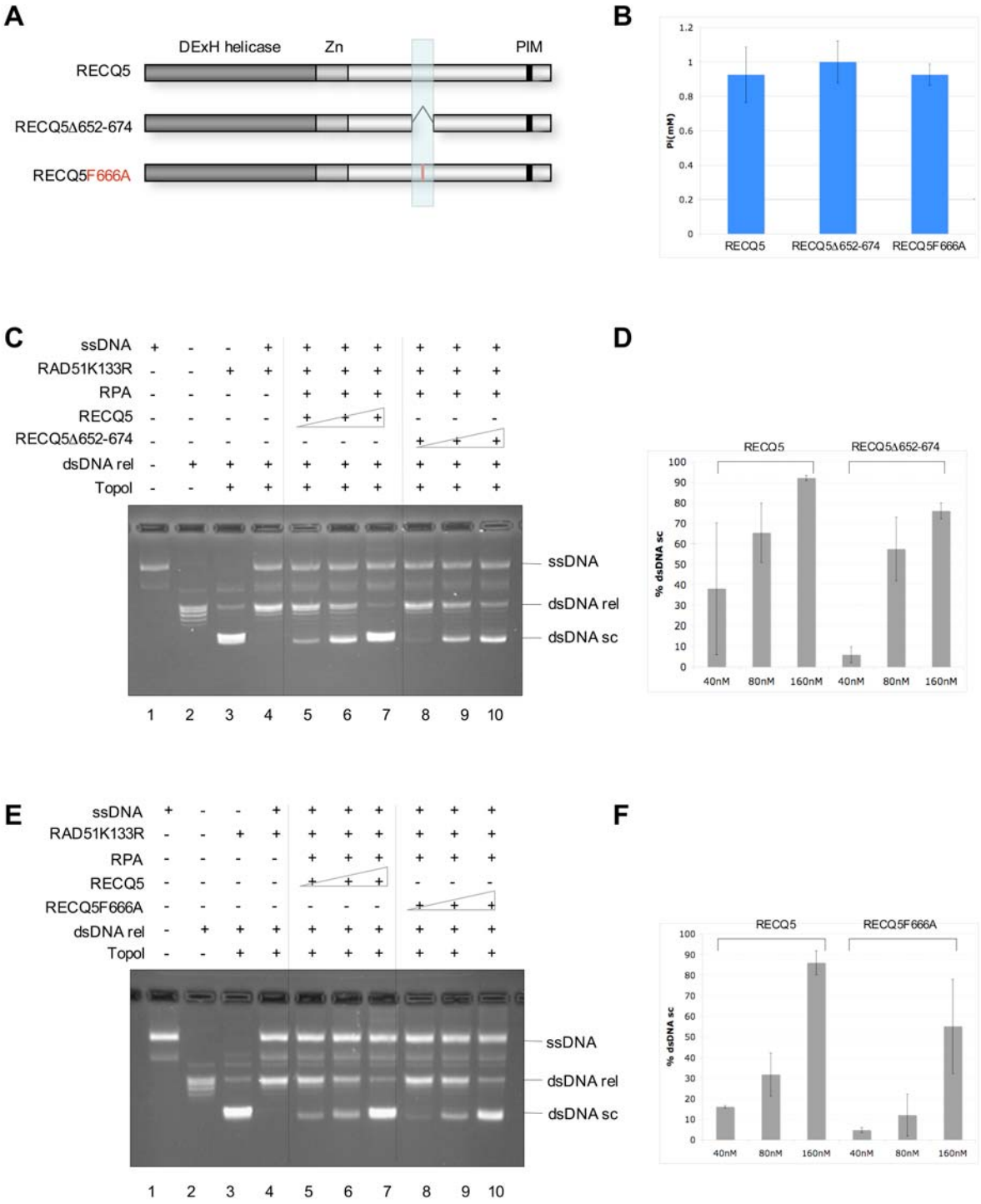

Figure 18

RAD51K133R filament-dissociation activity of RECQ5 mutants with disrupted RAD51-interaction site. (A) Scheme of RECQ5 variants used in the analysis. The amino acid stretch 652-674 is highlighted with a blue box. **(B)** ATPase activity of RECQ5 variants. ATPase activity was determined by colorimetric estimation of the amount of inorganic phosphate (P_i) released by ATP hydrolysis. ATPase reactions were carried out at 37°C for 30 min and contained 20 nM RECQ5, RECQ5Δ652-674, or RECQ5F666A and 25 μg/ml M13 ssDNA in buffer R supplemented with 2 mM ATP and 50 μg/ml BSA. Reactions were stopped by addition of EDTA, and the amount of P_i was determined using a malachite green assay described in Material and Methods. **(C)** and **(E)** RAD51K133R filament-disruption activity of

RECQ5 is stimulated *via* direct RAD51 binding. RAD51K133R filament-dissociation assay was carried out as described in Figure 17: the filament was pre-formed on 9 μM ssDNA (total nt) with 375 nM RAD51K133R, as indicated successively RECQ5, RECQ5Δ652-674 (C) or RECQ5F666A (E) (40, 80, 160 nM) together with 150 nM RPA and 7 μM relaxed dsDNA (total bp) together with 3 U wheat germ topoisomerase I were added. **(D)** and **(F)** The percentage of supercoiled dsDNA product in the RAD51K133R filament-dissociation assay was estimated as described in Materials and Methods. The estimation was done for two (D) or three (F) assays performed as described above.

ATP hydrolysis in the presence of ssDNA was measured and the concentrations of the mutant proteins were adjusted to have similar ATPase activities as wild-type RECQ5 (Fig. 18 B). Both RECQ5 mutants were capable to displace Rad51K133R from ssDNA, but showed a reduction in this activity compared with wild-type RECQ5 (RECQ5Δ652-674 Fig. 18 C/D and RECQ5F666A Fig. 18 E/F). This result suggests that direct RAD51 binding stimulates presynaptic filament disruption by RECQ5.

5.2.4 Analysis of RAD51K133R filament-disruption activity of RECQ5 C-terminal truncation variants

Mutational inactivation of the RAD51-interaction site on RECQ5 did not completely abolish the ability of RECQ5 to disrupt RAD51K133R filaments. It is possible that this residual activity results from action of the N-terminal portion of RECQ5 responsible for ssDNA-translocase activity of the enzyme [helicase domain and zinc-binding motif (appr. aa 1-470)] or that RECQ5 contains an additional domain that is involved in the RAD51 filament-disruption reaction. To address these hypotheses, we tested a series of C-terminal truncation variants of RECQ5 for the ability to disrupt RAD51K133R filaments. In this experiment, we used a C-terminal truncation variant of RECQ5 that contained the RAD51-interaction site (RECQ5 1-725), and two variants that lack this site of which the former ends at the beginning of the RAD51-interaction domain (RECQ5 1-651), whereas the latter is comprised of the ssDNA-translocase core only (RECQ5 1-475) (Fig. 19 A). We found that RECQ5 1-725 displayed similar RAD51K133R filament-disruption activity as wild-type RECQ5 (Fig. 19 C lane 6 and D). The activity of RECQ5 1-651 was

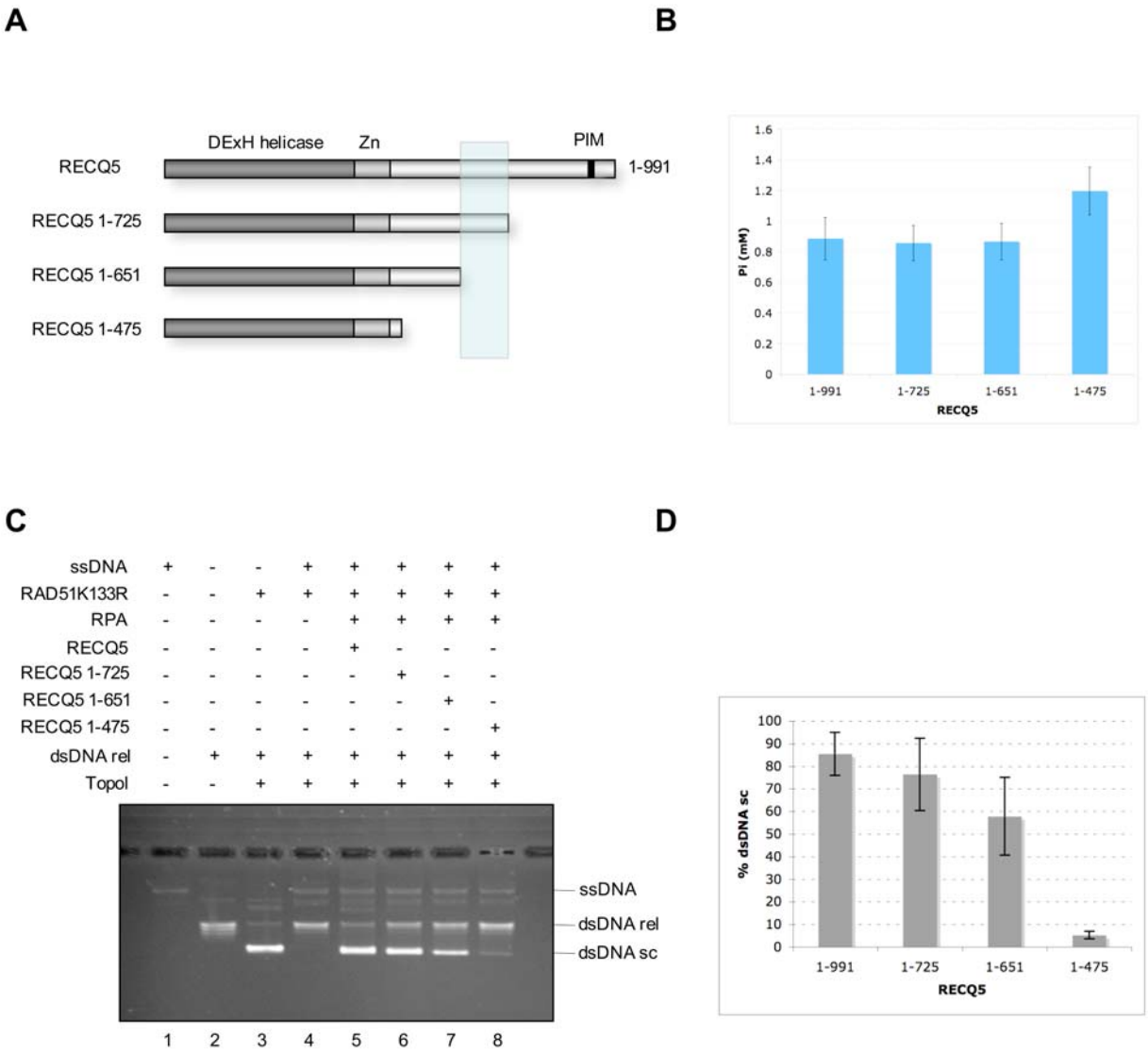

Figure 19
RAD51K133R filament-disruption activity of RECQ5 C-terminal truncation variants. (A) Scheme of RECQ5 variants used in the analysis. The location of the amino-acid stretch 652-725 is highlighted with a blue box. **(B)** ATPase activity of RECQ5 variants 1-991, 1-725, 1-651 and 1-475. ATP hydrolysis reactions were carried our as described in Figure 18 B using 20 nM enzyme, 25 μg/ml ssDNA and 2 mM ATP. (P_i), inorganic phosphate released by ATP hydrolysis. **(C)** Translocase activity of RECQ5 is not sufficient to disrupt efficiently the RAD51K133R filament. The dissociation assay was carried out as described in Figure 17: the filament was pre-formed on 9 μM ssDNA (total nt) with 375 nM RAD51K133R, as indicated successively 160 nM RECQ5 1-991, 1-725, 1-651, or 1-475 together with 150 nM RPA and 7 μM relaxed dsDNA (total bp) together with 3 U wheat germ topoisomerase I were added. **(D)** The percentage of supercoiled dsDNA product in the RAD51K133R filament-dissociation assay was estimated as described in Materials and Methods. The estimation was done for three assays performed as described above.

found to be in the range observed with RECQ5Δ652-674 and RECQ5F666A, confirming the importance of the RAD51-binding domain of RECQ5 for

RAD51K133R filament-disruption function (Fig. 19 C lane 7 and D and Fig 18). In contrast, RECQ5 1-475 could hardly promote the formation of supercoild dsDNA product (Fig. 19 C lane 8 and D) although it showed even higher ATPase activity relative to wild-type RECQ5, under our experimental conditions (Fig. 19 B). Moreover, this variant of RECQ5 was shown to be proficient in DNA unwinding (183,184). Collectively, these findings suggest an existence of an additional RECQ5 domain located between the zinc-binding motif and RAD51-interaction domain that plays an essential role in the RECQ5-mediated displacement of RAD51K133R from ssDNA. These findings suggest that DNA unwinding and disruption of protein-DNA complexes by RECQ5 occur *via* different mechanisms.

5.2.5 Analysis of RAD51K133R filament-disruption activity of BLM core and BLM:RECQ5 chimera

In a next experiment we wished to better define the contribution of the C-terminal part of RECQ5 to the RAD51K133R filament-disruption activity. For that purpose we used a BLM:RECQ5 chimera composed of the DNA translocase core domain of BLM and the C-terminal domain of RECQ5. Like RECQ5, BLM can directly bind RAD51. Two RAD51-interaction sites have been mapped on BLM, one at the N-terminus (aa 1-212) and one at the C-terminus (aa 1317-1417) of the protein (236). The full-size BLM has also been shown to be capable to disrupt RAD51 filaments *in vitro* (170). In our experiment, we used a translocase-competent core fragment of BLM (229) that lacks RAD51-interaction sites (BLM core aa 642-1290) and a BLM-RECQ5 chimera with the C-terminal part of RECQ5 starting just down-stream of the zinc-binding motif (Fig. 20 A). BLM core and BLM:RECQ5 were used in concentrations to have similar ATPase activities as wild-type RECQ5 (Fig. 20 B). In the RAD51K133R filament-dissociation assay, BLM core as well as the BLM:RECQ5 chimera showed hardly any activity (Fig. 20 C lanes 7/8 and 9/10). At present, it is not clear whether BLM:RECQ5 is in general not functional due to e.g. improper structural arrangement or whether the C-terminal part of RECQ5 has no effect on RAD51K133R filament-disruption function. The BLM core fragment was reported to exhibit DNA unwinding

activity (229) but as in the case of RECQ5 1-475, this appears not to be sufficient to displace the RAD51K133R protein from ssDNA.

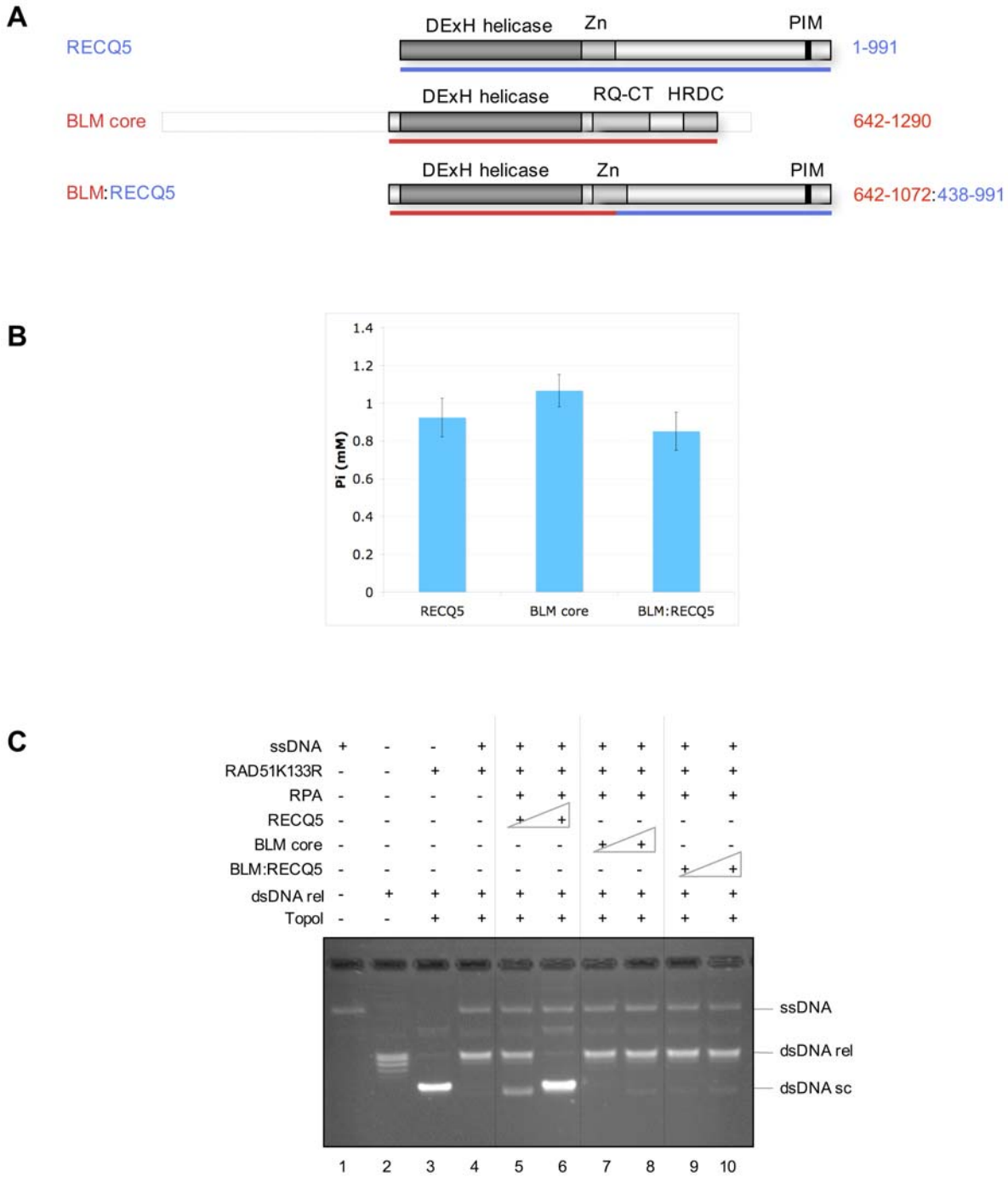

Figure 20
Analysis of RAD51K133R filament-disruption activity of BLM core and BLM:RECQ5 chimera. (A) Scheme of proteins used in the analysis: RECQ5, BLM core fragment, and BLM:RECQ5 chimera that is composed of the helicase part of BLM (red underlined) and the C-terminal part of RECQ5 (blue underlined). The domains indicated are: DExH helicase domain; Zn, zinc-binding motif; RQ-CT, RecQ C-terminal domain composed of a zinc-binding motif and a winged helix-turn-helix (WH) motif; HRDC, helicase and RNasD C-terminal

domain; and PIM, PCNA-binding motif. **(B)** ATPase activity of RECQ5, BLM core, and BLM:RECQ5. ATP hydrolysis reactions were carried our as described in Figure 18 B using 20 nM enzyme, 25 μg/ml ssDNA and 2 mM ATP. (P_i), inorganic phosphate released by ATP hydrolysis. **(C)** Translocase activity of BLM core is not sufficient to disrupt efficiently RAD51K133R presynaptic filaments. The displacement assay was carried out as described in Figure 17: the filament was pre-formed on 9 μM ssDNA (total nt) with 375 nM RAD51K133R, as indicated successively 50 or 100 nM RECQ5, BLM core, or BLM:RECQ5 together with 150 nM RPA and 7 μM relaxed dsDNA (total bp) together with 3 U wheat germ topoisomerase I were added.

6 DISCUSSION

6.1 Fork-regression activity of RECQ5

In the first part of the study, we analyzed the activity of the human RECQ5 helicase on large M13-based forked DNA structures with a leading-strand gap (Fig. 13 A). The model DNA used in our biochemical assays mimics a replication fork stalled by a lesion in the leading-strand template. Such structures with long ssDNA gaps were observed *in vivo* upon induction of replication-blocking lesions (101,118,119,138). Several pathways have been proposed to reactivate blocked replication forks (see chapter 3.4.2). One of these pathways includes replication-fork regression. We tested whether RECQ5 has the capacity to promote replication-fork regression *in vitro*.

RECQ5 was found to process forked DNA substrates with long leading-strand gaps in a reaction dependent on ATP hydrolysis (Fig. 13 B). Restriction enzymes were employed to monitor the formation of fork-regression intermediates. In a reaction with the forked substrate containing a 2.1kb leading-strand gap, RECQ5 was able to regress the fork junction through a region of at least 700bp (Fig. 14 B). In this experiment early regression intermediates were detected that form after unwinding of the lagging-strand arm and repairing of parental strands (Fig. 14 A). In addition, four-way regression-intermediates formed after annealing of the nascent stands were monitored by AclI cleavage (Fig. 14 C). The AclI-dependent release of a characteristic regressed arm fragment was found when RECQ5 was incubated with the forked substrate containing a 0.2kb leading-strand gap (Fig. 14 D). In contrast, RECQ5-promoted four-way intermediates were not detected by RusA cleavage (Fig. 15 E).

In our fork-regression experiments, we compared the activity of RECQ5 with that of the *E. coli* RecG helicase. RecG has been established to promote extensive fork regression of the substrate containing a 2.1kb leading-strand gap (111). Although RecG appeared to act in a non-processive manner, the catalyzed regression reaction was unidirectional and fast, proceeding at a rate of at least 240bp/s (111). Under our reaction conditions, we could observe formation of the linear fork-regression end-products with RecG (Fig. 13 B lanes 6 and 13). With RECQ5 we could not detect clearly these products (Fig. 13 lanes 2 and 9), indicating that RECQ5 may not promote the regression reaction efficiently and/or unidirectionally. Like other RecQ members, RECQ5 is thought to be a helicase with low processivity; frequent dissociation and rebinding during the unwinding process is expected. Helicase reloading and, consequently, branch migration of HJs could therefore take place in direction to regress fork further or to restore it.

On synthetic forked DNA structures, RECQ5 was demonstrated to have a preference for unwinding of the lagging-strand arm (131). In an assay with synthetic forked DNA structure with non-complementary arms lacking a leading strand, RECQ5 was shown to actively unwind the lagging-strand arm in a reaction stimulated by RPA (131). In agreement with these results, on M13-based fork structure with a 2.1kb leading-strand gap, RECQ5 appeared to unwind the lagging-strand arm (Fig. 14 A and B). Detection of the characteristic linear duplex fragments after restriction-enzyme cleavage indicated that the fork junction had regressed. RPA, expected to bind to the ssDNA of the leading-strand gap, slightly stimulated this reaction and did not interfere with pairing of the parental strands (Fig. 14 D (ii)). As mentioned above, RecQ helicases alone have a low processivity and cannot usually unwind more than 40-100bp of standard B-form DNA duplex. Interestingly, the BglII-dependent release of a 1.9kb duplex fragment indicated that RECQ5 without RPA could promote unwinding of more than 700bp of the lagging-strand arm (Fig. 14 B lane 13). Of course, pairing of parental strands at the fork junction could favor the RECQ5-promoted unwinding process by limiting re-annealing of the displaced lagging strand. However, the possibility that RECQ5 coordinates unwinding of the lagging strand and annealing of parental strands cannot be excluded. RecQ helicases are known to prefer complex

DNA structures as their substrates (175) and possess intrinsic a ssDNA annealing function (184,188-192). Biochemical studies suggested that RecQ helicases catalyze rather a strand-exchange reaction than a simple unwinding process. It was found for both, BLM and WRN that unwinding of synthetic duplex DNA could be enhanced by adding of a DNA oligomer complementary to one strand of the DNA substrate (274). In addition, unwinding activity of RECQ4 was only seen in the presence of excess complementary ssDNA (192). The unique C-terminal domain of RECQ5 has been demonstrated to possess DNA strand-annealing activity (184). For RECQ5, a potential way to process a forked structure could include annealing of the parental strands mediated by the C-terminal domain and unwinding of the lagging strand mediated by the N-terminal helicase domain. This hypothesis could be tested by using a C-terminal deletion mutant of RECQ5 lacking the annealing function.

Regression of the fork junction beyond the leading-strand gap is expected to result in a HJ-like DNA structure by annealing of the liberated nascent strands. By AcII and RusA cleavage, we tried to monitor the formation of these four-way DNA intermediates. We could detect the AclI-dependent release of a characteristic regressed arm fragment in reactions with RECQ5 (Fig. 14 C and D). In contrast, we were not able to see RECQ5-promoted RusA fragments (Fig. 15 E). We excluded the possibility that HJ cleavage by RusA was significantly hindered in the presence of RECQ5 (Fig. 15 C). This result challenged the finding that regressed arm fragments observed by AclI restriction analysis are formed by RECQ5-promoted fork regression. Another source of AclI-dependent fragments, we can think of, is direct strand breakage at the fork junction of the substrate. Since we did observe fork processing only in reactions with RECQ5 and ATP, this breakage would depend on mechanical stress caused by the helicase action of RECQ5. Direct visualization of fork-regression intermediates by electron microscopy would clarify this issue.

In summary, RECQ5 processes forked DNA structure in an ATP-dependent manner and unwinds the lagging-strand arm of the substrate with a long leading-strand gap. However, it is not clear if RECQ5 can convert the fork structure into a HJ-like intermediate. Other eukaryotic proteins with more

robust fork-regression activities are described in literature. The fork-regression activity of BLM was analyzed on a plasmid-based forked structure with a 14nt leading-strand gap (129). By restriction-enzymes digestion, BLM-promoted regressed arm fragments of more than 250bp in length were detected. Interestingly, bacterial RecQ, that is known to unwind the lagging strand at replication forks (196), did not shown fork-regression activity on that plasmid-based substrate (129). The FA protein, FANCM, has been shown to promote extensive fork regression of a plasmid-based fork structure with a short lagging-strand gap (128). HJ-like regression intermediates were detected both by restriction digest of the regressed arm and by direct cleavage of the junction by the HJ-specific endonuclease RuvC (128). Furthermore, the yeast Rad5, a member of the SWI/SNF family of ATPases, was shown to be able to regress plasmid-based fork structures (135). In experiments with synthetic forked molecules, Rad5 only unwound substrates with homologous arms. Concertedly unwinding and annealing of nascent and parental strands was observed without exposing ssDNA intermediates (135). In addition, there is *in vivo* evidence that yeast Rad5 is involved in a transient template switching mechanism for error-free damage-bypass following PCNA polyubiquitination (132). The biochemical properties of Rad5 suggest that it could directly convert blocked replication forks into HJ-like structures (135). A recently published study has suggested that the Rad6-Rad18-Rad5 error-free pathway operates under chronic low-dose UV light exposure in proliferating yeast cells and allows replication across the damaged template without DNA checkpoint activation (133). If such a pathway is operable in higher eukaryotes is not yet clear. However, in humans two Rad5 orthologs were identified, SHPRH and HLTF (136,137). Like yeast Rad5, SHPRH and HLTF contain SWI2/SNF2 subdomains and are involved in polyubiquitination of PCNA (136,137). If SHPRH and/or HLTF have the biochemical potential to regress a replication fork is not known.

6.2 Mechanism of RECQ5-mediated disruption of RAD51 nucleoprotein filaments

RECQ5 interacts physically with RAD51 and is suggested to prevent inappropriate HR events *via* RAD51 presynaptic filament disruption (169). In the second study, we analyzed the mechanism of RECQ5-mediated displacement of RAD51 from ssDNA using a topoisomerase-linked Rad51-trap assay. In particular, we tested whether physical interaction between RECQ5 and RAD51 is required for this activity of RECQ5.

We identified a single RAD51-interaction domain of RECQ5 that is located between aa 654-725 (Fig. 16 A-C). RAD51-RECQ5 complex formation *in vitro* and *in vivo* could be prevented either by deletion of aa 652-674 of RECQ5 or by changing phenylalanine 666 of RECQ5 to alanine (Fig. 16 C-E). RECQ5Δ652-674 and RECQ5F666A were tested for their ability to disrupt stable RAD51 filaments formed on ssDNA by an ATPase-defective mutant of RAD51, RAD51K133R. Both RECQ5 mutants were still capable to displace RAD51K133R from ssDNA, but showed a reduction in this activity compared with wild-type RECQ5 (Fig. 18 C-F). This result suggests that direct RAD51 binding stimulates presynaptic filament disruption by RECQ5. In agreement with this assumption, we found that the C-terminal truncation variants of RECQ5, RECQ5 1-725 that physically interacts with RAD51 (Fig. 16 B lane 9), displayed a similar RAD51K133R filament-disruption activity as wild-type RECQ5 (Fig. 19 C/D). The variant RECQ5 1-651, that failed to interact with RAD51 (Fig. 16 B lane 8), had a RAD51K133R filament-disruption activity in a range of those observed with RECQ5Δ652-674 and RECQ5F666A (Fig. 18/19). In contrast, the variant RECQ5 1-475 that was shown to be proficient in DNA unwinding (183,184) could hardly promote RAD51K133R filament disruption (Fig. 19 C/D). This finding suggests the involvement of an additional RECQ5 domain located between the zinc-binding motif and the RAD51-interaction domain in RECQ5-mediated displacement of RAD51K133R from ssDNA.

Using a BLM:RECQ5 chimera, we tested the hypothesis that the C-terminal part of RECQ5, starting downstream of the zinc-binding motif, confers the helicase/translocase domain of RECQ5 the ability to disrupt

RAD51K133R filaments. However, we found that, like the translocase core of BLM, the BLM:RECQ5 chimera was not capable of displacing RAD51K133R from ssDNA although it was proficient in ATP hydrolysis in the presence of ssDNA, a measure of DNA translocase activity (Fig. 20). This finding suggests that the DNA translocase domain of RECQ5 possesses some other unique features that are required for its RAD51K133R filament disruption activity.

Several helicases/translocases have been reported to remove proteins from ssDNA. It is not clear whether this activity is specific for a target DNA-binding protein or it is rather a side action that results from unidirectional translocation of these enzymes on ssDNA. Our result suggests that direct protein-protein interaction contributes to RECQ5-mediated RAD51K133R displacement from ssDNA but is not essential for it. RECQ5 variants with disrupted RAD51-interaction domain are still proficient in RAD51K133R filament disruption. The finding that the translocase/helicase competent RECQ5 1-475 fragment had lost RAD51K133R filament-disruption function, suggest a mechanistic difference between DNA unwinding and RAD51 filament disruption by RECQ5.

For the bacterial UvrD helicase, different mechanisms for DNA unwinding and protein displacement from ssDNA were proposed (153). The wrench-and-inchworm mechanism predicts that UvrD interacts directly with the duplex region of DNA during unwinding. UvrD proteins with mutations in dsDNA-binding motif or mutations that changes structural arrangement of the subdomains were found to have still robust DNA unwinding activity but had lost dsDNA-binding ability (153). The authors therefore suggested a second mode of action in which the protein stays in an open conformation during translocation along ssDNA and displaces the partner strand or bound protein like a wire-stripper. UvrD was reported to dismantle filaments of RecA as well as filaments of Rad51 (161). Recombinase-filament disruption across the species was also described for the *S. cerevisiae* Srs2 helicase. Srs2 interacts physically with Rad51 and can disrupt presynaptic filaments formed by Rad51 and RecA (165,166). It would be interesting to test if RECQ5 has also a general protein-displacement activity for nucleoprotein filament formed with the RecA/Rad51 family of recombinases. The RecA filament-disruption activity of UvrD and Srs2 was tested *in vitro* by monitoring RecA-promoted

DNA strand exchange. In such an assay, inhibition of RecA-promoted strand transfer by wild-type RECQ5 or RECQ5 variants could give further insight into the general domain requirement for filament-disruption function of RECQ5.

In yeast, Srs2 is thought to act as an anti-recombinase *in vivo* by disrupting Rad51 presynaptic filaments (165,166). In higher eukaryotes, regulation of HR at an early step by antagonizing RAD51 filament formation is expected to take place as well. However, an apparent ortholog of the related Srs2/UvrD helicases has not been identified. In humans, several potential candidates that could act in a similar way to yeast Srs2 are suggested. These include FBH1 (167), RTEL1 (168), BLM (170) and RECQ5 (169) (see chapter 3.5.3). In biochemical experiments, both BLM and RECQ5 have recently been shown to be able to displace RAD51 from ssDNA (169,170). Both helicases have a role in suppressing mitotic recombination as revealed by the finding that their deficiency causes an increase in SCE frequency. The observation that the rate of SCEs in the *recq5 blm* double-knockout mouse ES cells and chicken DT40 cells is significantly higher than that in either single mutant suggests that RECQ5 and BLM operate in different pathways to suppress mitotic recombination (266,267). A likely mechanism how BLM can suppress SCEs is by processing late HR intermediates. *In vitro*, BLM in complex with TOPOIIIα has been shown to resolve DHJs exclusively into non-crossover products (52). Although RECQ5 has been shown to coimmuno-precipitate with TOPOIIIα (265), it was not capable in conjuction with TOPOIIIα of catalyzing DHJ dissolution (187). Catalysis of the DHJ dissolution reaction seems highly specific for BLM (187). From biochemical experiments, BLM and RECQ5 are suggested to negative regulate the initial step of HR by disrupting the RAD51 presynaptic filament (169,170). Even though there are experimental differences in these studies the RAD51 filament-disruption function of BLM and RECQ5 could be diverse. In the presence of RPA and in a reaction dependent on ATP hydrolysis, RECQ5 can disrupt RAD51K133R filaments [(169) and our data], a stable and catalytically active form of presynaptic filaments (63). In contrast, BLM appears only capable of disrupting RAD51 filaments in inactive, ADP bound state (170). In a D-loop assay, BLM could inhibit RAD51-promoted strand invasion only when added

to the presynaptic filaments prior to their activation by Ca^{2+} ions (170). Interestingly, BLM inhibited under these conditions specifically strand exchange by the human RAD51, but not by the yeast Rad51 or human meiotic recombinase DMC1 (170). Under our condition with the stable RAD51K133R filament, we only tested the BLM core fragment (aa 642-1290) that lacks RAD51-interaction domains that have been mapped at the N-terminus (aa 1-212) and at the C-terminus (aa 1317-1417) of the protein (236). This translocase competent BLM core fragment (229) was not able to displace RAD51K133R from ssDNA (Fig. 20). It is not yet clear if this fragment is not sufficient for the RAD51 displacement function, similar to RECQ5 1-475 or if BLM is not capable of disrupting RAD51K133R filaments. The full-size BLM should therefore be tested for the ability to disrupt RAD51K133R filament to clarify this issue.

6.3 Conclusions and perspectives

RecQ DNA helicases display preference for complex DNA structures and are involved in cellular process where such DNA structures arise that is DNA replication and recombination. Defects in these enzymes are associated with hyper-recombination phenotype and genome instability. The human RECQ5 helicase associates with the replication machinery and accumulates at sites of stalled replication forks and DSBs (131,268). Moreover, recent studies suggested that RECQ5 regulates HR through disruption of RAD51 presynaptic filaments (169).

In the first study, we analyzed the activity of RECQ5 on M13-based forked DNA structures with a leading-strand gap. RECQ5 showed ATP-dependent activity on such structures, could unwind the lagging-strand arm, but was not efficient in converting fork structures into four-way DNA structures. Our biochemical result and fork-regression activities described in literature of other helicases/translocases, suggest that RECQ5 might not be the ideal enzyme to promote reactivation of stalled replication forks *via* a template-switching mechanism.

In the second study, we analyzed the mechanism underlying disruption of RAD51 filaments by RECQ5. We found that direct interaction between

RECQ5 and RAD51 enhances filament-disruption activity of RECQ5, but it is not essential for it. In addition, we found that the helicase/translocase core of RECQ5 is not sufficient to displace RAD51 from ssDNA suggesting a mechanistic difference between DNA unwinding and protein-DNA complex disruption by RECQ5.

There are still many open questions concerning the role of RECQ5 as an anti-recombinase. Firstly, it is not clear whether RECQ5 has a general protein-displacement activity for nucleoprotein filaments formed with the RecA/Rad51 family of recombinases, similar to yeast Srs2 and bacterial UvrD. Secondly, the redundancy between the RAD51 filament-disruption function of BLM and RECQ5 *in vitro* is not yet established. Comparing the activity of BLM and RECQ5 under identical reaction condition could show if there is a difference in disruption function concerning the stability and ATP-state of RAD51 filaments. Finally, the importance of the direct RECQ5-RAD51 interaction for anti-recombinase function of RECQ5 *in vivo* is not clear and will be analyzed in collaboration with Prof. Jeremy M. Stark. The repair by HR of a defined DSB in a reporter constructs will be analyzed in human cells over-expressing wild-type RECQ5 or RECQ5 mutants with disrupted RAD51-interaction domain.

We believe that apart from acting as an anti-recombinase in the classical DSBR pathway, RECQ5 has a potential to prevent stalled replication forks with ssDNA gaps from inappropriate recombination by displacing bound RAD51. Studies of the effect of RECQ5 deficiency on the rate of replication-fork progression will address this issue.

7 MATERIAL AND METHODS

Abbreviations

RT	room temperature
ATP	adenosine triphosphate
ATPγS	adenosine 5'-O-(3-thio)triphosphate

EDTA	ethylenediamine tetraacetic acid
EtBr	ethidium bromide
EtOH	ethanol
CTAB	cetyl trimethylammonium bromide (cationic tenside)
DTT	dithiothreitol
IPTG	isopropyl-1-thio-β-D-galactopyranoside
PEG	polyethylenglycol
PMSF	phenylmethylsulfonylfluoride
SDS-PAGE	sodium dodecylsulfate polyacrylamide gel electrophoresis

Preparation of bacteriophage M13 DNA

E. coli strain JM109 (containing the F episome and an amber suppressor mutation) was infected with M13mp8.32 (116) and grown in 2X YT medium overnight at 37°C. M13mp8.32 ssDNA was isolated from the supernatant of 1 l culture. The supernatant was heated to 70°C for 30 min, cooled down to RT and cleared by centrifugation (10 000 x g for 15 min). The phage particles were precipitated with 250 ml of 20% (w/v) PEG8000/2.5 M NaCl overnight at 4°C. The phage precipitate was collected by centrifugation (10 000 x g for 30 min at 4°C) and resuspended in a small volume of PBS (pH 7.4) (about 15 ml). The phage particles were allowed to dissolve by shaking moderately for 1-2 h at RT and cleared from residual bacterial cells by centrifugation (24 000 x g for 15 min at 4°C). To remove contaminating *E. coli* chromosomal DNA, the supernatant was supplemented with 50-60 U of DNaseI and 15 mM $MgCl_2$ and incubated for 2 h at 37°C. The DNaseI reaction was stopped by adding EDTA to a final concentration of 60 mM and heating to 80°C for 20 min. Thereafter, the capsid proteins which protect the M13mp8.32 ssDNA were digested with proteinase K (0.1 mg/ml, 37°C overnight). The free ssDNA was precipitated by adding 0.1 volume of 5% (w/v) CTAB/0.5M NaCl, kept for 10 min at RT and centrifuged (10 000 x g for 20 min). The pellet was dissolved in 5 ml 1.2 M NaCl and ssDNA was precipitated by adding 12.5 ml cold absolute EtOH. After incubation at -20°C for at least 1h, the suspension was centrifuged (23 000 x g for 30 min at 4°C), the pellet rinsed with 5 ml 70% RT EtOH and centrifuged again (23 000 x g for 10 min at 4°C). The DNA pellet was then air-dried and dissolved in a small volume (about 1 ml) of 10 mM

Tris-HCl (pH 8.0). Concentration of ssDNA was measured by absorbance at 260 nm using a conversion factor of 36 μg/ml (116). The yield was about 1 mg of M13mp8.32 ssDNA for 1 l of starting culture.

The supercoiled M13mp8.32 dsDNA was purified from infected JM109 cells using the QIAGEN Plasmid Maxi Kit. Briefly, cell pellet from 1 l 2X YT culture was washed with STE buffer [10 mM Tris-HCl (pH 8), 0.1 M NaCl, 1 mM EDTA] and DNA was prepared according to the manufacturer's protocol. Double amounts of the buffers P1, P2 and P3 were used. The obtained DNA was treated with 100 U of Plasmid-Safe ATP-Dependent DNase (Epicentre) in the manufacturer's reaction buffer (Epicentre) supplemented with 1 mM ATP overnight at 37°C. The enzyme was heat inactivated (70°C for 30 min) and DNA precipitated by adding 2.5 volumes of cold absolute EtOH and 0.1 volume of 3 M Na-acetate (pH 5.2) followed by incubation at -20°C overnight. The precipitated DNA was pelleted using an Eppendorf microcentrifuge (14 000 rpm for 20 min at 4°C). The pellet was washed with 70% RT EtOH (14 000 rpm for 10 min at 4°C), air-dried and dissolved in 10 mM Tris-HCl (pH 8). The yield of DNA was about 450 μg for 1 l culture. DNA concentration was determined by measuring absorbance at 260 nm using a conversion factor of 50 μg/ml.

Preparation of DNA substrate for fork-regression assay

DNA substrates that mimic stalled replication forks with a defined ssDNA gap on the leading strand (2.1kb, 0.2kb, 0.06kb or no gap) were assembled from a circular gapped duplex (gd) DNA and a homologous linear dsDNA arm ligated to a synthetic linker (116) (Fig. 12). Gd DNA was produced by a RecA-mediated strand-exchange reaction between circular M13mp8.32 ssDNA and a defined M13mp8.32 dsDNA fragment (5.2kb-[BsrGI-EcoRI], 7.1kb-[BglI-EcoRI], 7.3kb-[HindIII-EcoRI], or 7.3kb-[AccI-EcoRI]) (Fig. 21). The dsDNA fragments were purified from agarose gel using QIAquick Gel Extraction Kit (Qiagen). In more detail, the strand-exchange reaction was carried out with 6.7 μM RecA protein, 2 μM *E. coli* ssDNA binding protein (SSB), 20 μM circular ssDNA (total nt) and linear dsDNA fragment in excess (ssDNA and dsDNA molecules in a molar ratio of 1:1.3). The RecA-reaction buffer

contained 25 mM Tris-acetate (pH 7), 10 mM Mg-acetate, 3 mM potassium glutamate, 1 mM DTT, 5 % (v/v) glycerol and was supplemented with 3 mM ATP, 50 μg/ml BSA and an ATP regenerating system [10 U/ml creatine phosphokinase (SIGMA, C3755) and 12 mM phosphocreatine (SIGMA, P7936) (275). A large-scale gd DNA preparation was performed in a volume of 500-800 μl at 37°C. The RecA filament was preformed on ssDNA for 10 min and the strand-exchange reaction started by adding ATP, SSB and the dsDNA fragment. After incubation for 2 h, RecA was heat-inactivated (80°C for 20 min) and DNA deproteinized with trypsin (100 μg/ml). 1 M Tris-HCl (pH 8) was added to the reaction to a final concentration of 50 mM and the digest allowed to proceed for 2 h at 37°C. After trypsin-heat inactivation (70°C for 15 min), deproteinized DNA species were separated by 1% agarose gel electrophoresis at 40 V for 14-16 h in 0.5 x TBE buffer (45 mM Tris base, 45 mM Borate, 1 mM EDTA) at 4°C and gd DNA was extracted from gel by electroelution (111). Briefly, a small part of the gel was stained with EtBr to visualize the position of the gd DNA band. The band of gd DNA was cut out from the unstained part of the gel and the gd DNA extracted from the gel slice by electroelution in dialysis bag (Spectra/Por, molecular weight cutoff: 3.500). Electroelution was carried out in a standard agarose electrophoresis apparatus (GE Healthcare Minnie gel unit 80-6052-45) for 5 h at 100 V in 0.5 x TBE buffer at 4°C. The polarity of the current was reversed for 1 min before gd DNA was recovered from dialysis bag. The gd DNA, typically in a volume of 2-3 ml was concentrated using Centricon 30 (Amicon) and the buffer was exchanged for 10 mM Tris-HCl (pH 8). Concentration of purified gd DNA was estimated from agarose gel.

The arm fragment of the branched DNA substrate was prepared by digestion of supercoiled M13mp8.32 dsDNA with SapI and SmaI enzymes followed by purification of the 7.3kb-[SapI-SmaI] fragment by gel electrophoresis and extraction with QIAquick Gel Extraction Kit (Qiagen).

The linker DNA was prepared by annealing two synthetic oligonucleotides: the 5'-phosphorylated oligo 1MP 5'-CACCGAAGAGCGCACGGTGCC**G**CG**C**GC**G**GC**GCC**TCGACGGATCCCCGGG and the oligo 2M 5'- **GGC**GC**C**GC**G**CG**C**GGCACCGTGCGCTCTTCG

(Microsynth). The nucleotides in bold are mismatches with respect to M13mp8.32 sequence. One end of the linker (3-nt 5'-overhang) is complementary to the SapI cleavage site of the 7.3kb-[SapI-SmaI] fragment and the other end of the linker (16-nt 3'-overhang) is complementary to the gd DNA downstream of the EcoRI site. First, the linker was ligated with the 7.3kb-[SapI-SmaI] fragment using T4 DNA ligase. Typically, about 15 μg of

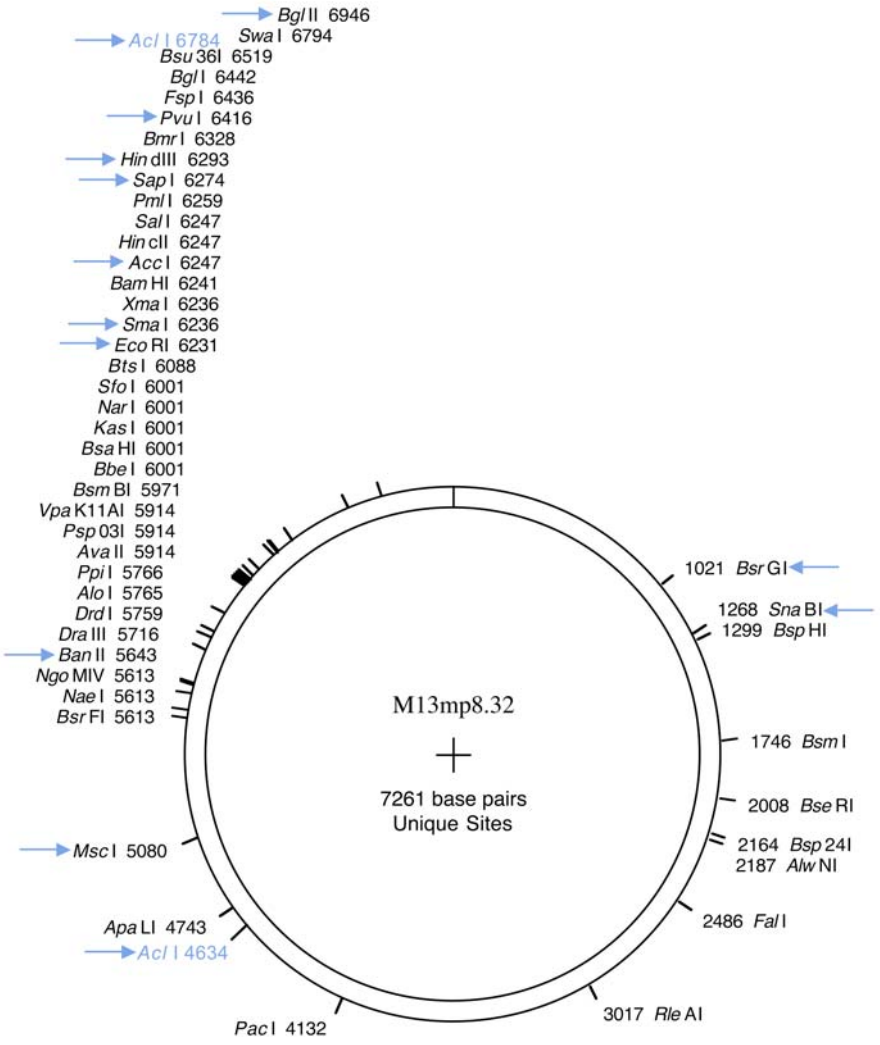

Figure 21.
Restriction map of M13mp3.82 DNA. Unique sites used are indicated by blue arrows. The used AclI double site is indicated in blue.

7.3kb-[SapI-SmaI] fragment and linker DNA in about 20-fold molar excess were incubated with 40 U T4 DNA ligase (New England Biolabs) in a volume of 240 μl of T4 DNA ligase buffer (New England Biolabs) for 16 h in a PCR

machine running a cycling program of endless change between 10°C for 30 sec and 30°C for 30 sec. The ligation product was purified by agarose gel electrophoresis, extracted with QIAquick Gel Extraction Kit (Qiagen) and ligated with the purified gd DNA using Taq DNA ligase (New England Biolabs). This reaction was carried out with gd DNA and linker-[SapI-SmaI] fragment in about 1:10 ratio, with 100 U of Taq DNA ligase in a volume of 200 μl of Taq reaction buffer (New England Biolabs) overnight at 45°C. The branched ligation product was either first linearized by MscI or directly purified by 0.7% agarose gel electrophoresis followed by electroelution as described above. Concentration of purified branched DNA molecules was estimated from agarose gel (see e.g. Fig. 12 C lanes 13-19).

Preparation of Holliday junction-containing DNA

We produced Holliday junction (HJ)-containing DNA *in vivo* using the *E. coli* strain RM40/pSD115 (273). In this strain expression of the XerC recombinase is under control of the lac promoter. RM40 is transformed with the plasmid pSD115 (4.95kb) harboring two copies of the *cer* recombination sites in direct orientation. 1 l RM40/pSD115 culture was grown at 37°C in LB medium containing 150 μg/ml ampicillin, 50 μg/ml diaminopimelic acid, and 1% glucose to maintain repression of the lac promoter. Expression of XerC was induced by adding 2 mM IPTG at an OD_{600} of 0.5. Under this condition *cer* sites of pSD115 are recombined intramolecularly, resulting in a HJ-containing plasmid. RM40 culture was allowed to grow under induced conditions for 1h at 37°C. Cells were then harvested and plasmid DNA isolated with the QIAGEN Plasmid Maxi Kit. The isolated DNA consisted of a mixture of pSD115 DNA in non-recombined, recombined and resolved conformations (Fig. 15 A). HJ-containing pSD115 plasmid, resembling a figure 8 structure, was converted into an α-structure by EcoRI cleavage and the α-structure was purified by 0.9% agarose gel electrophoresis (30 V for 16 h in 0.5 x TBE buffer at 4°C) and extracted from the gel by electroelution (described above).

Proteins used in the fork-regression assay

RECQ5 and RECQ5K58R proteins were produced as C-terminal fusions with self-cleaving Mxe-CBD affinity tag in bacteria and purified as previously described (184,276).

RecG purification was adapted from published protocol (277). The detection method used to follow RecG protein during purification was SDS-PAGE, using the known molecular weight of RecG (76 kDa). RecG protein was produced in *E. coli* BL21(DE3) transformed with the plasmid pAF201 harboring *RecG* gene under control of IPTG-inducible promoter. 2-4 l of cells were grown in LB medium containing 150 μg/ml ampicillin at 37°C. RecG expression was induced by adding 1 mM IPTG at an OD_{600} of 0.5. Cells were either grown for additional 6 h at 37°C or for 16 h at 18°C. Overall RecG expression was higher in cells grown at 37°C, but solubility of the protein was better in cells grown at 18°C. Cells were harvested by centrifugation, washed with STE buffer and dissolved in about 80 ml lysis buffer [20 mM Tris-HCl (pH 8.5), 400 mM NaCl, 1 mM DTT, 1 mM EDTA, 0.1 % Triton X-100, 10% glycerol]. Cell suspensions were frozen in liquid nitrogen, and stored at -80°C. After thawing cell suspensions, 0.5 mM of the protease inhibitor PMSF was added and cells were disrupted using a French press. Cell lysate was clarified by centrifugation (40 000 x g for 1h at 4°C). Nucleic acid in the supernatant was removed by the addition of polyethylenimine up to 0.5 %, incubation for 30 min at 4°C and centrifugation (40 000 x g for 30 min at 4°C). From the supernatant, proteins including RecG were precipitated with 70% saturation of ammonium sulfate (stirring on ice for 45 min). After centrifugation (40 000 x g for 30 min at 4°C), the protein pellet was resuspended in about 30 ml of R-buffer [20 mM Tris-HCl (pH 7.5), 1 mM DTT, 10 % glycerol] and dialyzed against 4 l of R-buffer/500 mM NaCl (Spectra/Por dialysis membrane, molecular weight cutoff: 3.500). Precipitates were removed from the dialyzed solution by centrifugation (40 000 x g for 30 min at 4°C), and 4 volumes of R-buffer were added. The solution was then applied to a DEAE-Sepharose FF column equilibrated with R-buffer/100 mM NaCl. The flow-through was loaded directly onto a SP-Sepharose column equilibrated with the same buffer and eluted with a linear gradient of NaCl (0.1-1.0 M) in R-buffer. Fractions

containing RecG, which were eluted around 500 mM NaCl, were pooled, diluted with R-buffer to approximately 200 mM NaCl and applied to a HiTrap heparin column equilibrated with R-buffer/200 mM NaCl. Proteins were eluted from the column with a linear gradient of NaCl (0.2-1.0 M) in R-buffer. Peak fractions containing about 95% pure RecG protein were aliquoted, frozen in liquid nitrogen, and stored at -80°C. Protein concentration was measured by Bradford method using BSA as a standard.

RusA protein was purified as described (278) with some modifications from 1 l culture of *E. coli* BL21pLysS harboring RusA expression vector pET19-b. Cells were grown in LB medium containing 150 μg/ml ampicillin and 25 μg/ml chloramphenicol at 37°C to an OD_{660} of 0.6 and protein synthesis was induced by adding 1 mM IPTG, followed by an 2 h incubtion at 37°C. Cells were harvested by centrifugation, washed with STE buffer, resuspended in 25 ml of 20 mM sodium phosphate (pH 7) supplemented with 0.5 mM PMSF and disrupted by sonication. Cell lysate was clarified by centrifugation (40 000 x g for 45 min at 4°C). The supernatant was subjected to fractional protein precipitation. An initial protein precipitation was induced with ammonium sulfate at 55 % saturation (stirring on ice for 1 h 20 min). After centrifugation (40 000 x g for 45 min at 4°C), further ammonium sulfate was added to the supernatant to a final concentration of 85 % saturation (stirring on ice for 1 h 20 min), following centrifugation as above. The protein pellet was then resuspended in 30 ml of HS buffer [20 mM sodium phosphate (pH 7), 1 mM DTT] and the solution applied to HiTrap SP column equilibrated with HS buffer. Proteins were eluted with a linear gradient of NaCl (0-2 M) in HS buffer. Fractions containing RusA in high concentration and purity of more than 95% were identified by SDS-PAGE, pooled (end volume 5 ml), supplemented with 0.1 mM PMSF and dialysed overnight against 0.5 l of storage buffer [50 mM Tris-HCl (pH 8), 200 mM NaCl, 1 mM DTT, 50 % glycerol] and stored at -20°C. Protein concentration was measured by Bradford method using BSA as a standard.

Human RPA was purified as described (279). Restriction enzymes and *E. coli* RecA protein were purchased from New England Biolabs. *E. coli* single-stranded DNA Binding Protein (SSB) was purchased from Promega.

Fork-regression assay

Reactions were carried out at 37°C in 1 x NEB4 buffer (New England BioLabs) supplemented with 50 µg/ml BSA in a volume of 15 µl. About 10 pM DNA substrate was incubated with indicated concentrations of RECQ5, RECQ5K58R or RecG in the presence of 2 mM ATP or ATPγS as indicated for 30-60 min. Where included, 20 or 40 nM RPA was pre-incubated with substrate DNA for 2 min before addition of the helicase. After the reaction, fork-regression products were directly deproteinized or further processed by restriction endonuculease or RusA cleavage as described below. To deproteinize and stop the reactions, samples were incubated for 20 min at 37°C with 1 % SDS, 12 mM EDTA, and 1 mg/ml proteinase K. The DNA products were then separated by 0.7% agarose gel electrophoresis, typically at 45 V for 4 h in 0.5 x TBE buffer, and transferred to a Zeta-Probe membrane (Bio-Rad catalog #162-0196) according to standard protocols for Southern blotting. The blots were shortly equilibrated in 2 x SSC buffer (0.3 M NaCl, 30 mM Na-citrate) and air-dried. Before hybridization, the membrane was soaked in 6 x SSC, pre-incubated with hybrisol I (CHEMICON, Cat. No. S4040) for 2 h at 45°C and further incubated with fresh hybrisol I containing radiolabeled probes (described below) overnight at 45°C. Next day, the membrane was rinsed with 2 x SSC, washed successively with 2 x SSC/0.1% SDS (at 41°C for 15 min), 0.5 x SSC/0.1% SDS (at 41°C for 15 min) and 0.1 x SSC/0.1% SDS (at RT for 2 min). DNA products on membrane were detected by autoradiography (Phosphor Screen from Molecular Dynamics, Typhoon 9400 scanner).

The probes for Southern blotting were prepared using the Random Primed DNA Labeling Kit from Roche (Cat. No. 1 004 760). The labeling reaction was performed according to manufacturer's protocol with [α-^{32}P]CTP and 50 ng of linear dsDNA fragment as template: M13mp8.32 1.2kb-[MscI-SapI], M13mp8.32 2.1kb-[EcoRI-BsrGI], or pSD115 0.95kb-[EcoRI-SalI]. Probes generated in one reaction lasted for 2-3 hybridizations.

RusA cleavage assay

RusA cleavage assay was carried out in 1 x NEB4 buffer directly after fork-regression assay described above. Fork-regression reaction-mixtures containing about 10 pM DNA substrate were supplemented with 5 nM RusA and 100 ng of oligonucleotide f-10-C [5'-GAGGTCACTCCAGTGAATTCGAGCTCGCAGCCCCTCTAGGTTACATGAC TGAATGATAGT-3'], that served as a trap for helicases, and incubated for additional 30 min at 37°C (end volume 20 μl).

For pSD115 α-structure, RusA cleavage reaction was carried out in 1 x NEB4 buffer supplemented with 50 μg/ml BSA for 30 min at 37°C. About 20 nM DNA was incubated with 10 nM RusA in the presence or absence of 2 mM ATP, 9 mM ATPγS and 100 ng ssDNA (oligo f-10-C) as indicated (reaction volume 15 μl). Where RECQ5 was included, DNA was pre-incubated with 50 nM RECQ5 and 2 mM ATP for 15 min before addition of RusA.

DNA products were deproteinized by proteinase K treatment and analyzed by agarose gel electrophoresis and Southern blotting as described above.

Plasmid constructs and recombinant proteins

To produce mutant variants of human RECQ5 for purification and for chitin-binding domain (CBD) pull-down assays, the following plasmid constructs were used. All plasmids are derivatives of the bacterial expression vectors pTXB1 (New England Biolabs), in which protein of interest is expressed as a C-terminal fusion with a self-cleaving Mxe-CBD affinity tag. Plasmid pPG10 codes for wild-type RECQ5 (amino acids 1-991), pPG17 for RECQ5 1-410, pPG19 for RECQ5 1-475, pPG21 for RECQ5 1-561, pPG20 for RECQ5 1-651, pPG18 for RECQ5 1-725, pPG11 for RECQ5 675-991, pPG16 for RECQ5 411-991, and pPG10K58R for RECQ5K58R (131,184).

In addition, the expression vector for RECQ5 529-725 fragment (pTXB1-hRQ5 529-725) was constructed by PCR amplification of the corresponding part of *RECQ5* cDNA from pPG10 (primers hRQ5-45 and hRQ5-21) and the PCR product cloned into pTXB1 *via* NdeI/SapI sites. The internal deletion variant RECQ5Δ640-653 (pPG10Δ640-653) was constructed

by PCR amplification of *RECQ5* cDNA in two separate PCR reactions. The primers used were hRQ5-3 and Del2-1918-1958R for the N-terminal coding sequence of *RECQ5* and hRQ5-4 and Del2-1918-1958F for the C-terminal coding sequence. The PCR products were cleaved with SacI and Acc651 (N-terminal coding sequence), Acc65I and Bsu36I (C-terminal coding sequence) and linked with the pPG10[Bsu36I-SacI] fragment in a three-fragment ligation reaction. Thereby two additional codons GGTACC (Acc65I site) were introduced between the N- and C- terminal portions of the *RECQ5* coding sequence. The internal deletion variant RECQ5Δ652-674 (pPG10Δ652-674) and RECQ5Δ652-725 (pPG10Δ652-725) were constructed using the same strategy but the isoschizomer KpnI was used instead of Acc65I. For RECQ5Δ652-674 the primers for the PCR reactions were hRQ5-3 and Del2-1954-2022R for the N-terminal coding sequence and hRQ5-4 and Del2-1954-2022F for the C-terminal coding sequence. For RECQ5Δ652-725 the primers were hRQ5-3 and Del2-1954-2022R (for N-terminal coding *RECQ5* cDNA), and hRQ5-4 and Del2-725F (for C-terminal coding *RECQ5* cDNA). Another three expression vectors for RECQ5Δ515-568 (pPG10Δ515-568), RECQ5Δ543-607 (pPG10Δ543-607) and RECQ5Δ571-653 (pPG10Δ571-653) variants were constructed using restriction enzymes. The pPG10Δ515-568 plasmid results from FspI/BsaAI deletion of pPG10. The pPG10Δ543-607 plasmid results from BamHI/EcoRV deletion of pPG10 where BamHI end was filled by Klenow fragment. The pPG10Δ571-653 plasmid results from BsaAI/Acc65I deletion of pPG10Δ640-653 where the Acc65I end was filled by Klenow fragment. Expression vector for RECQ5-R654A, RECQ5-F659A, RECQ5-F666A and RECQ5-E671A mutants were prepared using QuickChange Site-Directed Mutagenesis Kit (Stratagene) according to manufacturer's instructions. Wild-type and mutant RECQ5 proteins were purified as described previously (131,184).

Plasmid construction and protein purification for BLM core fragment encompassing amino acid residues 642-1290 were described (229). To construct the chimera protein BLM:RECQ5 composed of aa 642-1072 of BLM and aa 438-991 of RECQ5, a EagI site was introduced into the BLM encoding plasmid pJP73 by site-directed mutagenesis using the primers BLM-42/-43.

The EagI-SacII fragment of the resulting plasmid was replaced by the pPG10[EagI-SacII] fragment.

For ectopic expression of RECQ5, RECQ5Δ652-674 and RECQ5F666A in 293T cells, the mammalian expression vector pcDNA3.1/HisC (Invitrogen) was used. For wild-type RECQ5, a construct named pJP136 was already available in the laboratory. It was constructed by cloning *RECQ5* cDNA into the multiple cloning site of pcDNA3.1/HisC *via* BamHI/NdeI and EcoRI sites. Expression vector for RECQ5Δ652-674 (pJP136Δ652-674) was generated by ligation of the pJP136[Bsu36I-BstEII] fragment with the pPG10Δ652-674[BstEII-Bsu36I] fragment. The expression vector for RECQ5F666A was constructed using the same strategy.

Wild-type RAD51 and RAD51K133R used in protein interaction assays were purified by Igor Shevelev according to previously published protocol (280). The bacterial expression vector for wild-type RAD51 (pFB530) was obtained from Dr. Stephen West. The expression vector for RAD51K133R (pFB530KR) was generated by site-directed mutagenesis using the primers hRAD51KR-T/B.

Human RPA and *E.coli* Topoisomerase I were purified as described (279).

Wheat germ topoisomerase I (M2851) was purchased from Promega.

Primers

Name	Sequence (5'-3')	Restriction site
Del2-1918-1958F	GAGTAT**GGTACC**CGGGTGGGAGCTGGTTTCCCC	**Acc651**
Del2-1918-1958R	CACCCG**GGTACC**ATACTCATTGGGCTCCGGGGG	**Acc651**
Del2-1954-2022F	CTCAAA**GGTACC**ACGACTCGGATCAGGGAGCAAG	**Acc651**
Del2-1954-2022R	AGTCGT**GGTACC**TTTGAGCGAGTACACATGGGAG	**Acc651**
Del2-725F	AGTCGT**GGTACC**CCCTCCCCTGAGAAGAAGGC	**Acc651**

hRAD51KR-B	GACAGATCTGGGTC**C**TCCCAGTTCGGAATTC	-
hRAD51KR-T	GAATTCCGAACTGGGA**G**GACCCAGATCTGTC	-
hRQ5-21	AAGGCC**GCTCTTC**CGCACATCCCCCCATAGTGAGCGCTGCC	**SapI**
hRQ5-3	GGGAATTCCATATGAGCAGCCACCATACCACCTTTCCTTTT	**-**
hRQ5-4	AAGGCCGCTCTTCCGCATCTCTGGGGGCCACACAGGCCATGCCAG	-
hRQ5-45	GGGAATTC**CATATG**GATGAGAACTGTCCCCTGAAA	**NdeI**
BLM-42	TAATTGCTGTAAAACAAAGG**CGGCCG**AAACAAGAGATGTGACTGAC	**EagI**
BLM-43	ATTGGCATTGATATATAAGTCTTCATCCAA	**-**

Cell culture and preparation of total cell extracts

HEK 293T cells were cultivated in Dulbecco modified Eagle's medium (DMEM) (Gibco) supplemented with 5% fetal calf serum (Life Technologies), streptomycin (100 U/ml) and penicillin (100 μg/ml).

For extract preparation, cells at confluency of 90-100% were trypsinized, washed twice in PBS, and cell pellets frozen in liquid nitrogen and stored at -80°C. All centrifugation steps were done at 900 rpm for 5 min (Eppendorf centrifuge 5810R). Extracts were prepared before use. One frozen pellet (from a 15 cm dish) was thawed on ice, dissolved in 1 ml of IP buffer [50 mM Tris-HCl (pH 8), 120 mM NaCl, 0.5% (v/v) NP-40] supplemented with 0.3 mM PMSF and a protease inhibitor cocktail (complete EDTA free from Roche), incubated for 20-30 min at 4°C, and centrifuged at 14'000 rpm for 20 min at 4°C (Eppendorf microcentrifuge). The supernatant was transferred to a fresh tube and centrifuged for additional 10 min as above. This clarified supernatant was used as total cell extract in CBD pull-down assays. Protein concentration was measured by Bradford method using BSA as a standard.

Chitin Binding Domain (CBD) pull-down assay

RECQ5 protein and its variants were produced as C-terminal fusions with CBD tag in *E. coli* BL21(DE3). Cells were grown at 37°C in LB medium containing 150 μg/ml ampicillin and 25 μg/ml chloramphenicol to an OD_{600} of

about 0.3, induced by adding 0.2 mM IPTG and incubated overnight at 18°C. Cells harvested from a 10-ml culture were resuspended in 1 ml of CH buffer [20 mM Tris-HCl (pH 8), 500 mM NaCl, 1 mM EDTA, 0.1% (v/v) Triton X-100] supplemented with 0.5 mM PMSF and a protease inhibitor cocktail (complete EDTA free from Roche). Cells were disrupted by sonication and extracts clarified by centrifugation in a Eppendorf microcentrifuge at 14 000 rpm for 45 min at 4°C. Typically, 50 μl of the cleared extract were incubated with 25 μl of chitin beads (New England Biolabs) in a total volume of 500 μl of CH buffer supplemented with 0.2 mM PMSF and protease inhibitor cocktail for 2 h at 4°C. The beads were then washed once with 1 ml of CH buffer and three times with 1 ml of IP buffer [50 mM Tris-HCl (pH 8), 120 mM NaCl, 0.5% (v/v) NP-40]. After each wash, beads were collected by centrifugation at 5000 rpm for 2 min at 4°C (Eppendorf microcentrifuge). The washed beads were then incubated either with total cell extract from 293T cells (600-1000 μg) or with recombinant RAD51 protein (20-250 ng) in a volume of 500 μl of IP buffer supplemented with PMSF and protease inhibitor cocktail for 2 h at 4°C. The beads were again washed three times with IP buffer as above. Proteins were eluted from beads by boiling at 95°C for 7 min in 25 μl of 3 x SDS loading buffer, separated by 10% SDS-PAGE and analyzed by Western blotting with anti-RAD51 antibody.

Nickel pull-down assay

293T cells were transiently transfected with either the expression vector for RECQ5, RECQ5Δ652-674, RECQ5F666A or the corresponding empty vector (pCDNA3.1/HisC) using Metafecten reagent (Biontex). To do so, 1 x 10^6 cells were plated in 10 cm dishes one day before transfection. 2 μg of DNA in 100 μl DMEM were mixed with 7 μl of Metafecten in 100 μl DMEM, incubated at RT for 20 min and added to one 10 cm dish containing cells at about 40% confluency. Cells were harvested 48-64 h post-transfection. For that purpose, dishes were placed on ice, cells washed twice with 8 ml cold PBS and lysed in 500 μl of extraction buffer [50 mM Tris-HCl (pH 8), 120 mM NaCl, 20 mM NaF, 15 mM sodium pyrophosphate, 0.5% (v/v) NP-40] supplemented with 1 mM benzamidine, 0.2 mM PMSF, 0.5 mM sodium orthovanadate and

protease inhibitor cocktail (complete EDTA free from Roche). Cell suspension was gently scraped off the dish, snap frozen in liquid nitrogen, thawed and centrifuged at 14 000 rpm for 12 min at 4°C (Eppendorf microcentrifuge). The clarified supernatant (total protein extract) was used in Nickel (Ni) pull-down assay. To immobilize the ectopically expressed $(His)_6$-tagged RECQ5 variants, 800-1000 μg total protein extract was incubated with 25 μl Ni-NTA-Agarose beads (Qiagen) in a volume of 500 μl of extraction buffer supplemented with protease/phosphatase inhibitors as above and 20 mM imidazole for 2h or overnight at 4°C. Where required, 50 μg/ml EtBr was included in incubation or extracts were pre-treated with 20 U DNaseI (Roche) for 20 min at 25°C in the presence of 6 mM $MgCl_2$ and 1 mM $CaCl_2$. After incubation the beads were washed three times with 1 ml of extraction buffer supplemented only with PMSF and 20 mM imidazole, beads were collected after each washing step by centrifugation at 5000 rpm for 2 min at 4°C (Eppendorf microcentrifuge). Proteins were then eluted from nickel beads by boiling at 95°C for 10 min in 25 μl of 3 x SDS-loading buffer, separated by 10% SDS-PAGE and analyzed by Western blotting with anti-RAD51 antibody and anti-omni-probe antibody.

Western blot analysis

Proteins separated by 10% SDS-PAGE were transferred to Hybond-P PVDF membrane (GE Healthcare) according to standard protocols. To check the transfer, the membrane was stained with Ponceau dye. The membrane was blocked with 5% non-fat dry milk in TBS-T [20 mM Tris-HCl (pH 7.4), 150 mM NaCl, 0.1% (v/v) Tween-20] for 1-2 h at RT and probed with primary antibody overnight at 4°C in 5% non-fat dry milk in TBS-T. The membrane was afterward washed three times with TBS-T for 20 min at RT, incubated with corresponding horseradish peroxidase (HRP) coupled secondary antibody for 1 h at RT in 2.5% non-fat dry milk in TBS-T, followed three additional washing steps with TBS-T. Immune complexes were detected using enhanced chemiluminescence (ECL) reagent (GE Healthcare). The primary antibodies used were: rabbit polyclonal anti-RAD51 antibody (BD Pharmingen Cat. No. 551922), 1:5000; mouse monoclonal anti-RAD51 antibody ab1837 (Abcam),

1:500; goat polyclonal anti-omni-probe antibody sc-499-G (Santa Cruz Biotechnology), 1:1000. Additionally, the following HRP coupled secondary antibodies were used: sheep anti-mouse IgG (GE Healthcare NA931V); donkey anti-rabbit IgG (GE Healthcare NA934V); bovine anti-goat IgG sc-2350 (Santa Cruz Biotechnology).

DNA for enzyme assays

Bacteriophage M13mp8.32 ssDNA (116) was prepared as described above.

To generate topologically relaxed dsDNA plasmid, 4 μg of supercoiled pGEM-7Zf(+) DNA (Promega) were incubated with 2 μl *E. coli* Topoisomerase I (0.8 mg/ml) at 37°C for 30 min in 40 μl buffer R supplemented with 100 μg/ml BSA, followed by heat inactivation of the enzyme (65°C for 10 min).

RAD51 filament-dissociation assay

To measure displacement of RAD51 from ssDNA, a previously described topoisomerase-linked RAD51-trap assay (165,169) was adapted. Reactions were carried out at 37°C in an end-volume of 25 μl of buffer R [25 mM Tris-HCl (pH 7.5), 1 mM $MgCl_2$, 50 mM KCl, 1 mM DTT] supplemented with 100 μg/ml BSA, 2 mM ATP and an ATP-regenerating system consisting of 10 U/ml creatine phosphokinase (SIGMA, C3755) and 12 mM phosphocreatine (SIGMA, P7936). Indicated concentration of RAD51 or RAD51K133R was pre-incubated with circular M13mp8.32 ssDNA (9 μM nt) for 6 min, followed by addition of indicated concentrations of RECQ5 variants, BLM core, or BLM:RECQ5 and typically 150 nM RPA. After a 6-min incubation, topologically relaxed pGEM-7Zf(+) DNA (7 μM bp) and indicated concentrations of wheat germ topoisomerase I were added to complete the reaction. The reaction was incubated for additional 8 min and then terminated by the addition of 1% SDS, 12 mM EDTA, and 1 mg/ml proteinase K followed by a 25-min incubation at 37°C. DNA products were resolved by 1% agarose gel electrophoresis in 0.5 x TBE buffer at 100V for 2 h, stained in EtBr solution (0.5 μg/ml) and visualized on a UV transilluminator. Gel images were quantified using IMAGEQUANT software. The relative concentration of supercoiled dsDNA was expressed as percentage of total dsDNA. The values

for relaxed dsDNA were corrected using a factor of [dsDNA sc in positive control]/[ds DNA rel in negative control]. In the agarose gels shown, this corresponds to dsDNA bands in lane 3 / 4.

ATPase assay

ATPase activity of RECQ5 variants, BLM core or BLM:RECQ5 chimera was measured in the presence of saturating concentrations of ssDNA. The reactions were carried out at 37°C for 30 min with 20 nM enzyme, 25 μg/ml M13mp8.32 ssDNA in 20 μl of buffer R supplemented with 50 μg/ml BSA and 2 mM ATP. The reactions were terminated by addition of 20 μl of 0.1 M EDTA (pH 8). The amount of inorganic phosphate (P_i) released by ATP hydrolysis was determined by a colorimetric assay using malachite green (281,282). Briefly, 10 μl of stopped reaction mixture was added to 30 μl of 0.1 M EDTA (pH 8) in a 96-well microplate. To that mixture, 100 μl of freshly diluted 5.72% (w/v) ammonium molybdate/6 M HCl in H_20 (ratio 1:3) and 50 μl malachite green [0.0812% (w/v) in water] was added and incubated for a few minutes before absorbance at 620 nm was measured in a microplate reader (Molecular devices). The concetration of P_i released by ATP hydrolysis was determined from a calibration curve derived from solutions of known P_i concentration (KH_2PO_4). Reactions for individual proteins were done in triplicates.

8 REFERENCES

1. Jones, P.A. and Baylin, S.B. (2007) The epigenomics of cancer. *Cell*, **128**, 683-692.
2. Futreal, P.A., Coin, L., Marshall, M., Down, T., Hubbard, T., Wooster, R., Rahman, N. and Stratton, M.R. (2004) A census of human cancer genes. *Nat Rev Cancer*, **4**, 177-183.
3. Hanahan, D. and Weinberg, R.A. (2000) The hallmarks of cancer. *Cell*, **100**, 57-70.
4. Fearon, E.R. and Vogelstein, B. (1990) A genetic model for colorectal tumorigenesis. *Cell*, **61**, 759-767.
5. Evan, G.I. and Vousden, K.H. (2001) Proliferation, cell cycle and apoptosis in cancer. *Nature*, **411**, 342-348.

6. Sjoblom, T., Jones, S., Wood, L.D., Parsons, D.W., Lin, J., Barber, T.D., Mandelker, D., Leary, R.J., Ptak, J., Silliman, N. *et al.* (2006) The consensus coding sequences of human breast and colorectal cancers. *Science*, **314**, 268-274.
7. Parsons, R., Li, G.M., Longley, M.J., Fang, W.H., Papadopoulos, N., Jen, J., de la Chapelle, A., Kinzler, K.W., Vogelstein, B. and Modrich, P. (1993) Hypermutability and mismatch repair deficiency in RER+ tumor cells. *Cell*, **75**, 1227-1236.
8. Reitmair, A.H., Cai, J.C., Bjerknes, M., Redston, M., Cheng, H., Pind, M.T., Hay, K., Mitri, A., Bapat, B.V., Mak, T.W. *et al.* (1996) MSH2 deficiency contributes to accelerated APC-mediated intestinal tumorigenesis. *Cancer Res*, **56**, 2922-2926.
9. Lindahl, T. and Nyberg, B. (1972) Rate of depurination of native deoxyribonucleic acid. *Biochemistry*, **11**, 3610-3618.
10. Lindahl, T. (1993) Instability and decay of the primary structure of DNA. *Nature*, **362**, 709-715.
11. Kunkel, T.A. (2004) DNA replication fidelity. *J Biol Chem*, **279**, 16895-16898.
12. Hoeijmakers, J.H. (2001) Genome maintenance mechanisms for preventing cancer. *Nature*, **411**, 366-374.
13. Cory, S. and Adams, J.M. (2002) The Bcl2 family: regulators of the cellular life-or-death switch. *Nat Rev Cancer*, **2**, 647-656.
14. van Brabant, A.J., Ye, T., Sanz, M., German, I.J., Ellis, N.A. and Holloman, W.K. (2000) Binding and melting of D-loops by the Bloom syndrome helicase. *Biochemistry*, **39**, 14617-14625.
15. Friedberg, E.C. (2003) DNA damage and repair. *Nature*, **421**, 436-440.
16. Koike, G., Maki, H., Takeya, H., Hayakawa, H. and Sekiguchi, M. (1990) Purification, structure, and biochemical properties of human O6-methylguanine-DNA methyltransferase. *J Biol Chem*, **265**, 14754-14762.
17. Daniels, D.S., Woo, T.T., Luu, K.X., Noll, D.M., Clarke, N.D., Pegg, A.E. and Tainer, J.A. (2004) DNA binding and nucleotide flipping by the human DNA repair protein AGT. *Nat Struct Mol Biol*, **11**, 714-720.
18. Scharer, O.D. and Jiricny, J. (2001) Recent progress in the biology, chemistry and structural biology of DNA glycosylases. *Bioessays*, **23**, 270-281.
19. Gillet, L.C. and Scharer, O.D. (2006) Molecular mechanisms of mammalian global genome nucleotide excision repair. *Chem Rev*, **106**, 253-276.
20. Hess, M.T., Schwitter, U., Petretta, M., Giese, B. and Naegeli, H. (1997) Bipartite substrate discrimination by human nucleotide excision repair. *Proc Natl Acad Sci U S A*, **94**, 6664-6669.
21. Cleaver, J.E. (1968) Defective repair replication of DNA in xeroderma pigmentosum. *Nature*, **218**, 652-656.
22. Fousteri, M. and Mullenders, L.H. (2008) Transcription-coupled nucleotide excision repair in mammalian cells: molecular mechanisms and biological effects. *Cell Res*, **18**, 73-84.
23. Jiricny, J. (2006) The multifaceted mismatch-repair system. *Nat Rev Mol Cell Biol*, **7**, 335-346.
24. Strand, M., Prolla, T.A., Liskay, R.M. and Petes, T.D. (1993) Destabilization of tracts of simple repetitive DNA in yeast by mutations affecting DNA mismatch repair. *Nature*, **365**, 274-276.

25. Neale, M.J. and Keeney, S. (2006) Clarifying the mechanics of DNA strand exchange in meiotic recombination. *Nature*, **442**, 153-158.
26. Walker, J.R., Corpina, R.A. and Goldberg, J. (2001) Structure of the Ku heterodimer bound to DNA and its implications for double-strand break repair. *Nature*, **412**, 607-614.
27. Weterings, E. and Chen, D.J. (2008) The endless tale of non-homologous end-joining. *Cell Res*, **18**, 114-124.
28. Takata, M., Sasaki, M.S., Sonoda, E., Morrison, C., Hashimoto, M., Utsumi, H., Yamaguchi-Iwai, Y., Shinohara, A. and Takeda, S. (1998) Homologous recombination and non-homologous end-joining pathways of DNA double-strand break repair have overlapping roles in the maintenance of chromosomal integrity in vertebrate cells. *Embo J*, **17**, 5497-5508.
29. Yun, M.H. and Hiom, K. (2009) CtIP-BRCA1 modulates the choice of DNA double-strand-break repair pathway throughout the cell cycle. *Nature*.
30. Sartori, A.A., Lukas, C., Coates, J., Mistrik, M., Fu, S., Bartek, J., Baer, R., Lukas, J. and Jackson, S.P. (2007) Human CtIP promotes DNA end resection. *Nature*, **450**, 509-514.
31. Szostak, J.W., Orr-Weaver, T.L., Rothstein, R.J. and Stahl, F.W. (1983) The double-strand-break repair model for recombination. *Cell*, **33**, 25-35.
32. Assenmacher, N. and Hopfner, K.P. (2004) MRE11/RAD50/NBS1: complex activities. *Chromosoma*, **113**, 157-166.
33. San Filippo, J., Sung, P. and Klein, H. (2008) Mechanism of eukaryotic homologous recombination. *Annu Rev Biochem*, **77**, 229-257.
34. New, J.H., Sugiyama, T., Zaitseva, E. and Kowalczykowski, S.C. (1998) Rad52 protein stimulates DNA strand exchange by Rad51 and replication protein A. *Nature*, **391**, 407-410.
35. Sugawara, N., Wang, X. and Haber, J.E. (2003) In vivo roles of Rad52, Rad54, and Rad55 proteins in Rad51-mediated recombination. *Mol Cell*, **12**, 209-219.
36. Malkova, A., Ivanov, E.L. and Haber, J.E. (1996) Double-strand break repair in the absence of RAD51 in yeast: a possible role for break-induced DNA replication. *Proc Natl Acad Sci U S A*, **93**, 7131-7136.
37. Yonetani, Y., Hochegger, H., Sonoda, E., Shinya, S., Yoshikawa, H., Takeda, S. and Yamazoe, M. (2005) Differential and collaborative actions of Rad51 paralog proteins in cellular response to DNA damage. *Nucleic Acids Res*, **33**, 4544-4552.
38. Moynahan, M.E., Chiu, J.W., Koller, B.H. and Jasin, M. (1999) Brca1 controls homology-directed DNA repair. *Mol Cell*, **4**, 511-518.
39. Yuan, S.S., Lee, S.Y., Chen, G., Song, M., Tomlinson, G.E. and Lee, E.Y. (1999) BRCA2 is required for ionizing radiation-induced assembly of Rad51 complex in vivo. *Cancer Res*, **59**, 3547-3551.
40. Moynahan, M.E., Pierce, A.J. and Jasin, M. (2001) BRCA2 is required for homology-directed repair of chromosomal breaks. *Mol Cell*, **7**, 263-272.
41. Xia, F., Taghian, D.G., DeFrank, J.S., Zeng, Z.C., Willers, H., Iliakis, G. and Powell, S.N. (2001) Deficiency of human BRCA2 leads to impaired homologous recombination but maintains normal nonhomologous end joining. *Proc Natl Acad Sci U S A*, **98**, 8644-8649.
42. Heyer, W.D., Li, X., Rolfsmeier, M. and Zhang, X.P. (2006) Rad54: the Swiss Army knife of homologous recombination? *Nucleic Acids Res*, **34**, 4115-4125.

43. McIlwraith, M.J., Vaisman, A., Liu, Y., Fanning, E., Woodgate, R. and West, S.C. (2005) Human DNA polymerase eta promotes DNA synthesis from strand invasion intermediates of homologous recombination. *Mol Cell*, **20**, 783-792.
44. Sugiyama, T., New, J.H. and Kowalczykowski, S.C. (1998) DNA annealing by RAD52 protein is stimulated by specific interaction with the complex of replication protein A and single-stranded DNA. *Proc Natl Acad Sci U S A*, **95**, 6049-6054.
45. Sugiyama, T., Kantake, N., Wu, Y. and Kowalczykowski, S.C. (2006) Rad52-mediated DNA annealing after Rad51-mediated DNA strand exchange promotes second ssDNA capture. *Embo J*, **25**, 5539-5548.
46. Nimonkar, A.V., Sica, R.A. and Kowalczykowski, S.C. (2009) Rad52 promotes second-end DNA capture in double-stranded break repair to form complement-stabilized joint molecules. *Proc Natl Acad Sci U S A*, **106**, 3077-3082.
47. West, S.C. (1997) Processing of recombination intermediates by the RuvABC proteins. *Annu Rev Genet*, **31**, 213-244.
48. Constantinou, A., Chen, X.B., McGowan, C.H. and West, S.C. (2002) Holliday junction resolution in human cells: two junction endonucleases with distinct substrate specificities. *Embo J*, **21**, 5577-5585.
49. Ciccia, A., Constantinou, A. and West, S.C. (2003) Identification and characterization of the human mus81-eme1 endonuclease. *J Biol Chem*, **278**, 25172-25178.
50. Gaskell, L.J., Osman, F., Gilbert, R.J. and Whitby, M.C. (2007) Mus81 cleavage of Holliday junctions: a failsafe for processing meiotic recombination intermediates? *Embo J*, **26**, 1891-1901.
51. Ip, S.C., Rass, U., Blanco, M.G., Flynn, H.R., Skehel, J.M. and West, S.C. (2008) Identification of Holliday junction resolvases from humans and yeast. *Nature*, **456**, 357-361.
52. Wu, L. and Hickson, I.D. (2003) The Bloom's syndrome helicase suppresses crossing over during homologous recombination. *Nature*, **426**, 870-874.
53. Chaganti, R.S., Schonberg, S. and German, J. (1974) A manyfold increase in sister chromatid exchanges in Bloom's syndrome lymphocytes. *Proc Natl Acad Sci U S A*, **71**, 4508-4512.
54. Nassif, N., Penney, J., Pal, S., Engels, W.R. and Gloor, G.B. (1994) Efficient copying of nonhomologous sequences from ectopic sites via P-element-induced gap repair. *Mol Cell Biol*, **14**, 1613-1625.
55. Ferguson, D.O. and Holloman, W.K. (1996) Recombinational repair of gaps in DNA is asymmetric in Ustilago maydis and can be explained by a migrating D-loop model. *Proc Natl Acad Sci U S A*, **93**, 5419-5424.
56. Dupaigne, P., Le Breton, C., Fabre, F., Gangloff, S., Le Cam, E. and Veaute, X. (2008) The Srs2 helicase activity is stimulated by Rad51 filaments on dsDNA: implications for crossover incidence during mitotic recombination. *Mol Cell*, **29**, 243-254.
57. Sung, P. and Klein, H. (2006) Mechanism of homologous recombination: mediators and helicases take on regulatory functions. *Nat Rev Mol Cell Biol*, **7**, 739-750.
58. Gangloff, S., Soustelle, C. and Fabre, F. (2000) Homologous recombination is responsible for cell death in the absence of the Sgs1 and Srs2 helicases. *Nat Genet*, **25**, 192-194.

59. Tsuzuki, T., Fujii, Y., Sakumi, K., Tominaga, Y., Nakao, K., Sekiguchi, M., Matsushiro, A., Yoshimura, Y. and MoritaT. (1996) Targeted disruption of the Rad51 gene leads to lethality in embryonic mice. *Proc Natl Acad Sci U S A*, **93**, 6236-6240.
60. Lim, D.S. and Hasty, P. (1996) A mutation in mouse rad51 results in an early embryonic lethal that is suppressed by a mutation in p53. *Mol Cell Biol*, **16**, 7133-7143.
61. Sonoda, E., Sasaki, M.S., Buerstedde, J.M., Bezzubova, O., Shinohara, A., Ogawa, H., Takata, M., Yamaguchi-Iwai, Y. and Takeda, S. (1998) Rad51-deficient vertebrate cells accumulate chromosomal breaks prior to cell death. *Embo J*, **17**, 598-608.
62. Shin, D.S., Pellegrini, L., Daniels, D.S., Yelent, B., Craig, L., Bates, D., Yu, D.S., Shivji, M.K., Hitomi, C., Arvai, A.S. *et al.* (2003) Full-length archaeal Rad51 structure and mutants: mechanisms for RAD51 assembly and control by BRCA2. *Embo J*, **22**, 4566-4576.
63. Chi, P., Van Komen, S., Sehorn, M.G., Sigurdsson, S. and Sung, P. (2006) Roles of ATP binding and ATP hydrolysis in human Rad51 recombinase function. *DNA Repair (Amst)*, **5**, 381-391.
64. Mazin, A.V., Zaitseva, E., Sung, P. and Kowalczykowski, S.C. (2000) Tailed duplex DNA is the preferred substrate for Rad51 protein-mediated homologous pairing. *Embo J*, **19**, 1148-1156.
65. Sung, P. and Robberson, D.L. (1995) DNA strand exchange mediated by a RAD51-ssDNA nucleoprotein filament with polarity opposite to that of RecA. *Cell*, **82**, 453-461.
66. Ogawa, T., Yu, X., Shinohara, A. and Egelman, E.H. (1993) Similarity of the yeast RAD51 filament to the bacterial RecA filament. *Science*, **259**, 1896-1899.
67. Yu, X., Jacobs, S.A., West, S.C., Ogawa, T. and Egelman, E.H. (2001) Domain structure and dynamics in the helical filaments formed by RecA and Rad51 on DNA. *Proc Natl Acad Sci U S A*, **98**, 8419-8424.
68. Gupta, R.C., Folta-Stogniew, E., O'Malley, S., Takahashi, M. and Radding, C.M. (1999) Rapid exchange of A:T base pairs is essential for recognition of DNA homology by human Rad51 recombination protein. *Mol Cell*, **4**, 705-714.
69. Sinha, M. and Peterson, C.L. (2008) A Rad51 presynaptic filament is sufficient to capture nucleosomal homology during recombinational repair of a DNA double-strand break. *Mol Cell*, **30**, 803-810.
70. Thorslund, T. and West, S.C. (2007) BRCA2: a universal recombinase regulator. *Oncogene*, **26**, 7720-7730.
71. West, S.C. (2003) Molecular views of recombination proteins and their control. *Nat Rev Mol Cell Biol*, **4**, 435-445.
72. Ristic, D., Modesti, M., van der Heijden, T., van Noort, J., Dekker, C., Kanaar, R. and Wyman, C. (2005) Human Rad51 filaments on double- and single-stranded DNA: correlating regular and irregular forms with recombination function. *Nucleic Acids Res*, **33**, 3292-3302.
73. Bugreev, D.V. and Mazin, A.V. (2004) Ca2+ activates human homologous recombination protein Rad51 by modulating its ATPase activity. *Proc Natl Acad Sci U S A*, **101**, 9988-9993.

74. Sung, P. and Stratton, S.A. (1996) Yeast Rad51 recombinase mediates polar DNA strand exchange in the absence of ATP hydrolysis. *J Biol Chem*, **271**, 27983-27986.
75. Morrison, C., Shinohara, A., Sonoda, E., Yamaguchi-Iwai, Y., Takata, M., Weichselbaum, R.R. and Takeda, S. (1999) The essential functions of human Rad51 are independent of ATP hydrolysis. *Mol Cell Biol*, **19**, 6891-6897.
76. Carreira, A., Hilario, J., Amitani, I., Baskin, R.J., Shivji, M.K., Venkitaraman, A.R. and Kowalczykowski, S.C. (2009) The BRC repeats of BRCA2 modulate the DNA-binding selectivity of RAD51. *Cell*, **136**, 1032-1043.
77. Garg, P. and Burgers, P.M. (2005) DNA polymerases that propagate the eukaryotic DNA replication fork. *Crit Rev Biochem Mol Biol*, **40**, 115-128.
78. Pursell, Z.F., Isoz, I., Lundstrom, E.B., Johansson, E. and Kunkel, T.A. (2007) Yeast DNA polymerase epsilon participates in leading-strand DNA replication. *Science*, **317**, 127-130.
79. Nick McElhinny, S.A., Gordenin, D.A., Stith, C.M., Burgers, P.M. and Kunkel, T.A. (2008) Division of labor at the eukaryotic replication fork. *Mol Cell*, **30**, 137-144.
80. Garg, P., Stith, C.M., Sabouri, N., Johansson, E. and Burgers, P.M. (2004) Idling by DNA polymerase delta maintains a ligatable nick during lagging-strand DNA replication. *Genes Dev*, **18**, 2764-2773.
81. Ayyagari, R., Gomes, X.V., Gordenin, D.A. and Burgers, P.M. (2003) Okazaki fragment maturation in yeast. I. Distribution of functions between FEN1 AND DNA2. *J Biol Chem*, **278**, 1618-1625.
82. Pavlov, Y.I., Frahm, C., Nick McElhinny, S.A., Niimi, A., Suzuki, M. and Kunkel, T.A. (2006) Evidence that errors made by DNA polymerase alpha are corrected by DNA polymerase delta. *Curr Biol*, **16**, 202-207.
83. Krishna, T.S., Kong, X.P., Gary, S., Burgers, P.M. and Kuriyan, J. (1994) Crystal structure of the eukaryotic DNA polymerase processivity factor PCNA. *Cell*, **79**, 1233-1243.
84. Maga, G. and Hubscher, U. (2003) Proliferating cell nuclear antigen (PCNA): a dancer with many partners. *J Cell Sci*, **116**, 3051-3060.
85. Schvartzman, J.B. and Stasiak, A. (2004) A topological view of the replicon. *EMBO Rep*, **5**, 256-261.
86. Mulcair, M.D., Schaeffer, P.M., Oakley, A.J., Cross, H.F., Neylon, C., Hill, T.M. and Dixon, N.E. (2006) A molecular mousetrap determines polarity of termination of DNA replication in E. coli. *Cell*, **125**, 1309-1319.
87. Blow, J.J. and Dutta, A. (2005) Preventing re-replication of chromosomal DNA. *Nat Rev Mol Cell Biol*, **6**, 476-486.
88. Gilbert, D.M. (2001) Making sense of eukaryotic DNA replication origins. *Science*, **294**, 96-100.
89. Maisnier-Patin, S., Nordstrom, K. and Dasgupta, S. (2001) Replication arrests during a single round of replication of the Escherichia coli chromosome in the absence of DnaC activity. *Mol Microbiol*, **42**, 1371-1382.
90. Michel, B. (2000) Replication fork arrest and DNA recombination. *Trends Biochem Sci*, **25**, 173-178.
91. McGlynn, P. and Lloyd, R.G. (2002) Recombinational repair and restart of damaged replication forks. *Nat Rev Mol Cell Biol*, **3**, 859-870.
92. Michel, B., Ehrlich, S.D. and Uzest, M. (1997) DNA double-strand breaks caused by replication arrest. *Embo J*, **16**, 430-438.

93. Anderson, D.G. and Kowalczykowski, S.C. (1997) The translocating RecBCD enzyme stimulates recombination by directing RecA protein onto ssDNA in a chi-regulated manner. *Cell*, **90**, 77-86.
94. Seigneur, M., Bidnenko, V., Ehrlich, S.D. and Michel, B. (1998) RuvAB acts at arrested replication forks. *Cell*, **95**, 419-430.
95. Flores, M.J., Bierne, H., Ehrlich, S.D. and Michel, B. (2001) Impairment of lagging strand synthesis triggers the formation of a RuvABC substrate at replication forks. *Embo J*, **20**, 619-629.
96. Grompone, G., Seigneur, M., Ehrlich, S.D. and Michel, B. (2002) Replication fork reversal in DNA polymerase III mutants of Escherichia coli: a role for the beta clamp. *Mol Microbiol*, **44**, 1331-1339.
97. Grompone, G., Ehrlich, D. and Michel, B. (2004) Cells defective for replication restart undergo replication fork reversal. *EMBO Rep*, **5**, 607-612.
98. Heller, R.C. and Marians, K.J. (2005) The disposition of nascent strands at stalled replication forks dictates the pathway of replisome loading during restart. *Mol Cell*, **17**, 733-743.
99. Heller, R.C. and Marians, K.J. (2006) Replication fork reactivation downstream of a blocked nascent leading strand. *Nature*, **439**, 557-562.
100. Liu, J., Xu, L., Sandler, S.J. and Marians, K.J. (1999) Replication fork assembly at recombination intermediates is required for bacterial growth. *Proc Natl Acad Sci U S A*, **96**, 3552-3555.
101. Pages, V. and Fuchs, R.P. (2003) Uncoupling of leading- and lagging-strand DNA replication during lesion bypass in vivo. *Science*, **300**, 1300-1303.
102. Grompone, G., Sanchez, N., Dusko Ehrlich, S. and Michel, B. (2004) Requirement for RecFOR-mediated recombination in priA mutant. *Mol Microbiol*, **52**, 551-562.
103. Courcelle, J., Donaldson, J.R., Chow, K.H. and Courcelle, C.T. (2003) DNA damage-induced replication fork regression and processing in Escherichia coli. *Science*, **299**, 1064-1067.
104. Courcelle, C.T., Chow, K.H., Casey, A. and Courcelle, J. (2006) Nascent DNA processing by RecJ favors lesion repair over translesion synthesis at arrested replication forks in Escherichia coli. *Proc Natl Acad Sci U S A*, **103**, 9154-9159.
105. Courcelle, J. and Hanawalt, P.C. (1999) RecQ and RecJ process blocked replication forks prior to the resumption of replication in UV-irradiated Escherichia coli. *Mol Gen Genet*, **262**, 543-551.
106. Postow, L., Ullsperger, C., Keller, R.W., Bustamante, C., Vologodskii, A.V. and Cozzarelli, N.R. (2001) Positive torsional strain causes the formation of a four-way junction at replication forks. *J Biol Chem*, **276**, 2790-2796.
107. Olavarrieta, L., Martinez-Robles, M.L., Sogo, J.M., Stasiak, A., Hernandez, P., Krimer, D.B. and Schvartzman, J.B. (2002) Supercoiling, knotting and replication fork reversal in partially replicated plasmids. *Nucleic Acids Res*, **30**, 656-666.
108. Whitby, M.C. and Lloyd, R.G. (1998) Targeting Holliday junctions by the RecG branch migration protein of Escherichia coli. *J Biol Chem*, **273**, 19729-19739.
109. McGlynn, P. and Lloyd, R.G. (2000) Modulation of RNA polymerase by (p)ppGpp reveals a RecG-dependent mechanism for replication fork progression. *Cell*, **101**, 35-45.

110. McGlynn, P., Lloyd, R.G. and Marians, K.J. (2001) Formation of Holliday junctions by regression of nascent DNA in intermediates containing stalled replication forks: RecG stimulates regression even when the DNA is negatively supercoiled. *Proc Natl Acad Sci U S A*, **98**, 8235-8240.
111. Robu, M.E., Inman, R.B. and Cox, M.M. (2004) Situational repair of replication forks: roles of RecG and RecA proteins. *J Biol Chem*, **279**, 10973-10981.
112. Singleton, M.R., Scaife, S. and Wigley, D.B. (2001) Structural analysis of DNA replication fork reversal by RecG. *Cell*, **107**, 79-89.
113. Flores, M.J., Bidnenko, V. and Michel, B. (2004) The DNA repair helicase UvrD is essential for replication fork reversal in replication mutants. *EMBO Rep*, **5**, 983-988.
114. Flores, M.J., Sanchez, N. and Michel, B. (2005) A fork-clearing role for UvrD. *Mol Microbiol*, **57**, 1664-1675.
115. Baharoglu, Z., Petranovic, M., Flores, M.J. and Michel, B. (2006) RuvAB is essential for replication forks reversal in certain replication mutants. *Embo J*, **25**, 596-604.
116. Robu, M.E., Inman, R.B. and Cox, M.M. (2001) RecA protein promotes the regression of stalled replication forks in vitro. *Proc Natl Acad Sci U S A*, **98**, 8211-8218.
117. Heller, R.C. and Marians, K.J. (2006) Replisome assembly and the direct restart of stalled replication forks. *Nat Rev Mol Cell Biol*, **7**, 932-943.
118. Cordeiro-Stone, M., Zaritskaya, L.S., Price, L.K. and Kaufmann, W.K. (1997) Replication fork bypass of a pyrimidine dimer blocking leading strand DNA synthesis. *J Biol Chem*, **272**, 13945-13954.
119. Cordeiro-Stone, M., Makhov, A.M., Zaritskaya, L.S. and Griffith, J.D. (1999) Analysis of DNA replication forks encountering a pyrimidine dimer in the template to the leading strand. *J Mol Biol*, **289**, 1207-1218.
120. Masutani, C., Kusumoto, R., Yamada, A., Dohmae, N., Yokoi, M., Yuasa, M., Araki, M., Iwai, S., Takio, K. and Hanaoka, F. (1999) The XPV (xeroderma pigmentosum variant) gene encodes human DNA polymerase eta. *Nature*, **399**, 700-704.
121. Andersen, P.L., Xu, F. and Xiao, W. (2008) Eukaryotic DNA damage tolerance and translesion synthesis through covalent modifications of PCNA. *Cell Res*, **18**, 162-173.
122. Saleh-Gohari, N., Bryant, H.E., Schultz, N., Parker, K.M., Cassel, T.N. and Helleday, T. (2005) Spontaneous homologous recombination is induced by collapsed replication forks that are caused by endogenous DNA single-strand breaks. *Mol Cell Biol*, **25**, 7158-7169.
123. Rothstein, R., Michel, B. and Gangloff, S. (2000) Replication fork pausing and recombination or "gimme a break". *Genes Dev*, **14**, 1-10.
124. Lambert, S., Watson, A., Sheedy, D.M., Martin, B. and Carr, A.M. (2005) Gross chromosomal rearrangements and elevated recombination at an inducible site-specific replication fork barrier. *Cell*, **121**, 689-702.
125. Higgins, N.P., Kato, K. and Strauss, B. (1976) A model for replication repair in mammalian cells. *J Mol Biol*, **101**, 417-425.
126. Sogo, J.M., Lopes, M. and Foiani, M. (2002) Fork reversal and ssDNA accumulation at stalled replication forks owing to checkpoint defects. *Science*, **297**, 599-602.

127. Pellicioli, A. and Foiani, M. (2005) Signal transduction: how rad53 kinase is activated. *Curr Biol*, **15**, R769-771.
128. Gari, K., Decaillet, C., Delannoy, M., Wu, L. and Constantinou, A. (2008) Remodeling of DNA replication structures by the branch point translocase FANCM. *Proc Natl Acad Sci U S A*, **105**, 16107-16112.
129. Ralf, C., Hickson, I.D. and Wu, L. (2006) The Bloom's syndrome helicase can promote the regression of a model replication fork. *J Biol Chem*, **281**, 22839-22846.
130. Machwe, A., Xiao, L., Lloyd, R.G., Bolt, E. and Orren, D.K. (2007) Replication fork regression in vitro by the Werner syndrome protein (WRN): holliday junction formation, the effect of leading arm structure and a potential role for WRN exonuclease activity. *Nucleic Acids Res*, **35**, 5729-5747.
131. Kanagaraj, R., Saydam, N., Garcia, P.L., Zheng, L. and Janscak, P. (2006) Human RECQ5beta helicase promotes strand exchange on synthetic DNA structures resembling a stalled replication fork. *Nucleic Acids Res*, **34**, 5217-5231.
132. Hoege, C., Pfander, B., Moldovan, G.L., Pyrowolakis, G. and Jentsch, S. (2002) RAD6-dependent DNA repair is linked to modification of PCNA by ubiquitin and SUMO. *Nature*, **419**, 135-141.
133. Hishida, T., Kubota, Y., Carr, A.M. and Iwasaki, H. (2009) RAD6-RAD18-RAD5-pathway-dependent tolerance to chronic low-dose ultraviolet light. *Nature*, **457**, 612-615.
134. Johnson, R.E., Prakash, S. and Prakash, L. (1994) Yeast DNA repair protein RAD5 that promotes instability of simple repetitive sequences is a DNA-dependent ATPase. *J Biol Chem*, **269**, 28259-28262.
135. Blastyak, A., Pinter, L., Unk, I., Prakash, L., Prakash, S. and Haracska, L. (2007) Yeast Rad5 protein required for postreplication repair has a DNA helicase activity specific for replication fork regression. *Mol Cell*, **28**, 167-175.
136. Motegi, A., Sood, R., Moinova, H., Markowitz, S.D., Liu, P.P. and Myung, K. (2006) Human SHPRH suppresses genomic instability through proliferating cell nuclear antigen polyubiquitination. *J Cell Biol*, **175**, 703-708.
137. Motegi, A., Liaw, H.J., Lee, K.Y., Roest, H.P., Maas, A., Wu, X., Moinova, H., Markowitz, S.D., Ding, H., Hoeijmakers, J.H. *et al.* (2008) Polyubiquitination of proliferating cell nuclear antigen by HLTF and SHPRH prevents genomic instability from stalled replication forks. *Proc Natl Acad Sci U S A*, **105**, 12411-12416.
138. Lopes, M., Foiani, M. and Sogo, J.M. (2006) Multiple mechanisms control chromosome integrity after replication fork uncoupling and restart at irreparable UV lesions. *Mol Cell*, **21**, 15-27.
139. Soultanas, P. and Wigley, D.B. (2001) Unwinding the 'Gordian knot' of helicase action. *Trends Biochem Sci*, **26**, 47-54.
140. Caruthers, J.M. and McKay, D.B. (2002) Helicase structure and mechanism. *Curr Opin Struct Biol*, **12**, 123-133.
141. Tuteja, N. and Tuteja, R. (2004) Unraveling DNA helicases. Motif, structure, mechanism and function. *Eur J Biochem*, **271**, 1849-1863.
142. Singleton, M.R., Dillingham, M.S. and Wigley, D.B. (2007) Structure and mechanism of helicases and nucleic acid translocases. *Annu Rev Biochem*, **76**, 23-50.

143. Durr, H., Flaus, A., Owen-Hughes, T. and Hopfner, K.P. (2006) Snf2 family ATPases and DExx box helicases: differences and unifying concepts from high-resolution crystal structures. *Nucleic Acids Res*, **34**, 4160-4167.
144. Gorbalenya, A.E., Koonin, E.V., Donchenko, A.P. and Blinov, V.M. (1989) Two related superfamilies of putative helicases involved in replication, recombination, repair and expression of DNA and RNA genomes. *Nucleic Acids Res*, **17**, 4713-4730.
145. Pause, A. and Sonenberg, N. (1992) Mutational analysis of a DEAD box RNA helicase: the mammalian translation initiation factor eIF-4A. *Embo J*, **11**, 2643-2654.
146. Tanner, N.K., Cordin, O., Banroques, J., Doere, M. and Linder, P. (2003) The Q motif: a newly identified motif in DEAD box helicases may regulate ATP binding and hydrolysis. *Mol Cell*, **11**, 127-138.
147. Korolev, S., Yao, N., Lohman, T.M., Weber, P.C. and Waksman, G. (1998) Comparisons between the structures of HCV and Rep helicases reveal structural similarities between SF1 and SF2 super-families of helicases. *Protein Sci*, **7**, 605-610.
148. Mahdi, A.A., Briggs, G.S., Sharples, G.J., Wen, Q. and Lloyd, R.G. (2003) A model for dsDNA translocation revealed by a structural motif common to RecG and Mfd proteins. *Embo J*, **22**, 724-734.
149. Soultanas, P. and Wigley, D.B. (2000) DNA helicases: 'inching forward'. *Curr Opin Struct Biol*, **10**, 124-128.
150. Soultanas, P., Dillingham, M.S., Wiley, P., Webb, M.R. and Wigley, D.B. (2000) Uncoupling DNA translocation and helicase activity in PcrA: direct evidence for an active mechanism. *Embo J*, **19**, 3799-3810.
151. Walker, J.E., Saraste, M., Runswick, M.J. and Gay, N.J. (1982) Distantly related sequences in the alpha- and beta-subunits of ATP synthase, myosin, kinases and other ATP-requiring enzymes and a common nucleotide binding fold. *Embo J*, **1**, 945-951.
152. Velankar, S.S., Soultanas, P., Dillingham, M.S., Subramanya, H.S. and Wigley, D.B. (1999) Crystal structures of complexes of PcrA DNA helicase with a DNA substrate indicate an inchworm mechanism. *Cell*, **97**, 75-84.
153. Lee, J.Y. and Yang, W. (2006) UvrD helicase unwinds DNA one base pair at a time by a two-part power stroke. *Cell*, **127**, 1349-1360.
154. Bessler, J.B., Torredagger, J.Z. and Zakian, V.A. (2001) The Pif1p subfamily of helicases: region-specific DNA helicases? *Trends Cell Biol*, **11**, 60-65.
155. Ivessa, A.S., Zhou, J.Q., Schulz, V.P., Monson, E.K. and Zakian, V.A. (2002) Saccharomyces Rrm3p, a 5' to 3' DNA helicase that promotes replication fork progression through telomeric and subtelomeric DNA. *Genes Dev*, **16**, 1383-1396.
156. Ivessa, A.S., Zhou, J.Q. and Zakian, V.A. (2000) The Saccharomyces Pif1p DNA helicase and the highly related Rrm3p have opposite effects on replication fork progression in ribosomal DNA. *Cell*, **100**, 479-489.
157. Ivessa, A.S., Lenzmeier, B.A., Bessler, J.B., Goudsouzian, L.K., Schnakenberg, S.L. and Zakian, V.A. (2003) The Saccharomyces cerevisiae helicase Rrm3p facilitates replication past nonhistone protein-DNA complexes. *Mol Cell*, **12**, 1525-1536.
158. Torres, J.Z., Bessler, J.B. and Zakian, V.A. (2004) Local chromatin structure at the ribosomal DNA causes replication fork pausing and genome instability

in the absence of the S. cerevisiae DNA helicase Rrm3p. *Genes Dev*, **18**, 498-503.
159. Schulz, V.P. and Zakian, V.A. (1994) The saccharomyces PIF1 DNA helicase inhibits telomere elongation and de novo telomere formation. *Cell*, **76**, 145-155.
160. Boule, J.B., Vega, L.R. and Zakian, V.A. (2005) The yeast Pif1p helicase removes telomerase from telomeric DNA. *Nature*, **438**, 57-61.
161. Veaute, X., Delmas, S., Selva, M., Jeusset, J., Le Cam, E., Matic, I., Fabre, F. and Petit, M.A. (2005) UvrD helicase, unlike Rep helicase, dismantles RecA nucleoprotein filaments in Escherichia coli. *Embo J*, **24**, 180-189.
162. Rong, L. and Klein, H.L. (1993) Purification and characterization of the SRS2 DNA helicase of the yeast Saccharomyces cerevisiae. *J Biol Chem*, **268**, 1252-1259.
163. Aguilera, A. and Klein, H.L. (1988) Genetic control of intrachromosomal recombination in Saccharomyces cerevisiae. I. Isolation and genetic characterization of hyper-recombination mutations. *Genetics*, **119**, 779-790.
164. Klein, H.L. (2001) Mutations in recombinational repair and in checkpoint control genes suppress the lethal combination of srs2Delta with other DNA repair genes in Saccharomyces cerevisiae. *Genetics*, **157**, 557-565.
165. Krejci, L., Van Komen, S., Li, Y., Villemain, J., Reddy, M.S., Klein, H., Ellenberger, T. and Sung, P. (2003) DNA helicase Srs2 disrupts the Rad51 presynaptic filament. *Nature*, **423**, 305-309.
166. Veaute, X., Jeusset, J., Soustelle, C., Kowalczykowski, S.C., Le Cam, E. and Fabre, F. (2003) The Srs2 helicase prevents recombination by disrupting Rad51 nucleoprotein filaments. *Nature*, **423**, 309-312.
167. Chiolo, I., Saponaro, M., Baryshnikova, A., Kim, J.H., Seo, Y.S. and Liberi, G. (2007) The human F-Box DNA helicase FBH1 faces Saccharomyces cerevisiae Srs2 and postreplication repair pathway roles. *Mol Cell Biol*, **27**, 7439-7450.
168. Barber, L.J., Youds, J.L., Ward, J.D., McIlwraith, M.J., O'Neil, N.J., Petalcorin, M.I., Martin, J.S., Collis, S.J., Cantor, S.B., Auclair, M. *et al.* (2008) RTEL1 maintains genomic stability by suppressing homologous recombination. *Cell*, **135**, 261-271.
169. Hu, Y., Raynard, S., Sehorn, M.G., Lu, X., Bussen, W., Zheng, L., Stark, J.M., Barnes, E.L., Chi, P., Janscak, P. *et al.* (2007) RECQL5/Recql5 helicase regulates homologous recombination and suppresses tumor formation via disruption of Rad51 presynaptic filaments. *Genes Dev*, **21**, 3073-3084.
170. Bugreev, D.V., Yu, X., Egelman, E.H. and Mazin, A.V. (2007) Novel pro- and anti-recombination activities of the Bloom's syndrome helicase. *Genes Dev*, **21**, 3085-3094.
171. Nakayama, H., Nakayama, K., Nakayama, R., Irino, N., Nakayama, Y. and Hanawalt, P.C. (1984) Isolation and genetic characterization of a thymineless death-resistant mutant of Escherichia coli K12: identification of a new mutation (recQ1) that blocks the RecF recombination pathway. *Mol Gen Genet*, **195**, 474-480.
172. Hickson, I.D. (2003) RecQ helicases: caretakers of the genome. *Nat Rev Cancer*, **3**, 169-178.
173. Hanada, K. and Hickson, I.D. (2007) Molecular genetics of RecQ helicase disorders. *Cell Mol Life Sci*, **64**, 2306-2322.

174. Bachrati, C.Z. and Hickson, I.D. (2003) RecQ helicases: suppressors of tumorigenesis and premature aging. *Biochem J*, **374**, 577-606.
175. Bennett, R.J. and Keck, J.L. (2004) Structure and function of RecQ DNA helicases. *Crit Rev Biochem Mol Biol*, **39**, 79-97.
176. Sharma, S., Doherty, K.M. and Brosh, R.M., Jr. (2006) Mechanisms of RecQ helicases in pathways of DNA metabolism and maintenance of genomic stability. *Biochem J*, **398**, 319-337.
177. Ouyang, K.J., Woo, L.L. and Ellis, N.A. (2008) Homologous recombination and maintenance of genome integrity: cancer and aging through the prism of human RecQ helicases. *Mech Ageing Dev*, **129**, 425-440.
178. Bernstein, D.A. and Keck, J.L. (2003) Domain mapping of Escherichia coli RecQ defines the roles of conserved N- and C-terminal regions in the RecQ family. *Nucleic Acids Res*, **31**, 2778-2785.
179. Bernstein, D.A., Zittel, M.C. and Keck, J.L. (2003) High-resolution structure of the E.coli RecQ helicase catalytic core. *Embo J*, **22**, 4910-4921.
180. Morozov, V., Mushegian, A.R., Koonin, E.V. and Bork, P. (1997) A putative nucleic acid-binding domain in Bloom's and Werner's syndrome helicases. *Trends Biochem Sci*, **22**, 417-418.
181. Liu, J.L., Rigolet, P., Dou, S.X., Wang, P.Y. and Xi, X.G. (2004) The zinc finger motif of Escherichia coli RecQ is implicated in both DNA binding and protein folding. *J Biol Chem*, **279**, 42794-42802.
182. Guo, R.B., Rigolet, P., Zargarian, L., Fermandjian, S. and Xi, X.G. (2005) Structural and functional characterizations reveal the importance of a zinc binding domain in Bloom's syndrome helicase. *Nucleic Acids Res*, **33**, 3109-3124.
183. Ren, H., Dou, S.X., Zhang, X.D., Wang, P.Y., Kanagaraj, R., Liu, J.L., Janscak, P., Hu, J.S. and Xi, X.G. (2008) The zinc-binding motif of human RECQ5beta suppresses the intrinsic strand-annealing activity of its DExH helicase domain and is essential for the helicase activity of the enzyme. *Biochem J*, **412**, 425-433.
184. Garcia, P.L., Liu, Y., Jiricny, J., West, S.C. and Janscak, P. (2004) Human RECQ5beta, a protein with DNA helicase and strand-annealing activities in a single polypeptide. *Embo J*, **23**, 2882-2891.
185. Bernstein, D.A. and Keck, J.L. (2005) Conferring substrate specificity to DNA helicases: role of the RecQ HRDC domain. *Structure*, **13**, 1173-1182.
186. Liu, Z., Macias, M.J., Bottomley, M.J., Stier, G., Linge, J.P., Nilges, M., Bork, P. and Sattler, M. (1999) The three-dimensional structure of the HRDC domain and implications for the Werner and Bloom syndrome proteins. *Structure*, **7**, 1557-1566.
187. Wu, L., Chan, K.L., Ralf, C., Bernstein, D.A., Garcia, P.L., Bohr, V.A., Vindigni, A., Janscak, P., Keck, J.L. and Hickson, I.D. (2005) The HRDC domain of BLM is required for the dissolution of double Holliday junctions. *Embo J*, **24**, 2679-2687.
188. Machwe, A., Xiao, L., Groden, J., Matson, S.W. and Orren, D.K. (2005) RecQ family members combine strand pairing and unwinding activities to catalyze strand exchange. *J Biol Chem*, **280**, 23397-23407.
189. Macris, M.A., Krejci, L., Bussen, W., Shimamoto, A. and Sung, P. (2006) Biochemical characterization of the RECQ4 protein, mutated in Rothmund-Thomson syndrome. *DNA Repair (Amst)*, **5**, 172-180.

190. Cheok, C.F., Wu, L., Garcia, P.L., Janscak, P. and Hickson, I.D. (2005) The Bloom's syndrome helicase promotes the annealing of complementary single-stranded DNA. *Nucleic Acids Res*, **33**, 3932-3941.
191. Sharma, S., Sommers, J.A., Choudhary, S., Faulkner, J.K., Cui, S., Andreoli, L., Muzzolini, L., Vindigni, A. and Brosh, R.M., Jr. (2005) Biochemical analysis of the DNA unwinding and strand annealing activities catalyzed by human RECQ1. *J Biol Chem*, **280**, 28072-28084.
192. Xu, X. and Liu, Y. (2009) Dual DNA unwinding activities of the Rothmund-Thomson syndrome protein, RECQ4. *Embo J*, **28**, 568-577.
193. Sharma, S., Stumpo, D.J., Balajee, A.S., Bock, C.B., Lansdorp, P.M., Brosh, R.M., Jr. and Blackshear, P.J. (2007) RECQL, a member of the RecQ family of DNA helicases, suppresses chromosomal instability. *Mol Cell Biol*, **27**, 1784-1794.
194. Umezu, K., Nakayama, K. and Nakayama, H. (1990) Escherichia coli RecQ protein is a DNA helicase. *Proc Natl Acad Sci U S A*, **87**, 5363-5367.
195. Harmon, F.G. and Kowalczykowski, S.C. (1998) RecQ helicase, in concert with RecA and SSB proteins, initiates and disrupts DNA recombination. *Genes Dev*, **12**, 1134-1144.
196. Hishida, T., Han, Y.W., Shibata, T., Kubota, Y., Ishino, Y., Iwasaki, H. and Shinagawa, H. (2004) Role of the Escherichia coli RecQ DNA helicase in SOS signaling and genome stabilization at stalled replication forks. *Genes Dev*, **18**, 1886-1897.
197. Wu, X. and Maizels, N. (2001) Substrate-specific inhibition of RecQ helicase. *Nucleic Acids Res*, **29**, 1765-1771.
198. Magner, D.B., Blankschien, M.D., Lee, J.A., Pennington, J.M., Lupski, J.R. and Rosenberg, S.M. (2007) RecQ promotes toxic recombination in cells lacking recombination intermediate-removal proteins. *Mol Cell*, **26**, 273-286.
199. Hanada, K., Ukita, T., Kohno, Y., Saito, K., Kato, J. and Ikeda, H. (1997) RecQ DNA helicase is a suppressor of illegitimate recombination in Escherichia coli. *Proc Natl Acad Sci U S A*, **94**, 3860-3865.
200. Harmon, F.G., DiGate, R.J. and Kowalczykowski, S.C. (1999) RecQ helicase and topoisomerase III comprise a novel DNA strand passage function: a conserved mechanism for control of DNA recombination. *Mol Cell*, **3**, 611-620.
201. Suski, C. and Marians, K.J. (2008) Resolution of converging replication forks by RecQ and topoisomerase III. *Mol Cell*, **30**, 779-789.
202. Bennett, R.J., Sharp, J.A. and Wang, J.C. (1998) Purification and characterization of the Sgs1 DNA helicase activity of Saccharomyces cerevisiae. *J Biol Chem*, **273**, 9644-9650.
203. Bennett, R.J., Keck, J.L. and Wang, J.C. (1999) Binding specificity determines polarity of DNA unwinding by the Sgs1 protein of S. cerevisiae. *J Mol Biol*, **289**, 235-248.
204. Sun, H., Bennett, R.J. and Maizels, N. (1999) The Saccharomyces cerevisiae Sgs1 helicase efficiently unwinds G-G paired DNAs. *Nucleic Acids Res*, **27**, 1978-1984.
205. Huber, M.D., Lee, D.C. and Maizels, N. (2002) G4 DNA unwinding by BLM and Sgs1p: substrate specificity and substrate-specific inhibition. *Nucleic Acids Res*, **30**, 3954-3961.

206. Frei, C. and Gasser, S.M. (2000) The yeast Sgs1p helicase acts upstream of Rad53p in the DNA replication checkpoint and colocalizes with Rad53p in S-phase-specific foci. *Genes Dev*, **14**, 81-96.
207. Lu, J., Mullen, J.R., Brill, S.J., Kleff, S., Romeo, A.M. and Sternglanz, R. (1996) Human homologues of yeast helicase. *Nature*, **383**, 678-679.
208. Watt, P.M., Louis, E.J., Borts, R.H. and Hickson, I.D. (1995) Sgs1: a eukaryotic homolog of E. coli RecQ that interacts with topoisomerase II in vivo and is required for faithful chromosome segregation. *Cell*, **81**, 253-260.
209. Gangloff, S., McDonald, J.P., Bendixen, C., Arthur, L. and Rothstein, R. (1994) The yeast type I topoisomerase Top3 interacts with Sgs1, a DNA helicase homolog: a potential eukaryotic reverse gyrase. *Mol Cell Biol*, **14**, 8391-8398.
210. Bennett, R.J., Noirot-Gros, M.F. and Wang, J.C. (2000) Interaction between yeast sgs1 helicase and DNA topoisomerase III. *J Biol Chem*, **275**, 26898-26905.
211. Chang, M., Bellaoui, M., Zhang, C., Desai, R., Morozov, P., Delgado-Cruzata, L., Rothstein, R., Freyer, G.A., Boone, C. and Brown, G.W. (2005) RMI1/NCE4, a suppressor of genome instability, encodes a member of the RecQ helicase/Topo III complex. *Embo J*, **24**, 2024-2033.
212. Mullen, J.R., Nallaseth, F.S., Lan, Y.Q., Slagle, C.E. and Brill, S.J. (2005) Yeast Rmi1/Nce4 controls genome stability as a subunit of the Sgs1-Top3 complex. *Mol Cell Biol*, **25**, 4476-4487.
213. Ira, G., Malkova, A., Liberi, G., Foiani, M. and Haber, J.E. (2003) Srs2 and Sgs1-Top3 suppress crossovers during double-strand break repair in yeast. *Cell*, **115**, 401-411.
214. Liberi, G., Maffioletti, G., Lucca, C., Chiolo, I., Baryshnikova, A., Cotta-Ramusino, C., Lopes, M., Pellicioli, A., Haber, J.E. and Foiani, M. (2005) Rad51-dependent DNA structures accumulate at damaged replication forks in sgs1 mutants defective in the yeast ortholog of BLM RecQ helicase. *Genes Dev*, **19**, 339-350.
215. Cobb, J.A., Bjergbaek, L., Shimada, K., Frei, C. and Gasser, S.M. (2003) DNA polymerase stabilization at stalled replication forks requires Mec1 and the RecQ helicase Sgs1. *Embo J*, **22**, 4325-4336.
216. Bjergbaek, L., Cobb, J.A., Tsai-Pflugfelder, M. and Gasser, S.M. (2005) Mechanistically distinct roles for Sgs1p in checkpoint activation and replication fork maintenance. *Embo J*, **24**, 405-417.
217. Versini, G., Comet, I., Wu, M., Hoopes, L., Schwob, E. and Pasero, P. (2003) The yeast Sgs1 helicase is differentially required for genomic and ribosomal DNA replication. *Embo J*, **22**, 1939-1949.
218. Mullen, J.R., Kaliraman, V., Ibrahim, S.S. and Brill, S.J. (2001) Requirement for three novel protein complexes in the absence of the Sgs1 DNA helicase in Saccharomyces cerevisiae. *Genetics*, **157**, 103-118.
219. Kaliraman, V., Mullen, J.R., Fricke, W.M., Bastin-Shanower, S.A. and Brill, S.J. (2001) Functional overlap between Sgs1-Top3 and the Mms4-Mus81 endonuclease. *Genes Dev*, **15**, 2730-2740.
220. Cui, S., Klima, R., Ochem, A., Arosio, D., Falaschi, A. and Vindigni, A. (2003) Characterization of the DNA-unwinding activity of human RECQ1, a helicase specifically stimulated by human replication protein A. *J Biol Chem*, **278**, 1424-1432.

221. Cui, S., Arosio, D., Doherty, K.M., Brosh, R.M., Jr., Falaschi, A. and Vindigni, A. (2004) Analysis of the unwinding activity of the dimeric RECQ1 helicase in the presence of human replication protein A. *Nucleic Acids Res*, **32**, 2158-2170.
222. Muzzolini, L., Beuron, F., Patwardhan, A., Popuri, V., Cui, S., Niccolini, B., Rappas, M., Freemont, P.S. and Vindigni, A. (2007) Different quaternary structures of human RECQ1 are associated with its dual enzymatic activity. *PLoS Biol*, **5**, e20.
223. Kawabe, T., Tsuyama, N., Kitao, S., Nishikawa, K., Shimamoto, A., Shiratori, M., Matsumoto, T., Anno, K., Sato, T., Mitsui, Y. *et al.* (2000) Differential regulation of human RecQ family helicases in cell transformation and cell cycle. *Oncogene*, **19**, 4764-4772.
224. Doherty, K.M., Sharma, S., Uzdilla, L.A., Wilson, T.M., Cui, S., Vindigni, A. and Brosh, R.M., Jr. (2005) RECQ1 helicase interacts with human mismatch repair factors that regulate genetic recombination. *J Biol Chem*, **280**, 28085-28094.
225. LeRoy, G., Carroll, R., Kyin, S., Seki, M. and Cole, M.D. (2005) Identification of RecQL1 as a Holliday junction processing enzyme in human cell lines. *Nucleic Acids Res*, **33**, 6251-6257.
226. Luo, G., Santoro, I.M., McDaniel, L.D., Nishijima, I., Mills, M., Youssoufian, H., Vogel, H., Schultz, R.A. and Bradley, A. (2000) Cancer predisposition caused by elevated mitotic recombination in Bloom mice. *Nat Genet*, **26**, 424-429.
227. Karow, J.K., Newman, R.H., Freemont, P.S. and Hickson, I.D. (1999) Oligomeric ring structure of the Bloom's syndrome helicase. *Curr Biol*, **9**, 597-600.
228. Beresten, S.F., Stan, R., van Brabant, A.J., Ye, T., Naureckiene, S. and Ellis, N.A. (1999) Purification of overexpressed hexahistidine-tagged BLM N431 as oligomeric complexes. *Protein Expr Purif*, **17**, 239-248.
229. Janscak, P., Garcia, P.L., Hamburger, F., Makuta, Y., Shiraishi, K., Imai, Y., Ikeda, H. and Bickle, T.A. (2003) Characterization and mutational analysis of the RecQ core of the bloom syndrome protein. *J Mol Biol*, **330**, 29-42.
230. Brosh, R.M., Jr., Li, J.L., Kenny, M.K., Karow, J.K., Cooper, M.P., Kureekattil, R.P., Hickson, I.D. and Bohr, V.A. (2000) Replication protein A physically interacts with the Bloom's syndrome protein and stimulates its helicase activity. *J Biol Chem*, **275**, 23500-23508.
231. Mohaghegh, P., Karow, J.K., Brosh Jr, R.M., Jr., Bohr, V.A. and Hickson, I.D. (2001) The Bloom's and Werner's syndrome proteins are DNA structure-specific helicases. *Nucleic Acids Res*, **29**, 2843-2849.
232. Bachrati, C.Z., Borts, R.H. and Hickson, I.D. (2006) Mobile D-loops are a preferred substrate for the Bloom's syndrome helicase. *Nucleic Acids Res*, **34**, 2269-2279.
233. Sun, H., Karow, J.K., Hickson, I.D. and Maizels, N. (1998) The Bloom's syndrome helicase unwinds G4 DNA. *J Biol Chem*, **273**, 27587-27592.
234. Karow, J.K., Constantinou, A., Li, J.L., West, S.C. and Hickson, I.D. (2000) The Bloom's syndrome gene product promotes branch migration of holliday junctions. *Proc Natl Acad Sci U S A*, **97**, 6504-6508.
235. Bernardi, R. and Pandolfi, P.P. (2007) Structure, dynamics and functions of promyelocytic leukaemia nuclear bodies. *Nat Rev Mol Cell Biol*, **8**, 1006-1016.

236. Wu, L., Davies, S.L., Levitt, N.C. and Hickson, I.D. (2001) Potential role for the BLM helicase in recombinational repair via a conserved interaction with RAD51. *J Biol Chem*, **276**, 19375-19381.
237. Bischof, O., Kim, S.H., Irving, J., Beresten, S., Ellis, N.A. and Campisi, J. (2001) Regulation and localization of the Bloom syndrome protein in response to DNA damage. *J Cell Biol*, **153**, 367-380.
238. Sengupta, S., Linke, S.P., Pedeux, R., Yang, Q., Farnsworth, J., Garfield, S.H., Valerie, K., Shay, J.W., Ellis, N.A., Wasylyk, B. *et al.* (2003) BLM helicase-dependent transport of p53 to sites of stalled DNA replication forks modulates homologous recombination. *Embo J*, **22**, 1210-1222.
239. Davies, S.L., North, P.S. and Hickson, I.D. (2007) Role for BLM in replication-fork restart and suppression of origin firing after replicative stress. *Nat Struct Mol Biol*, **14**, 677-679.
240. Raynard, S., Bussen, W. and Sung, P. (2006) A double Holliday junction dissolvasome comprising BLM, topoisomerase IIIalpha, and BLAP75. *J Biol Chem*, **281**, 13861-13864.
241. Wu, L., Bachrati, C.Z., Ou, J., Xu, C., Yin, J., Chang, M., Wang, W., Li, L., Brown, G.W. and Hickson, I.D. (2006) BLAP75/RMI1 promotes the BLM-dependent dissolution of homologous recombination intermediates. *Proc Natl Acad Sci U S A*, **103**, 4068-4073.
242. Chan, K.L., North, P.S. and Hickson, I.D. (2007) BLM is required for faithful chromosome segregation and its localization defines a class of ultrafine anaphase bridges. *Embo J*, **26**, 3397-3409.
243. Perry, J.J., Yannone, S.M., Holden, L.G., Hitomi, C., Asaithamby, A., Han, S., Cooper, P.K., Chen, D.J. and Tainer, J.A. (2006) WRN exonuclease structure and molecular mechanism imply an editing role in DNA end processing. *Nat Struct Mol Biol*, **13**, 414-422.
244. Kamath-Loeb, A.S., Shen, J.C., Loeb, L.A. and Fry, M. (1998) Werner syndrome protein. II. Characterization of the integral 3' --> 5' DNA exonuclease. *J Biol Chem*, **273**, 34145-34150.
245. Huang, S., Li, B., Gray, M.D., Oshima, J., Mian, I.S. and Campisi, J. (1998) The premature ageing syndrome protein, WRN, is a 3'-->5' exonuclease. *Nat Genet*, **20**, 114-116.
246. Suzuki, N., Shimamoto, A., Imamura, O., Kuromitsu, J., Kitao, S., Goto, M. and Furuichi, Y. (1997) DNA helicase activity in Werner's syndrome gene product synthesized in a baculovirus system. *Nucleic Acids Res*, **25**, 2973-2978.
247. Shen, J.C., Gray, M.D., Oshima, J., Kamath-Loeb, A.S., Fry, M. and Loeb, L.A. (1998) Werner syndrome protein. I. DNA helicase and dna exonuclease reside on the same polypeptide. *J Biol Chem*, **273**, 34139-34144.
248. Shen, J.C. and Loeb, L.A. (2000) Werner syndrome exonuclease catalyzes structure-dependent degradation of DNA. *Nucleic Acids Res*, **28**, 3260-3268.
249. Brosh, R.M., Jr., Orren, D.K., Nehlin, J.O., Ravn, P.H., Kenny, M.K., Machwe, A. and Bohr, V.A. (1999) Functional and physical interaction between WRN helicase and human replication protein A. *J Biol Chem*, **274**, 18341-18350.
250. Constantinou, A., Tarsounas, M., Karow, J.K., Brosh, R.M., Bohr, V.A., Hickson, I.D. and West, S.C. (2000) Werner's syndrome protein (WRN) migrates Holliday junctions and co-localizes with RPA upon replication arrest. *EMBO Rep*, **1**, 80-84.

251. Kamath-Loeb, A.S., Loeb, L.A., Johansson, E., Burgers, P.M. and Fry, M. (2001) Interactions between the Werner syndrome helicase and DNA polymerase delta specifically facilitate copying of tetraplex and hairpin structures of the d(CGG)n trinucleotide repeat sequence. *J Biol Chem*, **276**, 16439-16446.
252. Crabbe, L., Verdun, R.E., Haggblom, C.I. and Karlseder, J. (2004) Defective telomere lagging strand synthesis in cells lacking WRN helicase activity. *Science*, **306**, 1951-1953.
253. Crabbe, L., Jauch, A., Naeger, C.M., Holtgreve-Grez, H. and Karlseder, J. (2007) Telomere dysfunction as a cause of genomic instability in Werner syndrome. *Proc Natl Acad Sci U S A*, **104**, 2205-2210.
254. Chang, S., Multani, A.S., Cabrera, N.G., Naylor, M.L., Laud, P., Lombard, D., Pathak, S., Guarente, L. and DePinho, R.A. (2004) Essential role of limiting telomeres in the pathogenesis of Werner syndrome. *Nat Genet*, **36**, 877-882.
255. Harrigan, J.A., Opresko, P.L., von Kobbe, C., Kedar, P.S., Prasad, R., Wilson, S.H. and Bohr, V.A. (2003) The Werner syndrome protein stimulates DNA polymerase beta strand displacement synthesis via its helicase activity. *J Biol Chem*, **278**, 22686-22695.
256. Saydam, N., Kanagaraj, R., Dietschy, T., Garcia, P.L., Pena-Diaz, J., Shevelev, I., Stagljar, I. and Janscak, P. (2007) Physical and functional interactions between Werner syndrome helicase and mismatch-repair initiation factors. *Nucleic Acids Res*, **35**, 5706-5716.
257. Prince, P.R., Emond, M.J. and Monnat, R.J., Jr. (2001) Loss of Werner syndrome protein function promotes aberrant mitotic recombination. *Genes Dev*, **15**, 933-938.
258. Saintigny, Y., Makienko, K., Swanson, C., Emond, M.J. and Monnat, R.J., Jr. (2002) Homologous recombination resolution defect in werner syndrome. *Mol Cell Biol*, **22**, 6971-6978.
259. Dietschy, T., Shevelev, I. and Stagljar, I. (2007) The molecular role of the Rothmund-Thomson-, RAPADILINO- and Baller-Gerold-gene product, RECQL4: recent progress. *Cell Mol Life Sci*, **64**, 796-802.
260. Sangrithi, M.N., Bernal, J.A., Madine, M., Philpott, A., Lee, J., Dunphy, W.G. and Venkitaraman, A.R. (2005) Initiation of DNA replication requires the RECQL4 protein mutated in Rothmund-Thomson syndrome. *Cell*, **121**, 887-898.
261. Petkovic, M., Dietschy, T., Freire, R., Jiao, R. and Stagljar, I. (2005) The human Rothmund-Thomson syndrome gene product, RECQL4, localizes to distinct nuclear foci that coincide with proteins involved in the maintenance of genome stability. *J Cell Sci*, **118**, 4261-4269.
262. Yin, J., Kwon, Y.T., Varshavsky, A. and Wang, W. (2004) RECQL4, mutated in the Rothmund-Thomson and RAPADILINO syndromes, interacts with ubiquitin ligases UBR1 and UBR2 of the N-end rule pathway. *Hum Mol Genet*, **13**, 2421-2430.
263. Woo, L.L., Futami, K., Shimamoto, A., Furuichi, Y. and Frank, K.M. (2006) The Rothmund-Thomson gene product RECQL4 localizes to the nucleolus in response to oxidative stress. *Exp Cell Res*, **312**, 3443-3457.
264. Sekelsky, J.J., Brodsky, M.H., Rubin, G.M. and Hawley, R.S. (1999) Drosophila and human RecQ5 exist in different isoforms generated by alternative splicing. *Nucleic Acids Res*, **27**, 3762-3769.

265. Shimamoto, A., Nishikawa, K., Kitao, S. and Furuichi, Y. (2000) Human RecQ5beta, a large isomer of RecQ5 DNA helicase, localizes in the nucleoplasm and interacts with topoisomerases 3alpha and 3beta. *Nucleic Acids Res*, **28**, 1647-1655.
266. Hu, Y., Lu, X., Barnes, E., Yan, M., Lou, H. and Luo, G. (2005) Recql5 and Blm RecQ DNA helicases have nonredundant roles in suppressing crossovers. *Mol Cell Biol*, **25**, 3431-3442.
267. Wang, W., Seki, M., Narita, Y., Nakagawa, T., Yoshimura, A., Otsuki, M., Kawabe, Y., Tada, S., Yagi, H., Ishii, Y. *et al.* (2003) Functional relation among RecQ family helicases RecQL1, RecQL5, and BLM in cell growth and sister chromatid exchange formation. *Mol Cell Biol*, **23**, 3527-3535.
268. Zheng, L., Kanagaraj, R., Mihaljevic, B., Schwendener, S., Sartori, A.A., Gerrits, B., Shevelev, I. and Janscak, P. (2009) MRE11 complex links RECQ5 helicase to sites of DNA damage. *Nucleic Acids Res*, **37**, 2645-2657.
269. Izumikawa, K., Yanagida, M., Hayano, T., Tachikawa, H., Komatsu, W., Shimamoto, A., Futami, K., Furuichi, Y., Shinkawa, T., Yamauchi, Y. *et al.* (2008) Association of human DNA helicase RecQ5beta with RNA polymerase II and its possible role in transcription. *Biochem J*, **413**, 505-516.
270. Aygun, O., Svejstrup, J. and Liu, Y. (2008) A RECQ5-RNA polymerase II association identified by targeted proteomic analysis of human chromatin. *Proc Natl Acad Sci U S A*, **105**, 8580-8584.
271. Sharples, G.J., Chan, S.N., Mahdi, A.A., Whitby, M.C. and Lloyd, R.G. (1994) Processing of intermediates in recombination and DNA repair: identification of a new endonuclease that specifically cleaves Holliday junctions. *Embo J*, **13**, 6133-6142.
272. Chan, S.N., Vincent, S.D. and Lloyd, R.G. (1998) Recognition and manipulation of branched DNA by the RusA Holliday junction resolvase of Escherichia coli. *Nucleic Acids Res*, **26**, 1560-1566.
273. McCulloch, R., Coggins, L.W., Colloms, S.D. and Sherratt, D.J. (1994) Xer-mediated site-specific recombination at cer generates Holliday junctions in vivo. *Embo J*, **13**, 1844-1855.
274. Machwe, A., Lozada, E.M., Xiao, L. and Orren, D.K. (2006) Competition between the DNA unwinding and strand pairing activities of the Werner and Bloom syndrome proteins. *BMC Mol Biol*, **7**, 1.
275. MacFarland, K.J., Shan, Q., Inman, R.B. and Cox, M.M. (1997) RecA as a motor protein. Testing models for the role of ATP hydrolysis in DNA strand exchange. *J Biol Chem*, **272**, 17675-17685.
276. Janscak, P., Sandmeier, U., Szczelkun, M.D. and Bickle, T.A. (2001) Subunit assembly and mode of DNA cleavage of the type III restriction endonucleases EcoP1I and EcoP15I. *J Mol Biol*, **306**, 417-431.
277. Fukuoh, A., Iwasaki, H., Ishioka, K. and Shinagawa, H. (1997) ATP-dependent resolution of R-loops at the ColE1 replication origin by Escherichia coli RecG protein, a Holliday junction-specific helicase. *Embo J*, **16**, 203-209.
278. Giraud-Panis, M.J. and Lilley, D.M. (1998) Structural recognition and distortion by the DNA junction-resolving enzyme RusA. *J Mol Biol*, **278**, 117-133.
279. Henricksen, L.A., Umbricht, C.B. and Wold, M.S. (1994) Recombinant replication protein A: expression, complex formation, and functional characterization. *J Biol Chem*, **269**, 11121-11132.

280. Benson, F.E., Stasiak, A. and West, S.C. (1994) Purification and characterization of the human Rad51 protein, an analogue of E. coli RecA. *Embo J*, **13**, 5764-5771.
281. Janscak, P., Abadjieva, A. and Firman, K. (1996) The type I restriction endonuclease R.EcoR124I: over-production and biochemical properties. *J Mol Biol*, **257**, 977-991.
282. Chan, K.M., Delfert, D. and Junger, K.D. (1986) A direct colorimetric assay for Ca2+ -stimulated ATPase activity. *Anal Biochem*, **157**, 375-380.

9 ACKNOWLEDGEMENT

I would like to express my gratitude to all those people who made this thesis possible.

First of all, Dr. Pavel Janscak for the possibility to join his group, for scientific supervision and support during the last four years of my PhD work. I appreciated that he was always open for discussion and I could go to his office anytime I needed help or advices.

Next, I would like to thank Prof. Josef Jiricny for his concern and being the doctor father of my thesis. I also thank Prof. Ian Hickson and Prof. Ulrich Hübscher for being in my thesis committee.

Special thanks to Raj who introduced me in the laboratory, helped me not only with many good scientific suggestions but also with his constructive and positive manner. In addition, I would like to thank all the past and present members of Pavel's gourp, Tracy, Nurten, Javi, Tobi, Dani, Boris, Igor and Shreya for understanding and help.

Many thanks to Christiane and Christine for their friendship and technical assistant. Giancarlo for always being around and taking care of everything. Marianne, Farah and Malika for support and sympathy during difficult times.

Special thanks to my family and friends for trust, interest and continuous support in all the years.

10 CURRICULUM VITAE

Sybille SCHWENDENER
Schützenmatt 29
CH-8046 Zurich
e-mail: sybille.schwendener@bluewin.ch

Nationality: Swiss
Marital status: Single
Date of birth: 17.08.1975
Place of citizenship: Buchs SG

EDUCATION

07/2005-07/2009	**PhD thesis at the Institute of Molecular Cancer Research of the University of Zurich** Title: Functional Characterization of the Human RECQ5 Protein. Supervisor: Dr. P. Janscak Responsible member of faculty: Prof. Dr. J. Jiricny
09/2002-05/2005	**Diploma studies at ETH Zurich** Major: Biochemistry, Molecular Biology Minor: Cell Biology, Immunology, Virology
04/2004-10/2004	**Diploma thesis at the Institute of medical Virology of the University of Zurich** Title: Analysis of Triplex Formation at the Polypurine Tract of HIV-1 Supervisor: Dr. J. Heinrich Responsible member of faculty: Prof. Dr. K. Mölling
08/2003-11/2003	**Semester work at the Institute of medical Virology of the University of Zurich**
09/2000-08/2002	**Basic studies in Biology and Chemistry at the ETH Zurich**
1997-2000	**Matura (Typus C), AKAD Zurich**
1995-1996	**Vorkurs, Schule für Gestaltung Zurich**
1991-1994	**Diplommittelschule Zurich**
1982-1991	**Primar- und Sekundarschule Wädenswil**

PUBLICATIONS

Schwendener S, Raynard S, Paliwal S, Cheng A, Kanagaraj R, Shevelev I, Stark JM, Sung P and Janscak P " Physical interaction of RECQ5 helicase with RAD51 facilitates its anti-recombinase activity" J Biol Chem. 2010 May 21;285(21):15739-45. Epub 2010 Mar 25.

Speina E, Dawut L, Hedayati M, Wang Z, May A, **Schwendener S**, Janscak P, Croteau DL, Bohr VA "Human RECQL5{beta} stimulates flap endonuclease 1" Nucleic Acids Res. 2010 May;38(9):2904-16. Epub 2010 Jan 16.

Zheng L, Kanagaraj R, Mihaljevic B, **Schwendener S**, Janscak P. "MRE11 complex links RECQ5 helicase to sites of DNA damage" Nucleic Acids Res. 2009 May;37(8):2645-57. Epub 2009 Mar 6.

EMPLOYMENT HISTORY

1998-2000	Part-time employment as **photo lab assistant, Mini Print**, Wädenswil
1996-1999	**Keeper, Tierheim Uster** (part-time)
1996-1998	**Crew, Mc Donald's**, Wädenswil (part-time)
1995-1996	**Keeper, Bearded Collie Breeding,** Schönenberg, (part-time)
1994-1995	**Internship in food industry** (Kern und Sammet, Wädenswil; Zweifel Pomy-Chips AG, Spreitenbach; Biscuit-Suter, Schönenberg)
1993	**Patient care traineeship**, Stadtspital Triemli, Zurich (one month)

SKILLS AND HOBBIES

Languages	**German**: mother tongue **English**: good **French**: basic knowledge
IT	Operating system: MS Windows, Mac OS MS Office: Word, Excel, PowerPoint Basic knowledge in Bioinformatics
Sports	Jogging, Gymnastics, Hiking
Hobbies	Drawing and Painting, Reading

11 APPENDIX

Publications

Schwendener S, Raynard S, Paliwal S, Cheng A, Kanagaraj R, Shevelev I, Stark JM, Sung P and Janscak P " Physical interaction of RECQ5 helicase with RAD51 facilitates its anti-recombinase activity" J Biol Chem. 2010 May 21;285(21):15739-45. Epub 2010 Mar 25.
http://www.jbc.org/content/285/21/15739.long

Speina E, Dawut L, Hedayati M, Wang Z, May A, **Schwendener S**, Janscak P, Croteau DL, Bohr VA "Human RECQL5{beta} stimulates flap endonuclease 1" Nucleic Acids Res. 2010 May;38(9):2904-16. Epub 2010 Jan 16.
http://nar.oxfordjournals.org/cgi/content/full/gkp1217v1?view=long&pmid=20081208

Zheng L, Kanagaraj R, Mihaljevic B, **Schwendener S**, Janscak P. "MRE11 complex links RECQ5 helicase to sites of DNA damage" Nucleic Acids Res. 2009 May;37(8):2645-57. Epub 2009 Mar 6.
http://nar.oxfordjournals.org/cgi/content/full/37/8/2645?view=long&pmid=19270065